

GW - 31

REPORTS

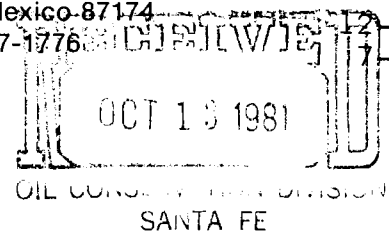
YEAR(S):

1974 - 1984

Union Geothermal Company of New Mexico

4100 Southern Blvd. SE - Suite 180C
P.O. Box 15225
Rio Rancho, New Mexico 87174
Telephone (505) 897-1776

2-600.1
7-740



October 9, 1981

Carl Ulvog
State of New Mexico
Oil Conservation Division
P.O. Box 2088
Santa Fe, New Mexico 87501

Dear Mr. Ulvog:

Enclosed please find a copy of the Baca Geothermal Demonstration Project Jemez Watershed Monitoring Program for water year 1979-1980. Chapter 2 contains a description of equipment in the Redondo Creek monitoring station.

Since the publication of the report, one additional ISCO unit has been installed to collect a 100 ml sample from Redondo Creek every eight hours. The ISCO set to collect only during increased flow has been set to collect with an increase of 0.1 cfs. Water year 1980-1981 did not experience the variability of flow related to the spring runoff that 1979-1980 experienced.

Recording pH and conductivity meters are presently being reviewed and a meter to backup the Analytical Measurements meter will be purchased to decrease downtime.

I hope the report will be useful to you.

Sincerely,

Lyle Rae Berger
Ecologist

LRB/dp
Enclosure

BACA GEOTHERMAL DEMONSTRATION PROJECT

JEMEZ WATERSHED MONITORING PROGRAM

WATER YEAR 1979-1980

L. R. BERGER

JANUARY, 1981

JEMEZ WATERSHED MONITORING PROGRAM

WATER YEAR 1979-1980

The Jemez River watershed monitoring program was designed to make monthly checks on water from seven sites located either upstream or downstream from Redondo Creek and the Baca Project. Location of the seven sites is designated by number on the map in Figure 1.

Monitoring was begun August 24, 1979 and has been conducted monthly since then.

SAMPLING PROCEDURE:

At each sample site, water temperature and pH are measured using a Beckman Chem-Mate pH Meter with a futura combination field electrode. Temperature is checked with a hand held thermometer. Conductivity is measured using a YSI field conductivity meter. Flow rate is calculated by measuring the time it takes a plastic cup filled with water to pass through a measured volume of stream. A sample of water is collected for transmittal to a local analytical laboratory.

Field data plus pertinent weather and activity information are logged at each site. Figure 2 is a sample log sheet.

Initially, raw water was collected, held at 4⁰C and taken to a laboratory for analysis within six hours. All seven sites were visited in one day.

In February of 1980 a routine check on the laboratory used at the time resulted in the project changing laboratories. The "new" laboratory requested samples be filtered. All water was filtered from May 13 until July 23, 1980 because project policy requires a laboratory receive samples in the condition it requested. Filtering samples increased collection time from one day to two to four days. Since fewer samples were submitted each day, the laboratory was not providing a discount promised for seven samples. The result was a 10% cost increase for analysis and one to three additional days pay for technician services for less useful water quality data.

The problems of increased time elapsed between site collections and increased cost were discussed with the laboratory. It was agreed that raw water from such a source as the Jemez watershed would be acceptable. From August 1980, all water has been collected without filtering. The water has always been held at 4⁰C and transported within six hours of collection.

JEMEZ WATERSHED MONITORING PROGRAM
WATER YEAR 1979-1980

2.

DATA COLLECTION HISTORY:

Initially, water was collected by supervisory personnel. A field technician was hired to collect watershed samples in conjunction with maintaining Redondo Creek monitoring station in December 1979. Scheduling problems arose from only one person being available which resulted in no water collection for April 1980.

One additional person has been trained to collect samples so that scheduling problems should not occur again. Additionally, backup technical help allows two people to make collections in winter months and during periods of runoff when wading some streams is hazardous.

Two sites, east fork of the Jemez River (7) and Sulfur Creek at Union Gate (2) could not be sampled some winter months because they freeze over.

Flow data could not be collected for any stream some winter months because of ice buildup in the stream course.

Most data collection problems are technician related and involve the Beckman pH meter probe.

COLLECTION PROCEDURE:

A. Collection of a Grab Sample

1. A container, usually of a plastic, is rinsed several times in the water to be sampled and the rinse water is discarded downstream.
2. The rinsed container is then submerged, if possible, into the stream flow and a volume of water is collected.
3. The full container is lifted quickly from the stream and the water is poured carefully into clean bottles supplied by the laboratory.
4. If the sample requires no acidification or other preparation, the cap to the bottle is filled with sample water then carefully sealed to the bottle.
5. If the sample requires acidification, careful measurement of the volume of acid is required. This measurement will be used to calibrate the actual volume of water left in the sample. When the sample has been appropriately treated, the bottle cap is rinsed and sealed to the bottle.

JEMEZ WATERSHED MONITORING PROGRAM
WATER YEAR 1979-1980

3.

COLLECTION PROCEDURE (Cont'd)

6. The bottle should have the following information placed on its surface:
 - a. sample site
 - b. date and time of day
 - c. sample temperature (taken in stream)
 - d. sample pH (taken in stream or bottle)
 1. If sample was acidified, "natural" pH should be distinguished from acidified and both should be indicated.
 - e. flow rate at sample site
 - f. conductivity at sample site
7. All samples should be kept cool (4°C) and out of the sun.
8. Samples should be collected at same site each sample period.

B. Collection of Field Temperature

1. Place a field thermometer well into the stream for several minutes.
2. Read thermometer directly.
3. Replace thermometer into stream for several more minutes.
4. Read thermometer again.

C. Collection of Field pH

1. Calibrate pH meter.
2. Rinse electrodes with stream water.
3. Insert electrodes well into stream for several seconds.
4. Read pH.
5. Rinse electrodes with stream water.
6. Reinsert into stream several seconds.
7. Read pH.
8. Rinse electrodes well with distilled water.

JEMEZ WATERSHED MONITORING PROGRAM
WATER YEAR 1979-1980

4.

COLLECTION PROCEDURE (Cont'd)

D. Collection of Field Conductance

1. Same procedure as field pH using conductivity meter.

E. Collection of Flow Rate

1. Select a fairly uniform site.
2. With a tape measure average width of stream.
3. Measure average depth of stream.
4. Measure a given distance on stream bank -- example, 3 feet between point A and B.
5. Drop a floatable object at point A and measure time it takes object to reach point B with a stop watch.
6. Repeat several times.
7. Calculate volume of water measured.
8. Calculate CFS using average time for water to move from A to B and volume of water between points A and B.

F. Collection of Small Flow Rate - Springs

1. If flow is small enough, collect all water flowing in a large container whose volume is known.
2. Measure time to fill the container using a stop watch.
3. Repeat several times.
4. Calculate CFS using volume and average time needed to fill the volume.

BACA SURFACE WATER MONITORING PROGRAM

SAMPLING SITES

JEMEZ WATER SHED

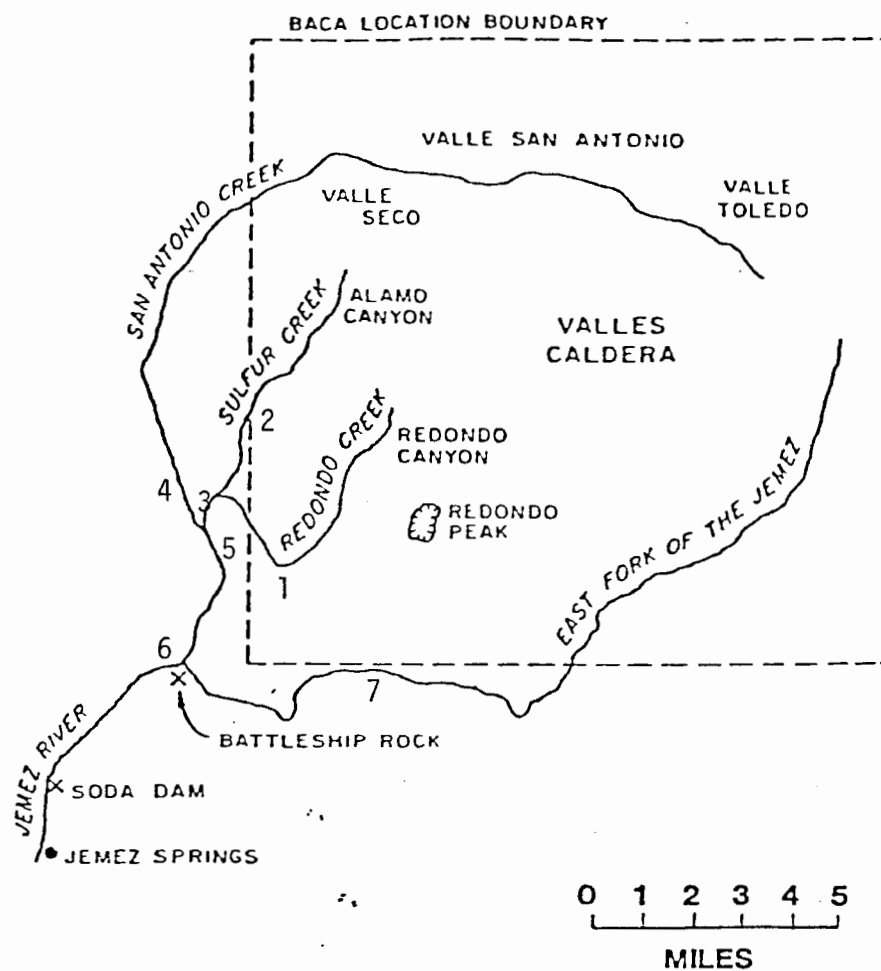


FIGURE 1

FIGURE 2:
INTERFACE WATER QUALITY SUMMARY SHEETS
LACA PROJECT, JEMEZ WATERSHED

SITE _____

<u>FIELD DATA</u>		<u>COMMENTS</u>
Date:		Weather Conditions:
Time:		Comments:
Water Temp:		Comments on Equipment:
pH:		
uhmos/cm		
cfs		

SITE _____

<u>FIELD DATA</u>		<u>COMMENTS</u>
Date:		Weather Conditions:
Time:		Comments:
Water Temp:		Comments on Equipment:
pH:		
uhmos/cm		
cfs		

SITE _____

<u>FIELD DATA</u>		<u>COMMENTS</u>
Date:		Weather Conditions:
Time:		Comments:
Water Temp:		Comments on Equipment:
pH:		
uhmos/cm		
cfs		

JEMEZ WATERSHED MONITORING PROGRAM
WATER YEAR 1979-1980

5.

Tables 1-7 outline chemical constituents measured in water samples and values of those constituents for each monitoring site. Monthly water quality data sheets are received from the laboratory by Union and copies are submitted to WESTEC and PNM.

Redondo Creek water quality data (Table 1) shows a marked difference from other collection periods November 1979 and August 1980. There is a marked rise in field conductivity; boron levels, sodium, calcium, chloride, sulfate and magnesium ions and a decrease in bicarbonate ions and pH in November 1979.

August 1980 data show similar elevation in chloride and sodium concentrations, a potential elevation in sulfate concentrations and conductivity. Less significant ion concentration elevations occur in January 1980.

The November 1979 data, and possibly the January and August 1980 data, probably reflect contribution to Redondo Creek from temporary drain lines in the geo-thermal well field. Such a potential contribution will be eliminated with installation of permanent pipelines in 1981-82.

Water quality data from Sulfur Creek at Union Gate (Table 2) demonstrates a great deal of variability between monthly collections. The variability probably reflects the percent contribution Sulfur receives from hot springs located one mile upstream from the collection site. The site was selected because it is the first point where Sulfur Creek waters enter public land, and it is above the confluence of Sulfur and Redondo Creeks. The variability of the quality of the waters makes comment difficult.

Table 3 lists water quality data for Sulfur Creek about one mile below the confluence with Redondo Creek. Sulfur and Redondo contribute approximately equal volumes to the sampling site. The water quality excursions discussed for Redondo Creek (Table 1) are not reflected in water quality data for Sulfur at La Cueva. The low SO_4 reading of November 1979 is probably a typographical error from the lab (undocumented by the lab).

February BOD_5 reading on Table 3 is extremely high. Succeeding readings indicate that the source of pollution was probably ephemeral.

Water quality data for San Antonio Creek above La Cueva may be found in Table 4. Dilution effect due to increased flow is the most probable explanation for the major water quality excursion for this site which occurred in May 1980 during spring runoff.

Increased BOD_5 readings for June and July 1980 could indicate contamination from local sewage facilities, possibly from the San Antonio Campground.

Table 5 lists water quality data for San Antonio Creek about 100 yards below its confluence with Sulfur Creek. Sulfur contributes $\approx 10\%$ of San Antonio's volume at this point.

JEMEZ WATERSHED MONITORING PROGRAM
WATER YEAR 1979-1980

6.

Chloride appears to be the only chemical constituent that changes in the water quality of San Antonio Creek below its confluence with Sulfur. No other clear contribution by Sulfur appears when Tables 3, 4 and 5 are compared.

San Antonio Creek and the East Fork of the Jemez (see Table 7) contribute approximately equal volumes to form the Jemez River at Battleship Rock (see Table 6).

Table 5 shows San Antonio Creek samples to have slightly elevated flourine concentrations when compared to Tables 6 and 7.

Table 7 shows East Fork waters consistently to have lower concentrations of bicarbonate, calcium, sodium and sulfate ions than either San Antonio Creek or Jemez River below Battleship Rock. Conductivity of East Fork samples is also lower than the other two sites. Boron concentration is consistently higher in East Fork samples and Jemez River at Battleship Rock than waters of San Antonio Creek when Tables 5, 6 and 7 are compared.

Slightly elevated BOD_5 concentrations from East Fork samples during June and July may indicate fecal contamination from cattle.

The extremely high BOD_5 concentration recorded in February at the Jemez River site at Battleship Rock could indicate a camper had illegally emptied sanitary tanks recently or that some other temporary pollution source was present near the collection site. Both sites in Tables 6 and 3 are near roads which could be used as illegal dumping points. Such extreme values for BOD_5 should be reflected in other tables if the samples had been improperly handled during the February collection or analysis.

TABLE 1: WATER QUALITY DATA - REDONDO CREEK

REDONDO	AUGUST 79	SEPTEMBER 79	OCTOBER 79	NOV. 79	DEC. 79	JAN. 80	FEB. 80	MARCH 80	MAY 80	JUNE 80	JULY 80	AUG. 80	SEPT. 80
	BOD ₅ mg/l	---	---	---	---	---	6.3	---	3.0	5.0	5.0	2.4	0.25
As	< 0.02	< 0.02	< 0.02	< 0.02	< 0.02	< 0.02	0.01	< 0.02	0.05	0.01	0.01	< 0.01	< 0.01
Ba	"	"	"	"	"	"	2.5	2.0	1.5	---	0.01	< 0.01	0.02
Hg	"	0.00012*	< 0.00001*	0.00025*	0.00054*	0.00012*	< 0.00001*	< 0.001	< 0.0001*	0.001	0.001	< 0.001	< 0.001
NO ₃	"	0.48	0.05	0.005	0.34	1.5	0.5	0.5	0.7	0.78	0.58	0.10	0.03
F	"	0.47	0.6	0.28	0.6	0.47	< 0.1	0.14	0.22	0.05	0.10	0.42	0.10
B	"	0.2	0.3	0.02	1.1	0.25*	1.75	0.2	0.1	0.03	0.10	0.02	0.50
HCO ₃	"	45.2	29.1	31.9	19.5	30.0	37.5	33.4	48.0	45.0	41.1	37.4	37.3
Ca	"	7.6	4.8	8.8	35.4	7.6	16.7	15.0	18.7	11.0	7.4	7.9	18.0
Cl	"	13.4	12.0	16.0	109.8	18.8	44.0	18.1	23.0	15.9	6.0	17.9	24.8
Fe (diss)	< 0.02	0.05	0.09	< 0.02	< 0.02	< 0.02	.30	< 0.02	0.35	0.02	0.09	0.07	0.17
Hg	"	0.8	1.1	1.3	6.7	0.8	1.8	1.4	2.3	1.1	0.79	0.78	2.0
K	"	1.6	2.0	1.8	12.4	1.6	4.7	2.8	2.9	3.8	1.2	1.8	4.6
Na	"	6.0	6.9	6.4	50.8	6.0	26.6	13.0	15.7	7.1	11.0	4.0	31.0
SO ₄	"	11.0	7.0	10.0	135.0	12.0	6.0	8.0	10.0	6.6	0.8	0.1	4.0
pH		6.4+	7.2	5.4	7.7	7.3	6.8	7.5	7.2	7.6	7.1	7.8	7.0
umhos conductance	50	40	70	440	188	130	79	112	70	63	78	245	
Ave. Flow Rt. cfs							1.6	1.6	1.8	2.2			
Temp °C	17°	8°	7°	13°	0°	2°	3.5°	5°	7°	13°	15°	13°	10°
PO ₄	"	.09	0.45	0.23	0.05	0.24	0.1	0.11	< 0.1	0.13	0.07	0.08	0.12

* data questionable - no known technique assures such accuracy
+ pH electrode questionable
pH, conductance and water temperature are field data

TABLE 2: WATER QUALITY DATA - SULFUR AT UNION GATE

- * data questionable - no known technique assures such accuracy
- + pH electrode questionable
- pH, conductance and water temperature are field data

TABLE 3: WATER QUALITY DATA - SULFUR AT LA CUEVA

SULFUR AT LA CUEVA	AUGUST 79	SEPTEMBER 79	OCTOBER 79	NOV. 79	DEC. 79	JAN. 80	FEB. 80	MARCH 80	MAY 80	JUNE 80	JULY 80	AUG. 80	SEPT. 80
BOD ₅ mg/l	--	--	--	<0.02	<0.02	<0.02	<0.02	<0.01	1.5	0.03	0.02	<0.01	0.6
As	"	<0.02	<0.02	<0.02	<0.02	<0.02	<0.02	0.5	1.5	--	--	<0.01	0.04
Ba	"	--	--	--	--	--	<0.001	<0.001	<0.001	<0.001	<0.001	<0.001	0.02
Hg	"	<0.001	<0.001	<0.001	<0.001	<0.001	<0.001	<0.001	<0.001	<0.001	<0.001	<0.001	<0.001
NO ₃	"	0.68	0.086	0.003	0.32	1.6	1.3	0.19	0.6	0.10	0.03	0.03	<0.01
F	"	0.36	0.65	0.4	0.43	0.29	0.2	0.24	0.51	0.10	0.27	0.07	0.09
B	"	0.1	0.2	<0.02	0.75	0.2	0.05	0.29	0.1	0.07	0.09	0.04	0.15
HCO ₃	"	22.0	27.6	28.0	32.0	27.0	66.0	78.0	79.8	19.5	29.8	32.1	37.3
Ca	"	10.2	8.6	17.6	7.6	20.8	84.7	45.0	62.3	12.0	13.0	12.0	29.6
Cl	"	18.4	10.8	14.9	45.2	24.8	26.4	29.3	15.2	6.0	6.0	8.0	24.8
Fe (diss.)	<0.02	0.42	0.43	0.06	<0.02	<0.02	0.03	<0.02	<0.01	0.07	0.16	0.62	0.41
Mg	"	1.8	2.2	3.3	1.6	4.1	9.9	6.2	6.9	1.7	1.5	1.5	2.0
K	"	2.4	3.8	1.9	5.2	7.1	2.0	9.8	9.1	2.2	2.1	2.4	2.4
Na	"	8.8	10.9	11.2	22.6	18.8	24.7	30.0	30.1	46.0	11.0	6.1	10.0
SO ₄	"	50.0	34.0	65.0	7.0	90.0	195.0	188.0	135.0	45.0	37.0	21.0	12.0
pH	--	6.3	6.3	6.2	5.7	--	4.4	4.6	5.2	7.2	6.5	7.1	
chloride con-													
ductance													
Temp °C	23°	12°	8°	0°	6°	0°	1°	5°	4°	14°	17°	9°	
PO ₄ mg/l	0.1	0.09	0.43	0.28	0.11	0.025	0.03	<0.1	0.09	0.04	0.11	0.02	0.08
LOW RATE	3.6	3.0	1.0	-	-	-	-	-	-	9 cfs	5.5	2.5	1.6

* data questionable - no known technique assures such accuracy
+ pH electrode questionable
pH, conductance and water temperature are field data

TABLE 4: WATER QUALITY DATA - SAN ANTONIO ABOVE LA CUEVA

SAN ANTONIO VE LA CUEVA	AUGUST 79	SEPTEMBER 79	OCTOBER 79	NOV. 79	DEC. 79	JAN. 80	FEB. 80	MARCH 80	MAY 80	JUNE 80	JULY 80	AUG. 80	SEPT. 80	
BOD ₅ mg/l	--	--	--	<0.02	<0.02	--	--	0.6	--	1.2	10.7	10.2	0.9	0.75
As "	<0.02	--	<0.02	<0.02	<0.02	<0.02	<0.02	<0.02	<0.02	<0.02	0.02	0.01	<0.01	0.06
Ba "	--	--	--	--	--	<0.02	<0.02	<0.02	2.0	--	0.1	0.03	<0.01	0.13
Hg "	0.00026*	0.00001*	0.00013*	0.00001*	0.00001*	<0.00001*	<0.00001*	<0.00001*	<0.00001*	<0.0001	0.05	<0.001	<0.001	<0.001
NO ₃ f	0.51	0.068	0.002	0.57	1.7	0.6	0.6	0.6	0.8	0.06	0.96	0.03	0.06	<0.01
B "	0.02	0.2	0.02	0.2	0.2	0.05	0.05	0.05	<0.02	<0.02	0.08	0.07	0.07	0.02
HCO ₃	67.6	68.5	78.0	68.0	74.0	62.0	58.6	78.0	38.5	102.0	107.0	89.6	120.1	
Ca "	4.6	3.7	6.4	5.2	4.2	11.7	13.0	20.4	9.1	17.0	17.0	16.0	22.2	
Cl "	12.2	3.6	3.6	3.2	4.8	4.0	7.9	6.0	1.0	2.0	3.0	3.0	4.0	
Fe (diss.)	<0.02	0.04	0.16	0.1	0.1	<0.02	<0.02	<0.02	<0.02	0.10	0.05	0.10	0.59	0.26
Mg "	1.1	1.4	1.8	1.6	1.45	1.6	1.8	2.9	1.60	2.5	2.2	1.90	1.80	
K "	2.8	2.6	2.4	2.2	2.4	3.0	2.8	4.7	2.3	2.5	2.8	2.9	2.2	
Na "	13.8	16.7	17.9	16.8	18.2	18.2	13.0	32.7	4.2	15.0	16.0	15.0	17.0	
SO ₄	14.0	9.0	10.0	8.0	12.0	15.0	12.0	17.0	10.0	2.0	0.5	5.0	<0.1	
pH	6.2	7.3	6.7	7.6	6.7	--	6.4	7.5	7.5	7.2	7.5	7.6		
hos conductance	110.0	120.0	100.0	90.0	75.0	82.0	72.0	105.0	68.0	138.0	165.0			
Temp °C	19°C	17°C	10°C	13°C	2°C	1.5°C	2°C	8°C	7°C	14°C	14°C			
PO ₄ mg/l	0.1	0.13	0.70	0.14	--	0.1	0.1	0.3	0.11	0.12	0.05	0.05	0.12	
flow rate	74.0	18.0	12.0	--	--	--	--	--	--	132.0	18.5	20.0		
													11.3	

* Data questionable - no known technique assures such accuracy
+ pH electrode questionable
pH, conductance and water temperature are field data

TABLE 5: WATER QUALITY DATA - SAN ANTONIO BELOW LA CUEVA

AN ANTONIO LOW LA CUEVA	AUGUST 79	SEPTEMBER 79	OCTOBER 79	NOV. 79	DEC. 79	JAN. 80	FEB. 80	MARCH 80	APRIL 80	JUNE 80	JULY 80	AUG. 80	SEPT. 80	
BOD ₅	mg/l	--	--	<0.02	<0.02	<0.02	<0.02	1.2	--	0.9	4.8	5.0	3.0	1.9
As	"	<0.02	--	--	--	--	<0.02	<0.02	<0.02	0.03	<0.01	<0.01	0.01	0.01
Ba	"	--	--	--	--	--	<0.001	<0.001	1.5	--	<0.1(?)	0.11	<0.01	0.11
Hg	"	<0.001	<0.001	<0.001	<0.001	<0.001	<0.001	<0.001	<0.001	<0.001	<0.001	<0.001	<0.001	<0.001
NO ₃	"	0.72	0.023	0.003	0.7	2.0	0.5	1.1	0.6	0.07	0.07	0.01	1.20	<0.01
f	"	1.25	1.11	1.21	1.34	1.12	0.84	1.28	0.94	0.22	0.74	0.34	1.10	0.81
B	"	<0.02	0.8	<0.02	0.45	0.05	<0.02	<0.02	0.3	0.07	0.09	0.12	0.06	0.13
HCO ₃	"	82.2	61.4	65.5	67.0	61.0	51.0	58.6	63.6	42.0	74.6	90.9	84.6	89.6
Ca	"	5.0	4.0	6.0	7.9	4.5	10.0	37.6	19.6	8.9	15.0	16.0	19.0	21.3
Cl	"	8.8	4.8	4.8	3.6	4.6	6.0	9.2	5.0	9.0	1.0	2.0	28.8(?)	4.8
Fe (diss.)	"	<0.02	0.09	0.18	<0.02	<0.02	0.12	<0.02	0.12	<0.02	0.17	0.05	0.11	0.25
Mg	"	1.1	1.48	1.7	2.0	1.35	1.3	2.7	3.3	1.60	2.20	2.20	2.20	1.6
K	"	3.2	3.1	2.3	2.0	2.38	2.7	1.4	2.3	1.9	2.3	2.7	3.2	2.0
Na	"	14.6	15.2	14.3	16.6	15.8	13.3	26.4	28.2	3.8(?)	14.0	11.0	22.0	11.2
SO ₄	"	11.0	11.0	5.0	13.5	17.0	15.0	19.0	17.0	12.0	12.0	4.1(?)	7.0	<0.1(?)
pH	"	6.1	7.1	7.0	6.4	6.1	--	8.0*	7.3	7.5	6.9	7.2	7.8	
mhos conductance		140	120	100	80	85	80	82	122	75	122	148	148	
Temp °C		20	18	7	5	2	1	4	9	8	13	17	13	
Po ₄ mg/l		0.2	0.18	0.55	0.16	0.19	0.1	0.08	0.33	0.10	0.10	0.06	0.05	0.04
LOW RATE		15.0	20.0	15.0	-	-	-	-	-	184.0	23.0	18.0	16.7	

* Data questionable - no known technique assures such accuracy
+ pH electrode questionable
pH, conductance and water temperature are field data

TABLE 6: WATER QUALITY DATA - JEMEZ RIVER AT BATTLESHIP ROCK

JEMEZ RIVER AT BATTLESHIP ROCK		AUGUST 79	SEPTEMBER 79	OCTOBER 79	NOV. 79	DEC. 79	JAN. 80	FEB. 80	MARCH 80	MAY 80	JUNE 80	JULY 80	AUG. 80	SEPT. 80
BOD ₅ mg/l		--	--	--	<0.02	<0.02	<0.02	<0.02	--	2.4	2.0	2.7	1.6	
As "		<0.02	--	--	--	--	--	<0.02	0.02	0.01	<0.01	<0.01	0.03	
Ba "		--	--	--	--	--	--	<0.02	0.5	2.0	--	0.01	0.03	<0.01
Hg "		<0.00011*	<0.000011*	0.000114*	0.00042*	<0.00001*	<0.00001*	<0.0001	0.00001*	<0.001	<0.001	<0.001	<0.001	<0.001
NO ₃ f		0.55	0.02	0.003	0.5	0.6	0.9	0.47	0.06	0.07	0.07	0.02	0.02	<0.01
B "		0.72	0.9	1.0	0.51	1.06	0.66	0.86	0.83	0.18	0.60	0.68	0.74	0.63
HCO ₃		61.0	61.7	69.0	73.0	62.0	58.0	66.4	60.6	35.7	76.2	77.5	84.6	89.6
Ca		7.8	3.8	5.0	4.2	3.5	11.2	13.0	21.6	12.0	12.0	14.0	14.0	0.14
Cl		16.4	4.4	4.4	6.2	5.2	6.0	12.0	6.2	3.0	1.0	2.0	6.0	4.0
Fe (diss.)		<0.02	<0.02	0.09	0.02	<0.02	<0.02	0.23	0.02	0.9	0.06	0.07	0.13	0.14
Mg "		1.0	8.2	2.1	2.2	1.5	2.0	2.2	3.1	1.6	1.2	1.10	2.30	1.8
K "		2.4	2.6	0.2	2.1	2.3	3.1	3.2	2.1	2.8	1.9	2.4	2.4	2.1
Na "		13.6	17.8	15.2	19.1	17.5	17.3	24.0	24.9	8.0	9.5	12.0	15.0	11.3
SO ₄		11.0	9.5	10.0	8.0	14.0	16.0	15.0	17.0	11.0	7.0	0.8	3.0	<0.1
pH		6.4+	7.0	6.8	7.6	--	--	7.4	7.5	7.5	7.2	6.9	7.9	
Dissolved con- ductance		120.0	110.0	85.0	90.0	--	88.0	90.0	120.0	61.0	122.0	148.0	140.0	
Temp °C		17°C	18°C	9°C	3.5°C	--	0°C	4°C	8°C	7°C	18°C	19°C	18°C	
PO ₄ mg/l		0.14	0.13	0.45	0.16	0.2	0.08	0.06	0.01	0.09	0.10	0.05	0.04	0.10
FLOW RATE		36.0	30.0	24.0	--	--	--	--	--	305.0	44.0	50.0	27.0	

* Data questionable - no known technique assures such accuracy
+ pH electrode questionable
pH, conductance and water temperature are field data

TABLE 7: WATER QUALITY DATA - EAST FORK OF JEMEZ

EAST FORK OF JEMEZ		AUGUST 79	SEPTEMBER 79	OCTOBER 79	NOV. 79	DEC. 79	JAN. 80	FEB. 80	MARCH 80	APRIL 80	JUNE 80	JULY 80	AUG. 80	SEPT. 80
BOD ₅ mg/l		--	--	--	--	<0.02	<0.02	<0.02	--	1.0	4.2	8.0	1.5	1.1
As "		<0.02	<0.02	<0.02	<0.02	<0.02	<0.02	<0.02	<0.02	0.04	0.01	0.01	0.02	0.02
Ba "		--	--	--	--	--	--	--	3.0	--	0.1	0.04	<0.01	0.02
Hg "		0.00018*	0.00001*	0.00026	<0.00001*	0.00001*	<0.00001*	<0.00001*	<0.0001	<0.0001	<0.001	<0.001	<0.001	<0.001
NO ₃		0.47	0.032	0.006	0.006	0.006	0.006	0.006	0.5	0.03	0.01	0.02	0.03	<0.01
f "		0.67	0.85	0.79	0.79	0.79	0.79	0.79	0.23	0.18	0.43	0.20	0.52	0.44
B "		0.02	0.9	0.02	0.02	0.02	0.02	0.02	0.7	0.12	0.09	.05	<0.01	0.15
HCO ₃		44.1	37.8	41.0	41.0	47.2	47.2	45.9	35.7	47.5	40.1	52.3	52.3	52.3
Ca "		4.3	2.5	4.0	4.0	2.3	2.3	17.6	9.4	7.1	8.0	6.3	8.7	8.7
Cl "		17.8	3.0	9.2	9.2	4.2	4.2	7.6	5.0	1.5	0.4	1.0	1.0	1.0
Fe (diss.)		<0.02	<0.02	<0.02	<0.02	<0.02	<0.02	3.0	0.75	0.06	0.17	0.29	0.27	0.27
Mg "		0.9	1.0	1.0	1.0	0.72	0.72	2.2	1.3	1.20	1.1	1.1	1.0	1.0
K "		1.8	2.4	1.8	1.8	2.1	2.1	4.6	1.9	1.4	1.7	1.5	1.6	1.6
Na "		10.4	9.4	9.3	9.3	11.5	11.5	21.6	4.5	9.5	6.4	11.0	6.8	6.8
SO ₄		7.0	4.5	55.0	55.0	8.0	8.0	8.0	2.0	<0.1	<0.1	<0.1	<0.1	<0.1
pH		5.8+	6.4	7.8	7.8	6.0	6.0	7.6	7.4	7.3	7.1	7.1	7.6	7.6
Dissolved con- ductance		90.0	40.0	50.0	50.0	65.00	65.00	58.0	48.0	70.0	78.0	70.0	70.0	70.0
Temp °C		18°C	10°C	8°C	8°C	1°C	1°C	-1°C	16°C	16°C	18°C	14°C	14°C	14°C
PO ₄ mg/l		0.3	0.11	0.20	0.20	0.17	0.17	0.1	0.10	0.10	0.02	0.02	0.02	0.02
LOW RATE		23.0	20.0	20.0	20.0	-	-	-	-	-	112.0	24.0	18.0	14.0

- * Data questionable - no known technique assures such accuracy
+ pH electrode questionable
pH, conductance and water temperature are field data

SURFACE WATER MONITORING DATA

REDONDO CREEK

WATER YEAR 1979-1980

SURFACE WATER MONITORING DATA, REDONDO CREEK

WATER YEAR 1979-1980

The Redondo Creek water quality monitoring station is located about 1.5 miles downstream from the Baca project. The station consists of a steel Parshall measuring flume with a 30" throat, 24" depth and a listed 23.94 cfs capacity maximum set into the creek bed. A shelter covers the flume and its attached stilling well to protect monitoring equipment from temperature extremes and weather. The station cannot be held at constant temperature or humidity. A butane heater and a backup electric heater prevent the recorders from freezing. Flow rate, pH and water temperature are recorded continuously at the station from the stilling well. Flow increase triggers collection of up to 28 aliquots directly from Redondo Creek. A field technician is required to ensure that all equipment is functioning and that collected samples are processed in a timely manner. The instruments are checked at least once each week, charts are collected and transported to Union's Rio Rancho office each Friday.

Flow is recorded on a Stevens type F meter with an 8 day hand wind clock, 5" float, 1.2" per day time scale and a 1:1 English gauge scale. The Stevens recorder was selected because of its long history of durability and dependability under field operating conditions.

Selection of a field operable pH/temperature recorder required extensive research. Temperature and pH are recorded by an Analytical Model 30 AC pH/temperature recording meter with ranges of 2-12 pH, 0°-50°C. The instrument carries an automatic temperature compensation, gear train set for 1/4" per hour and is run by electric hook-up. Although Analytical Instruments are a relatively new firm, this instrument appeared to have the sturdiness necessary for field conditions that other instrumentation lacked without exorbitant cost.

A Barton temperature meter with a 7 day hand wind clock and a range of 0-100°F serves as a backup for the Analytical instrument. There is no backup pH recording unit.

Samples of water from Redondo Creek are collected automatically by an ISCO Model 2100 Sampler. Samples are collected by a peristaltic pump with a self purging mode between sample collections and a precollection wash mode. ISCO is run by direct electric hook-up but may be battery operated. ISCO is set to collect samples during increased flow only and to shut off after flow has decreased. It is capable of collecting up to 28 sequential samples of predetermined volume at predetermined frequency. Considerable variation in trigger levels and collection frequency have occurred over the year; to be discussed later.

SURFACE WATER MONITORING DATA
REDONDO CREEK
WATER YEAR 1979-1980

2.

DISCUSSION

The Parshall flume was installed into Redondo Creek August 14, 1979. The instrument stand was installed over the stilling basin and the shelter built by August 24, 1980. On August 24th the Stevens flow meter and ISCO were installed. ISCO was run by battery. The Analytical temperature meter had not yet been purchased. pH and temperature were collected at the site as frequently as a technician was present. A flow rate was measured regularly to calibrate the readings from the flume. The Analytical meter was installed November 30, 1979 when electricity was available to the water shelter. From that time ISCO was also run by electricity. The instruments are calibrated with field measurements regularly. The station has been fully operational since December 1, 1979.

Data is collected on continuous graph charts that must be tabulated. Table 1 has hourly averages of water temperature and pH from December 1, 1979 through September 30, 1980. Blank spaces following a value for pH or temperature indicate that no change occurred. Sections of the table that reflect periods where no data were collected are marked "no data". Loss of data usually occurred because of improper placement of the paper roll in the instrument. Additional admonishment of field technicians resulted in a decrease in the frequency of this type of loss. Data loss for the period from May 29 to July 30, 1980 resulted from periods when a local electric company was working on wires in the area, which resulted in power surges or cutoffs to the water station. ISCO was set to battery operate during the problem period but the Analytical meter had to be shut off. Contiguously, a short in the Analytical pH probe cable was discovered and the cable had to be replaced. Data was lost from August 1 to August 8, 1980. Additional probes have been purchased to eliminate future problems.

The Barton temperature meter collected temperature data for part of the time the Analytical meter was down. Barton data from June 26 through July 31, 1980 and from August 1 through August 8, 1980 may be found in Table 2. ($^{\circ}\text{F}$ have been converted to $^{\circ}\text{C}$.)

Flow data may be found in Tables 3 and 4. Table 3 lists daily average flows after the style of USGS Water Resources data for New Mexico. Possible explanation for certain flow changes have been listed. Those days for which data are not available are marked by a blank space. Data was usually lost because a technician was not available to change charts as frequently as necessary. Additional technicians have been trained in monitoring the water station to prevent such losses in the future.

Figures 1 thru 14 graph hourly water temperature, pH and flow available with ambient temperatures and precipitation data collected 1.5 miles above Redondo Station. Blanks in graphs indicate no data.

SURFACE WATER MONITORING DATA
REDONDO CREEK
WATER YEAR 1979-1980

3.

Table 4 indicates hourly flow changes in Redondo Creek. Total daily flow change is recorded as an activity index (sum of changes without regard to sign x 100). The activity index pinpoints those days of peak activity. Field notes and the station log can be checked or interviews of field personnel conducted to determine the cause of activity. Activity during June through October can usually be traced to precipitation in Redondo Canyon. Data from the 200' MET tower rain gauge have not been compared to flow data for analysis. Activity November through February/March are typically caused in early mornings by ice buildup below the station and in mid-day by snow melt. Sunny days all winter produced runoff from south facing slopes. Beginning in March through June spring runoff produced very large activity indexes due to almost hourly flow changes.

The magnitude of fluctuations in flow due to runoff caused problems with setting the ISCO sampler.

The ISCO is triggered by a transducer placed above ambient water level. As water touches the transducer an electric impulse triggers the sampler to begin collecting. As water subsides, the trigger stops the sampler. Frequency of collection is determined by a clock inside the sampler.

The trigger was set during the winter months at a point about .05 feet above the stream on the flume scale. During periods of runoff, the trigger and timer were moved regularly in an attempt to be sensitive to flow increases without being overly sensitive. ISCO sample collections are indicated on Table 4.

Representative aliquots were regularly selected from the sampler and analyzed for the following constituents:

TDS	(mg/l)
TSS	(mg/l)
pH	
Conductivity	$\mu\text{mhos}/\text{cm}$
SO_4	(mg/l)
C1	"
B	"
Br	"
As	"
Hg	"
Si	"

Grab samples were taken from Redondo Creek between periods of peak flow in an attempt to characterize Redondo's waters. Table 6 lists the constituents tested for in samples and values for each. ISCO samples are indicated by an ISCO # in the table. If no number is present, the values represent a grab sample collected at Redondo Station. Possible reasons ISCO was triggered are listed below specific samples.

SURFACE WATER MONITORING DATA
REDONDO CREEK
WATER YEAR 1979-1980

4.

The only convenient way to ensure that potential samples from a geo-thermal spill are collected during periods of runoff would be to set a series of samplers with triggers set at increasing distances above base flow. A single sampler may be set so it is filled before such a spill would reach it, or that samples might not be collected from a small spill.

Ensuring against the first case with a single sampler would require a full time 24 hour surveillance. Ensuring against the second case could produce the first case.

During spring runoff for 1980, the field technician regularly checked the ISCO no more than once a week. The sampler frequently was full and out of operation for over half a week at a time. Increasing the number of sample bottles available and training additional staff should prevent such problems in 1981. A laboratory will be available in Redondo Canyon from spring 1981 so that ISCO sample bottles may be cleaned on site. Turbidity measurements could also be made of samples on site.

The majority of problems with data collection at the Redondo Creek Station are technician related. The work supports only a part time position which limits the availability of personnel. Initially, the technician in charge of the WSSI air quality MET towers was to check the water station. Problems arose when the technician was called away frequently without notifying supervisors that the water station would not be monitored.

It was decided to hire a technician to strictly work with the water station and collect monthly water shed samples. The technician selected was a UNM student who had several years experience collecting water samples.

Problems again arose from periods when the technician was not available to monitor the station when charts required change. Two additional people have, therefore, been hired to monitor the station on a more regular basis. Both persons work at other activities in the vicinity of the water station. Since the additional personnel have been acquired, data loss is expected to drop significantly.

CONCLUSION

Since the Redondo Creek Station has been operational all equipment at the station has had some down time, but generally equipment has operated satisfactorily for the first year. The companies selling equipment, with the exception of Beckman, have been helpful and have provided speedy assistance when necessary.

SURFACE WATER MONITORING DATA
REDONDO CREEK
WATER YEAR 1979-1980

5.

The major problems with operating the water station relate to the difficulty of finding a qualified technician to monitor the station daily. Two technicians are presently monitoring the station. One checks the instruments nearly daily. A second is available to bring samples to Albuquerque.

The thorniest problem with the collection of data is the setting of the ISCO sampler so that critical samples are not missed.

The water budget for 1980 was overrun. Analysis of ISCO samples accounted for about 1/3 of the total cost of water analysis. Runoff water has been sufficiently analyzed so that analysis of few ISCO samples should be necessary for 1981.

The critical questions that water samples should clarify are whether flow increase in Redondo Creek carries geothermal water, and secondly whether runoff is carrying an increased salt load over time. Silt load changes in Redondo Creek should also be monitored. A technique that samples all increased flows, allowing for analysis of any sample, has yet to be successfully worked out.

TABLE 1: REDONDO CREEK pH/WATER TEMPERATURE (T_i) ($^{\circ}\text{C}$)

DECEMBER 1 - 15, '79

TABLE I (CONT'D):

pH/WATER TEMPERATURE (T) (°C)

DECEMBER 16 - 31 '79

? FLOW ↑

TABLE 1 (CONT'D):

REDONDO CREEK

JANUARY 1 - 15, '80

TIME	DATE:	1	2	3	4	5	6	7	8	9	10	11	12	13	14	15	
		pH	T	pH	T	pH	T	pH	T	pH	T	pH	T	pH	T	pH	T
0000		6.8	3.0	6.9	3.0	6.8	2.0	6.9	2.6	6.8	2.6	6.8	2.8	6.9	3.0	6.8	2.2
01																2.9	
02																2.8	2.3
03																2.7	
0400																	
05																2.6	2.4
06																2.5	2.5
07																	
0800																2.4	2.6
09																	
10																2.3	
11																	
1200																2.2	6.9
13																	
14																	
15																	
1600																6.8	2.7
17																	
18																2.8	
19																	
2000																	
21																2.9	
22																7.0	3.1
23																	3.2
MEAN		6.9	3.0	6.9	2.5	6.8	2.0	6.8	2.3	6.9	2.6	6.8	2.6	6.9	2.6	6.9	3.0
H1		6.9	"	6.9	"	6.9	2.6	"	"	"	2.7	6.9	3.0	"	6.9	2.9	7.0
L0		6.8	"	6.8	"	6.8	2.0	"	"	"	2.6	6.8	2.8	"	6.8	2.2	6.9
RANGE		.1	0	.1 (1.0)	0	.1	0	0	0	0	.1	0	0	.1	.1	.1	.1

JANUARY 16 - 31 '80

DATE:	REDONDO CREEK												PH/WATER TEMPERATURE (T) (OC)																		
	16		17		18		19		20		21		22		23		24		25		26		27		28		29		30		31
TIME	pH	T	pH	T	pH	T	pH	T	pH	T	pH	T	pH	T	pH	T	pH	T	pH	T	pH	T	pH	T	pH	T	pH	T			
0000	7.0	3.3	7.0	3.0	7.0	3.0	7.0	2.8	7.0	3.0	7.1	3.0	7.0	2.0	7.0	2.0	7.2	2.0	7.1	2.0	7.0	2.0	7.2	2.0	7.1	2.2	7.0	2.0			
01																															
02																															
03																															
0400																															
05																															
06																															
07																															
0800																															
09																															
0																															
1																															
1200																															
13																															
14																															
15																															
1600																															
17																															
18																															
19																															
2000																															
21																															
22																															
23																															
MEAN	7.0	3.2	7.0	3.0	7.0	2.9	7.1	3.0	7.1	2.6	7.0	2.0	7.1	2.0	7.2	2.0	7.1	2.0	7.1	2.0	7.1	2.2	7.0	2.3							
HI	"	3.3	"	"	"	2.9	7.1	"	7.1	2.2	"	"	"	"	"	"	"	"	"	"	"	"	"	"	"	2.5					
LO	"	3.0	"	"	"	2.9	"	2.8	7.0	"	7.0	3.0	"	"	"	"	"	"	"	"	"	"	"	"	"	2.0					
RANGE	Ø	.3	Ø	Ø	Ø	.1	Ø	.1	Ø	.1	Ø	.1	Ø	.1	Ø	.1	Ø	.1	Ø	.1	Ø	.1	Ø	.1	.5	Ø	.2	Ø	Ø		

TABLE 1 (CONT'D):

pH/WATER TEMPERATURE (T) ($^{\circ}\text{C}$)

FEBRUARY 1 - 15, '80

DATE:	1			2			3			4			5			6			7			8			9			10			11			12			13			14			15		
	pH	T	pH	T																																									
1/0000	7.2	2.5	7.1	2.5	7.0	2.0	7.1	2.5	7.2	3.0	7.1	2.2	7.0	2.0	7.0	2.2	7.1	2.8	7.1	2.0	7.0	1.5	7.1	2.0	7.1	2.0	7.0	2.0	7.0	2.0															
1/01																																													
1/02																																													
1/03																																													
1/0400																																													
1/05																																													
1/06																																													
1/07																																													
1/0800																																													
1/09																																													
1/10																																													
1/11																																													
1/1200																																													
1/13																																													
1/14																																													
1/15																																													
1/1600																																													
1/17																																													
1/18																																													
1/19																																													
1/2000																																													
1/21																																													
1/22																																													
1/23																																													
MEAN	7.2	2.5	7.1	2.3	7.0	2.0	7.1	2.3	7.1	2.0	7.2	2.6	7.1	2.2	7.0	2.1	7.0	2.5	7.1	2.4	7.1	1.6	7.0	1.4	7.1	1.8	7.1	2.0	7.1	2.0															
"	"	"	7.1	2.5	"	7.2	3.0	"	3.0	"	2.5	"	2.2	"	2.2	"	2.8	"	2.8	"	2.8	"	2.0	"	1.5	7.1	2.0	"	"	"	"														
"	"	"	7.0	2.0	"	2.0	2.5	"	2.5	"	2.1	"	2.0	"	2.0	"	2.0	"	2.0	"	2.0	"	1.2	7.0	1.5	"	"	"	"	"	"														
"	"	"	0	.1	"	.5	0	.5	0	.5	0	.8	0	.1	0	.2	0	.1	0	.6	0	.8	0	.1	0	.5	0	.3	0	.1	0	0													

FEBRUARY 16 - 29 '80

TABLE 1 (CONT'D): REDONDO CREEK pH/WATER TEMPERATURE (T) (°C)

TABLE 1 (CONT'D) REDONDO CREEK

TIME	DATE:	PH/WATER TEMPERATURE (T) (OC)												MARCH 1 - 15, '80															
		1	2	3	4	5	6	7 *	8	9	10	11	12	13 *	14	15	pH	T											
0000	01	6.8	2.5	6.8	2.5	6.8	2.5	6.8	2.5	6.8	3.0	7.1	3.0	7.4	3.0	(8.4)	3.0	7.2	3.0	7.6	3.0	7.6	3.0	7.8	2.6	7.8	2.6	7.3	3.0
0100	02																												
0200	03																												
0300	04																												
0400	05																												
0500	06																												
0600	07																												
0700	08																												
0800	09																												
0900	10																												
1000	11																												
1100	12																												
1200	13																												
1300	14																												
1400	15																												
1500	16																												
1600	17																												
1700	18																												
1800	19																												
1900	20																												
2000	21																												
2100	22																												
2200	23																												

* CALIB.
7 MAR.
1500* CALIB.
13 MAR.{ 7.0 @ 0730 } FLOW
{ 7.0 @ 1400 } FLUX
{ 7.0 @ 1930 }
{ 7.2 @ 0830 }

TABLE 1 (CONT'D): BEDONDO CREEK pH/WATER TEMPERATURE (T) ($^{\circ}\text{C}$)

TIME	DATE:	16	17	18	19	20	21	22	23	24	25	26	27	28	29	30	31			
		pH	T	pH	T	pH	T	pH	T	pH	T	pH	T	pH	T	pH	T	pH	T	
0000		7.8	3.0	7.6	3.0	7.6	2.8	7.6	2.8	7.4	3.0	7.4	3.0	7.3	3.5	7.2	3.0	7.2	3.0	
01																				
02																				
03																				
0400																				
05																				
06																				
07																				
0800																				
09																				
10																				
11																				
1200																				
13																				
14																				
15																				
1600																				
17																				
18																				
19																				
2000																				
21																				
22																				
23																				
MEAN		7.7	3.0	7.6	2.5	7.6	2.8	7.5	2.8	7.4	3.0	7.3	3.3	7.3	3.5	7.2	3.0	7.2	3.0	
MIN		7.8	"	7.6	3.0	"	"	7.6	"	7.4	5.0	"	3.5	7.3	"	3.5	"	"	"	
MAX		7.7	"	7.5	2.0	"	"	7.4	"	7.0	3.0	"	3.0	7.2	"	3.0	"	"	"	
RANGE		.1	0	.1	(1.0)	0	0	0.2	0	0	(.4)	(2.0)	0	.5	1	0	0	0	0	

TABLE 1 (CONT'D): REDONDO CREEK

PH/WATER TEMPERATURE (T) (°C)

APRIL 1 - 15, '80

DATE:	1*	2*	3	4	5*	6	7	8	9	10	11	12	13	14	15	
TIME	pH	T	pH	T	pH	T	pH	T	pH	T	pH	T	pH	T	pH	
0000	7.2	3.0	7.2	2.0			7.1	3.8	7.7	4.0	7.6	4.0	7.5	4.0	7.1	
01							7.6	3.9	3.9						3.0	
02							3.8	7.5	3.8				7.4	3.9	7.1	
03							3.7		3.6	7.4	3.7				4.0	
0400							3.6		3.4	7.3	3.6		3.9		3.8	
05							3.5		3.2			3.5			3.7	
06							3.0				3.4				3.6	
07									7.2		3.2		3.7			
0800										3.0		3.6		7.1	3.5	
09										3.1				7.3		
10										3.2						
11										7.5	3.5					
1200										3.4	7.4	3.6		7.2	3.4	
13										3.5		3.8		3.1		
14										3.6	4.0		3.2(7.6)(6.0)			
15										1st *	3.8	7.3		3.3		
1600										READING @ 1730	4.0	(7.9) 4.5	3.8	7.1	3.4	5.9
17											7.1	4.0 (7.8) 4.5	7.1	4.0	3.5	5.1
18											4.4	7.7 4.3	7.0	3.6	4.8	
19											4.2	7.6 4.1	3.8	4.5		
2000											4.0	4.0	3.9	7.1	4.0	4.3
21											3.9	7.7	3.8		4.2	
22											3.8		3.6		4.1	
23														7.5	4.0	3.1
MEAN	7.2	2.0	7.2	2.0	NO	NO	7.1	3.9	7.1	3.9	7.6	3.7	7.4	4.1	7.3	4.6
HIGH	"	3.0	"	"	CHART	CHART	"	4.0	7.8	4.5	7.9	4.5	7.6	4.0	7.6	6.0
LOW	"	"	"	"	IN	IN	"	3.8	7.1	3.4	7.3	3.0	7.1	3.6	7.2	"
RANGE	Ø	(2.0)	Ø	Ø	RECODER	RECODER	Ø	(.7)(1.1)	(.6)(1.5)	.5	.4	(.5)(2.4)	.2	(1.0)	.3	.9

ICE
BUILD-UP

NEW TAPE FLOW

* END OF TAPE 2 APR
FLOW

?

* START NEW TAPE FLOW

APRIL 16 - 30 '80

TABLE 1 (CONT'D): REDONDO GREEK pH/WATER TEMPERATURE (T) ($^{\circ}\text{C}$)

DATE:	16			17			18			19			20			21			22			23			24 *			25			26			27			28			29			30		
	pH	T	pH	T	pH	T	pH	T	pH	T	pH	T	pH	T	pH	T	pH	T	pH	T	pH	T	pH	T	pH	T																			
	7.5	4.2	7.4	4.0	7.4	4.5	7.4	4.0	7.3	4.0	6.9	4.0	6.8	4.0	6.8	4.6	6.8	5.0	6.7	4.4	7.2	4.0	7.3	4.6	7.5	4.6	7.6	5.0	7.5	5.0	7.5	5.0													
	7.4	4.1					3.9	7.2			3.9																																		
	4.0		7.3				3.8				3.8																																		
	7.3						7.3	3.7	7.1		3.6																																		
							7.2	4.4	7.2	3.6	3.9		3.2																																
	7.2						7.1			3.4	3.8	3.0																																	
							7.3			7.0		3.2	3.7																																
	7.1									3.0	7.0	3.6																																	
							3.9	7.2		4.3	7.1		3.5																																
	7.0	3.8					4.2			3.4																																			
							3.7			4.1		3.2																																	
	3.6	7.1	3.9							3.0																																			
							7.0	3.8	4.0	7.0																																			
										3.4	3.5	6.8	3.3																																
										(4.0)	4.0	(4.0)																																	
										4.4	4.5	4.5																																	
										4.8	4.8	5.0																																	
										4.0	4.1	5.0	5.0																																
										(5.0)	4.0	(7.4)(5.0)	(6.0)	(6.0)	6.0	4.1																													
										(7.4)	5.6	(5.0)	(6.0)	(7.2)	6.5	(7.0)	5.5	4.2	4.7	4.3																									
											5.4	7.1		7.3		6.5	5.0	4.4	4.8	6.7	4.4																								
											5.0	7.2	4.9	5.5	6.0		6.0																												
											4.2	7.3	4.8	(4.5)	5.5	5.5	4.3	4.6	5.0																										
											4.1	7.4	4.6	4.0	4.5	(4.5)	4.1																												
											7.3	4.6	7.2	4.4	7.2	5.0	7.1	5.0	6.8	4.3	6.8	4.3	6.8	4.3	6.8	4.3	7.1	4.2	7.3	4.3	7.4	4.5	7.6	4.5	7.5	5.0									
											7.5	5.6	7.4	5.0	7.4	6.0	7.4	6.5	7.3	7.0	6.9	6.0	"	4.6	"	5.0	(11.7)5.0	7.4	4.4	7.4	4.6	7.5	4.8	7.8	4.9	7.6	"	7.7	"						
											7.0	3.6	7.0	3.8	7.0	4.0	7.0	3.0	6.9	3.0	6.8	3.0	"	4.0	"	4.6	6.7	4.3	6.7	4.0	7.2	4.0	7.3	4.2	7.5	4.0	7.4	"	7.2	"					
											(1.5)	(2.0)	(1.2)	.4	(2.0)	.4	(3.5)	.4	(4.0)	.1	(3.0)	.6	Ø	(5.0)	.7	(7.7)	.4	.2	.6	.2	.6	.3	.9	.2	.6	.3	.9	.2	.6	.3	.9	.2	.6		

MAY 1 - 15 '80

TABLE 1 (CONT'D): REDONDO CREEK pH/WATER TEMPERATURE (T) ($^{\circ}\text{C}$)

RAIN, SLEET, SNOW →

MAY 16 - 31 '80

TABLE 1 (CONT'D): REDONDO CREEK

END OF
CONTINUITY
IN TAPE ?

CALIB.
PHG

TABLE 1 (CONT'D): REDONDO CREEK
pH/WATER TEMPERATURE (T) (°C)

TABLE 1 (CONT'D): REDONDO CREEK pH/WATER TEMPERATURE (T) ($^{\circ}\text{C}$)

TABLE 1 (CONT'D): REDONDO CREEK

pH/WATER TEMPERATURE (T) (°C)

AUG. 16 - 31 '80

TABLE I (CONT'D): REDONDO CREEK

PH/WATER TEMPERATURE (T) (°C)

SEPT. 1 - 15 '80

TIME	DATE:	1	2	3	4	5	6	7	8	9	10	11	12	13	14	15	
	pH	T	pH	T	pH	T	pH	T	pH	T	pH	T	pH	T	pH	T	
0000		7.3	12	7.2	12	7.3	12	7.0	13	7.1	13	7.2	12.5	7.0	12	7.0	12
01								7.2									
02								7.4									
03																	
0400																	
05																	
06																	
07																	
0800																	
09	START TAPE																
10		7.4	11														
11								7.2	7.2								
1200																	
13																	
14																	
15																	
1600																	
17																	
18																	
19																	
2000																	
21																	
22																	
2300																	
MEAN		7.3	11.5	7.3	11.5	7.3	12	7.2	12	7.1	12.5	7.2	12.5	7.0	12	7.0	11.5
H1		7.4	12	7.3	12	7.3	12	7.3	12.5	7.4	13	7.4	13	7.2	12.5	12.5	12
LO		7.2	11	7.2	11	7.2	12	7.1	12	7.0	12	6.9	12	12	11	11	11.5
RANGE		0.2	1.0	0.1	1.0	0.1	0.5	0.2	0.5	0.1	0.5	0.1	0.5	0.5	0.5	0.5	0.5

TABLE 1 (CONT'D): REDONDO CREEK pH/WATER TEMPERATURE (T) ($^{\circ}\text{C}$)

TABLE 2: REDONDO CREEK WATER TEMPERATURE - BARTON METER (CONVERTED TO °C)

TABLE 2 (CONT'D)

WATER TEMPERATURE - BARTON METER (CONVERTED TO °C)

TABLE 2 (CONT'D): RECONDITO CREEK
WATER TEMPERATURE - BUOYON METER (CONVERTED TO 8°C)

AUG. '20

TABLE 3: REDONDO CREEK

AVERAGE DAILY FLOW RATE (cfs)

	1	2	3	4	5	6	7	8	9	10	11	12	13	14	15	16	17	18	19	20	21	22	23	24	25	26	27	28	29	30	31				
AUG. '79	2.0	1.9	1.8	1.9	1.8	1.7	1.8	2.0	2.0	2.0	2.0	2.0	2.0	2.0	2.0	2.0	2.0	2.0	2.0	2.0	2.0	2.0	2.0	2.0	2.0	1.9	1.8	1.7	1.7	1.8					
SEP. '79	1.2	1.2	1.2	1.2	1.2	1.2	1.2	1.2	1.2	1.2	1.2	1.2	1.2	1.2	1.2	1.2	1.2	1.2	1.2	1.2	1.2	1.2	1.2	1.2	1.2	1.2	1.2	1.2	1.2	1.2	1.2				
OCT. '79	1.6	1.6	1.55	1.6	1.6	1.6	1.6	1.6	1.6	1.6	1.6	1.6	1.6	1.6	1.6	1.6	1.6	1.6	1.6	1.6	1.6	1.6	1.6	1.6	1.6	1.6	1.6	1.6	1.6	1.6	1.6				
NOV. '79	1.9	1.6	1.6	1.6	1.6	1.6	1.6	1.6	1.6	1.6	1.6	1.6	1.6	1.6	1.6	1.6	1.6	1.6	1.6	1.6	1.6	1.6	1.6	1.6	1.6	1.6	1.6	1.6	1.6	1.6	1.6				
DEC. '79	1.9	1.6	1.6	1.6	1.52	1.56	1.56	1.56	1.56	1.56	1.56	1.56	1.56	1.56	1.56	1.56	1.56	1.56	1.56	1.56	1.56	1.56	1.56	1.56	1.56	1.56	1.56	1.56	1.56	1.56	1.56	1.56	1.56		
JAN. '80	1.9	1.9	2.9	1.9	1.9	1.9	1.9	1.9	1.9	1.9	1.9	1.9	1.9	1.9	1.9	1.9	1.9	1.9	1.9	1.9	1.9	1.9	1.9	1.9	1.9	1.9	1.9	1.9	1.9	1.9	1.9	1.9	1.9	1.9	1.9
FEB. '80	1.9	1.9	1.9	1.9	1.9	1.9	1.9	1.9	1.9	1.9	1.9	1.9	1.9	1.9	1.9	1.9	1.9	1.9	1.9	1.9	1.9	1.9	1.9	1.9	1.9	1.9	1.9	1.9	1.9	1.9	1.9	1.9	1.9	1.9	1.9
MAR. '80	3.4	3.4	3.4	3.4	3.4	3.4	3.4	3.4	3.4	3.4	3.4	3.4	3.4	3.4	3.4	3.4	3.4	3.4	3.4	3.4	3.4	3.4	3.4	3.4	3.4	3.4	3.4	3.4	3.4	3.4	3.4	3.4	3.4	3.4	3.4
APR. '80	5.7	3.4	3.4	3.4	4.5	5.7	6.8	7.8	7.8	7.8	7.8	7.8	7.8	7.8	7.8	7.8	7.8	7.8	7.8	7.8	7.8	7.8	7.8	7.8	7.8	7.8	7.8	7.8	7.8	7.8	7.8	7.8	7.8	7.8	7.8
MAY '80	22.4	20.9	20	20.6	21.8	22.4	23.5	25.0	24.5	24.5	24.5	24.5	24.5	24.5	24.5	24.5	24.5	24.5	24.5	24.5	24.5	24.5	24.5	24.5	24.5	24.5	24.5	24.5	24.5	24.5	24.5	24.5	24.5	24.5	
JUNE '80	15	15	14.8	14.6	14.2	14	14	13.3	12.4	11.6	11.0	10.8	10.5	10.3	10.3	10.3	10.3	10.3	10.3	10.3	10.3	10.3	10.3	10.3	10.3	10.3	10.3	10.3	10.3	10.3	10.3	10.3	10.3	10.3	
JULY '80	7.8	7.8	7.1	7.1	(6.4	5.7	5.1	4.5	3.9	3.9	3.9	3.9	3.9	3.9	3.9	3.9	3.9	3.9	3.9	3.9	3.9	3.9	3.9	3.9	3.9	3.9	3.9	3.9	3.9	3.9	3.9	3.9	3.9	3.9	3.9
AUG. '80	3.1	3.4	3.3	3.1	3.1	3.1	3.1	4.0	4.5	5.1	3.0	2.5	2.5	2.8	2.7	2.7	2.7	2.7	2.7	2.7	2.7	2.7	2.7	2.7	2.7	2.7	2.7	2.7	2.7	2.7	2.7	2.7	2.7	2.7	2.7
SEP. '80	2.3	2.3	1.9	1.7	1.7	1.7	1.8	1.8	1.8	1.9	2.0	2.0	2.0	2.0	2.0	2.0	2.0	2.0	2.0	2.0	2.0	2.0	2.0	2.0	2.0	2.0	2.0	2.0	2.0	2.0	2.0	2.0	2.0	2.0	2.0

*3 Based on
slope of
flume
readings** Thunder-
storms** "Heavy
thunder-
storm
upper
water-
shed"
RP** Thunder-
storm?*1 "Removed
stones
from
flume" RP
EMPTY SPACES INDICATE MISSING DATA

TABLE 4: REDONDO CREEK

GROSS FLOW FLUCTUATIONS NET CHANGES (FEET)

TABLE 4 (CONT'D): REDONDO CREEK

TABLE 4 (CONT'D): REDONDO CREEK

GROSS FLOW FLUCTUATIONS

ISCO TAKEN (X)

TABLE 4 (CONT'D): REDONDO CREEK

TABLE 4 (CONT'D): REDONDO CREEK

TABLE 4 (CONT'D): REDONDO GREEK GROSS FLOW FLUCTUATIONS
NET CHANGES (FEET)

TABLE 4 (CONT'D.): REDONDO CREEK

TABLE 4 (CONT'D): REDONDO CREEK GROSS FLOW
 NET CHANNEL

TABLE 4 (CONT'D): REDONDO CREEK

GROSS FLOW FLUCTUATIONS
NET. CHANGES (FEET)

TIME	DATE:	APRIL '80																														
		1	2	3	4	5	6	7	8	9	10	11	12	13	14	15	16	17	18	19	20	21	22	23	24	25	26	27	28	29	30	31
0000																																
01	+ .01																															
02	+ .02 - .01	- .01																														
03	+ .02																															
0400	+ .02	- .01																														
05	+ .02	- .01																														
06	+ .02 + .01																															
07	+ .02																															
0800	+ .02																															
09	- .03	+ .02																														
10	- .03	+ .02 - .01																														
11	+ .02																															
1200	- .05 + .01 + .02 - .03	+ .01																														
13	- .03																															
14	+ .02	- .01 + .01	+ .01																													
15	+ .02 + .01 + .01 + .01 + .02 + .02																															
1600	+ .01 + .01 + .01																															
17	+ .01																															
18																																
19		- .01 - .01																														
2000	- .01	- .01																														
21	- .01	- .01																														
22	- .02	- .01																														
23		- .01																														
ACTIVITY INDEX (Sum of Changes x 100)	(34) 3 (8) Ice build-up	(12) 4 (8) 3 (17) 5 (12) 3 4 4 (13) (6) (15) (10) (20) (16) (15) (18) Snow melt																														
ISCO TAKEN (X)		X																														

APPROX. 5 cm deep
stones have washed into
the stream at mea-
suring point RP

TABLE 4 (CONT'D): REDONDO CREEK

TIME	DATE:	GROSS FLOW FLUCTUATIONS NET CHANGES (FEET)												MAY '80																		
		1	2	3	4	5	6	7	8	9	10	11	12	13	14	15	16	17	18	19	20	21	22	23	24	25	26	27	28	29	30	31
0000																																
01																																
02																																
03																																
0400																																
05																																
06																																
07																																
0800																																
09																																
10																																
11																																
1200																																
13																																
14																																
15																																
1600																																
17																																
18																																
19																																
2000																																
21																																
22																																
23																																
ACTIVITY INDEX (Sum of Changes x 100)	1	3	2	4	0	3	(6)	1	(5)																							
ISCO TAKEN (X)		X																														

* Practice continuous monitoring into flume (nm)

X

(8) 4 0 0 1 1 3 2 2 2 2 3 (5) 1

X X X X

DRIVE STOPPED

+ .01 - .01 - .01

+ .01 - .01

- .01 + .01

+ .01

+ .01

+ .01

- .01 + .01

+ .01

- .01 + .01

+ .01

- .01 + .01

+ .01

- .01 + .01

+ .01

- .01 + .01

+ .01

- .01 + .01

+ .01

- .01 + .01

+ .01

- .01 + .01

+ .01

- .01 + .01

+ .01

+ .01

+ .01

+ .01

+ .01

+ .01

+ .01

+ .01

TABLE 4 (CONT'D): REDONDO CREEK

GROSS FLOW FLUCTUATIONS
NET CHANGES (FEET)

TIME	DATE:	1	2	3	4	5	6	7	8	9	10	11	12	13	14	15	16	17	18	19	20	21	22	23	24	25	26	27	28	29	30	31
0000																																
01																																
02																																
03																																
0400		+.01																														
05																																
06		+.01																														
07																																
0800																																
09		+.01																														
10																																
11																																
1200		-.01																														
13																																
14		-.01																														
15																																
1600		-.01	-.01	-.01	-.01	-.01	-.01	-.01	-.01	-.01	-.01	-.01	-.01	-.01	-.01	-.01	-.01	-.01	-.01	-.01	-.01	-.01	-.01	-.01	-.01	-.01	-.01	-.01	-.01			
17																																
18																																
19																																
2000																																
21																																
22																																
23		+.01																														
ACTIVITY INDEX (Sum of Changes x 100)	1	2	2	2	2	1	2	2	2	1	1	2	2	2	2	2	2	2	2	2	2	2	2	2	2	2	2	2	2	2		
ISCO TAKEN (X)												X	X																		X	

JUNE '80

TABLE 4 (CONT'D): REDONDO CREEK

TABLE 4 (CONT'D): REDONDO CREEK

FIGURE 1

union
GEOTHERMAL

AUGUST 1979

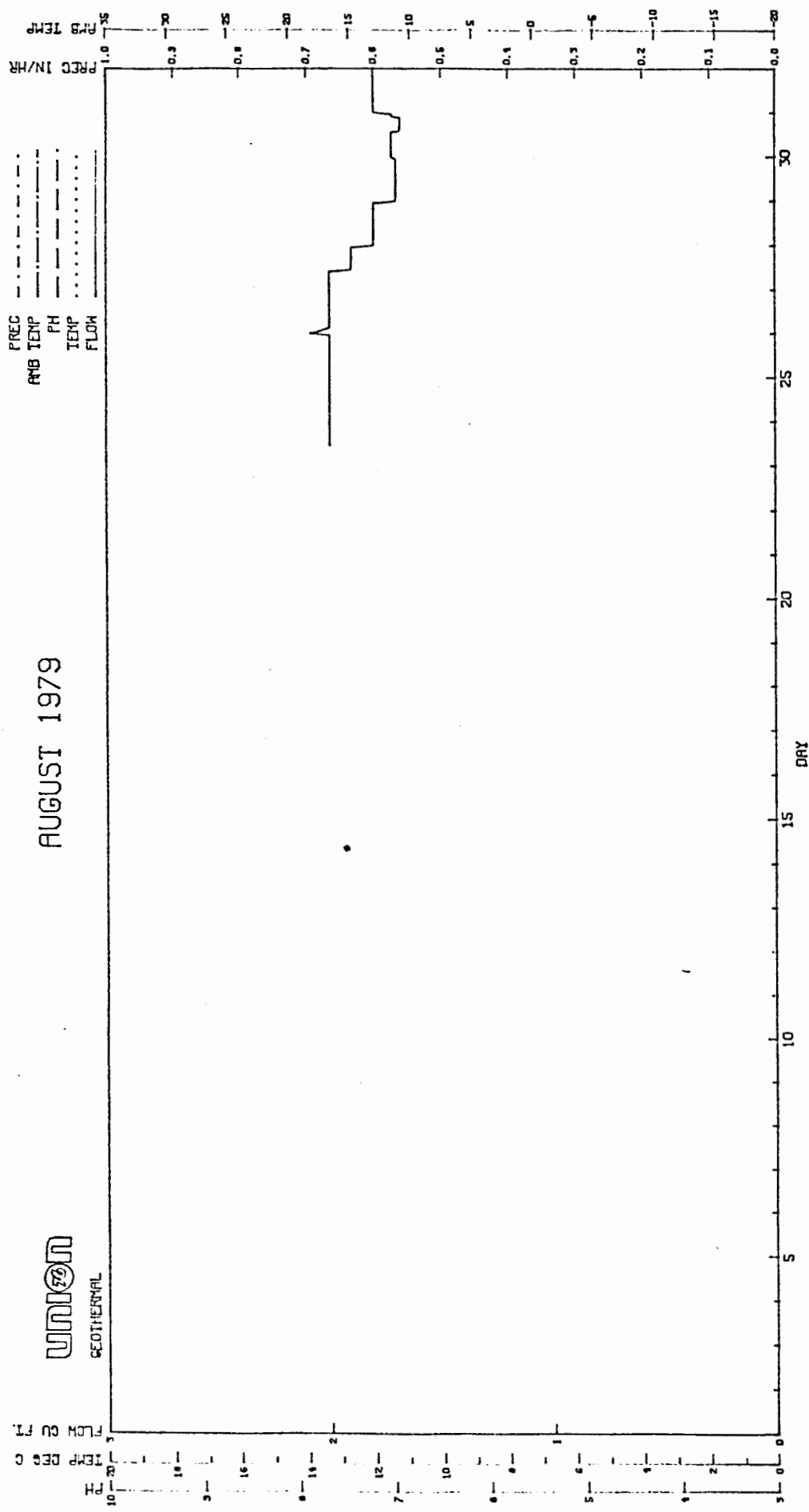


FIGURE 2

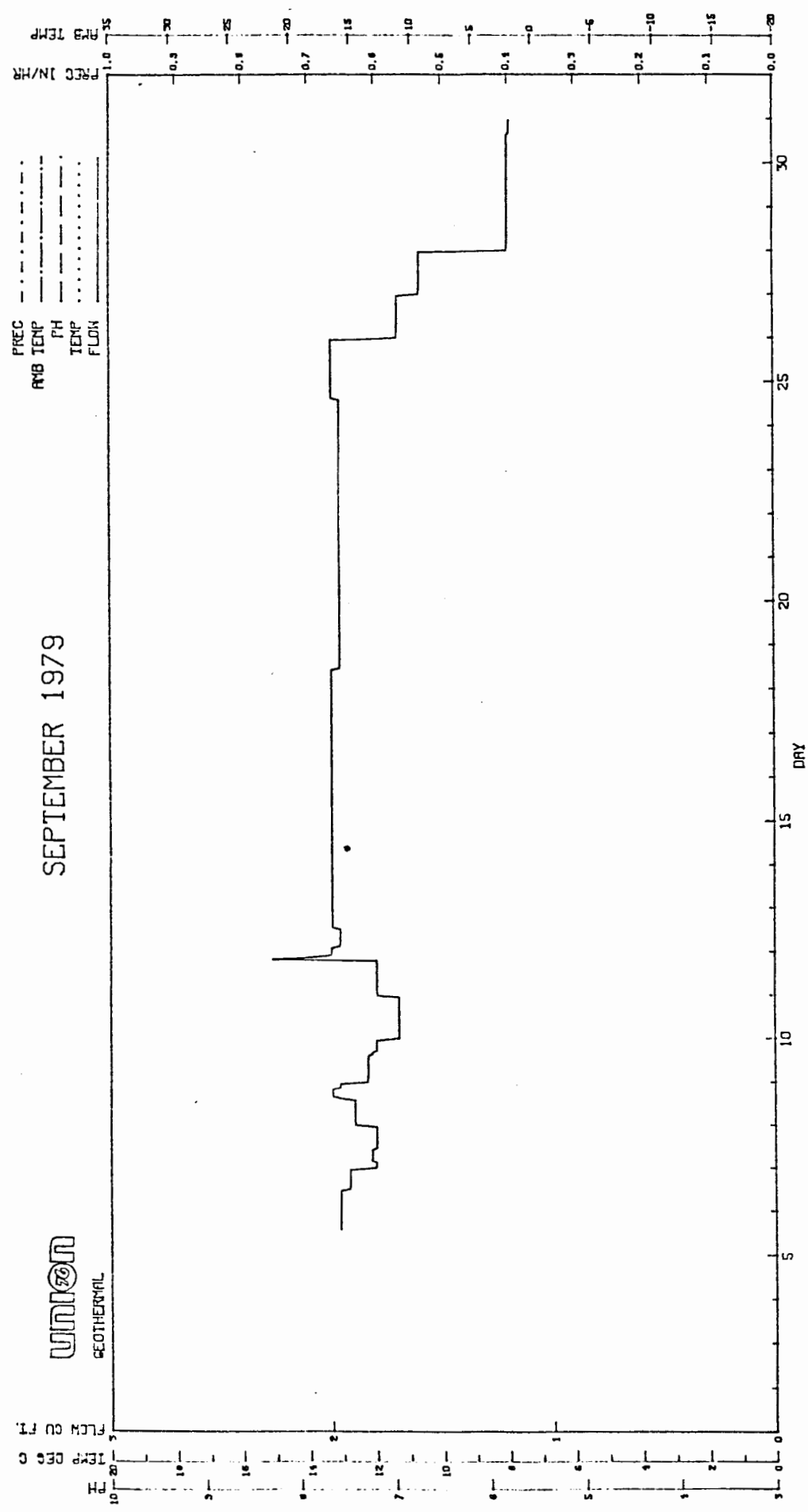


FIGURE 3

UNIVERSITY
OF MICHIGAN

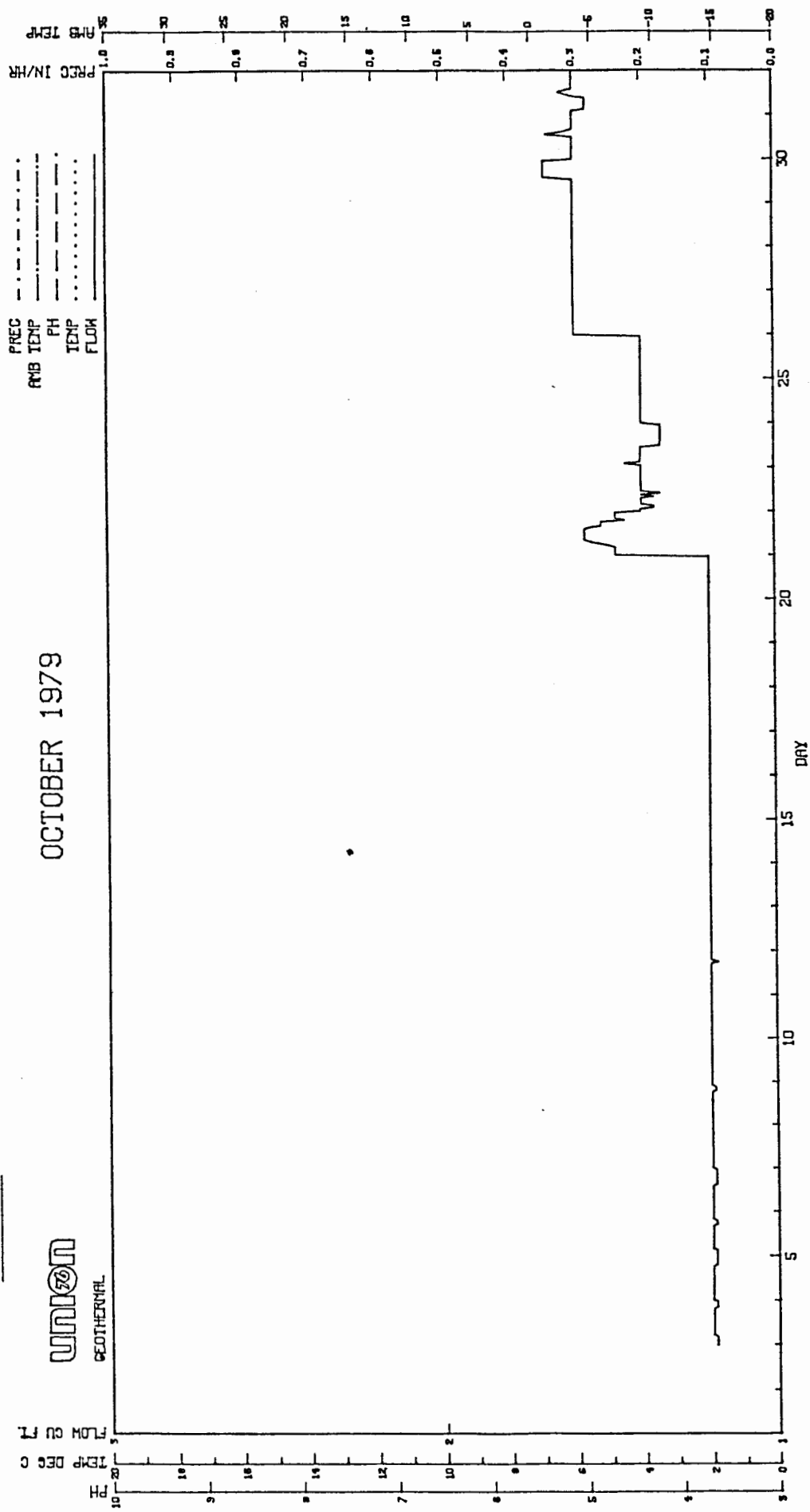


FIGURE 4

UNION
22
GEOGRAPHICAL

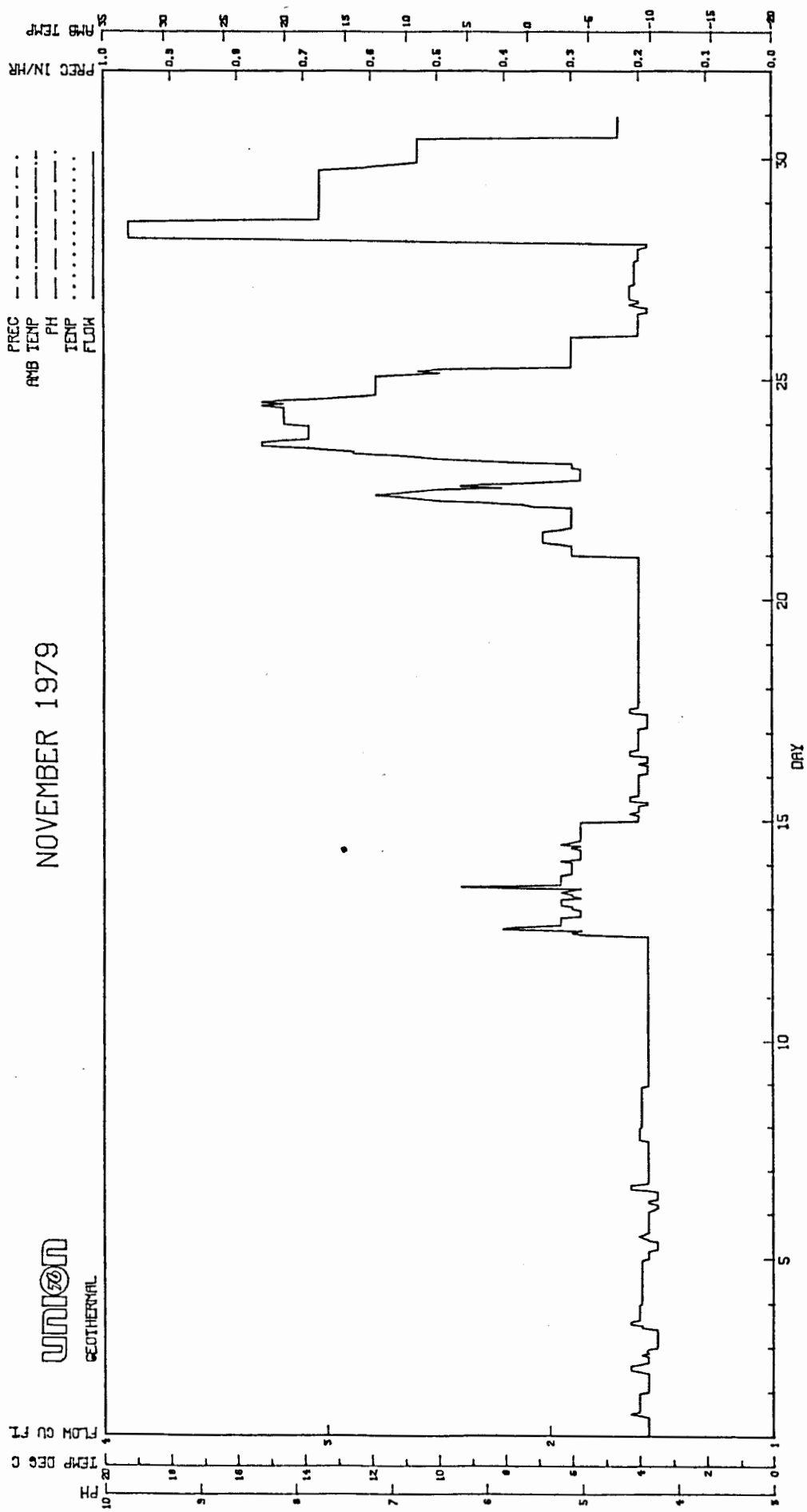


FIGURE 5

UNION
GEOOTHERMAL

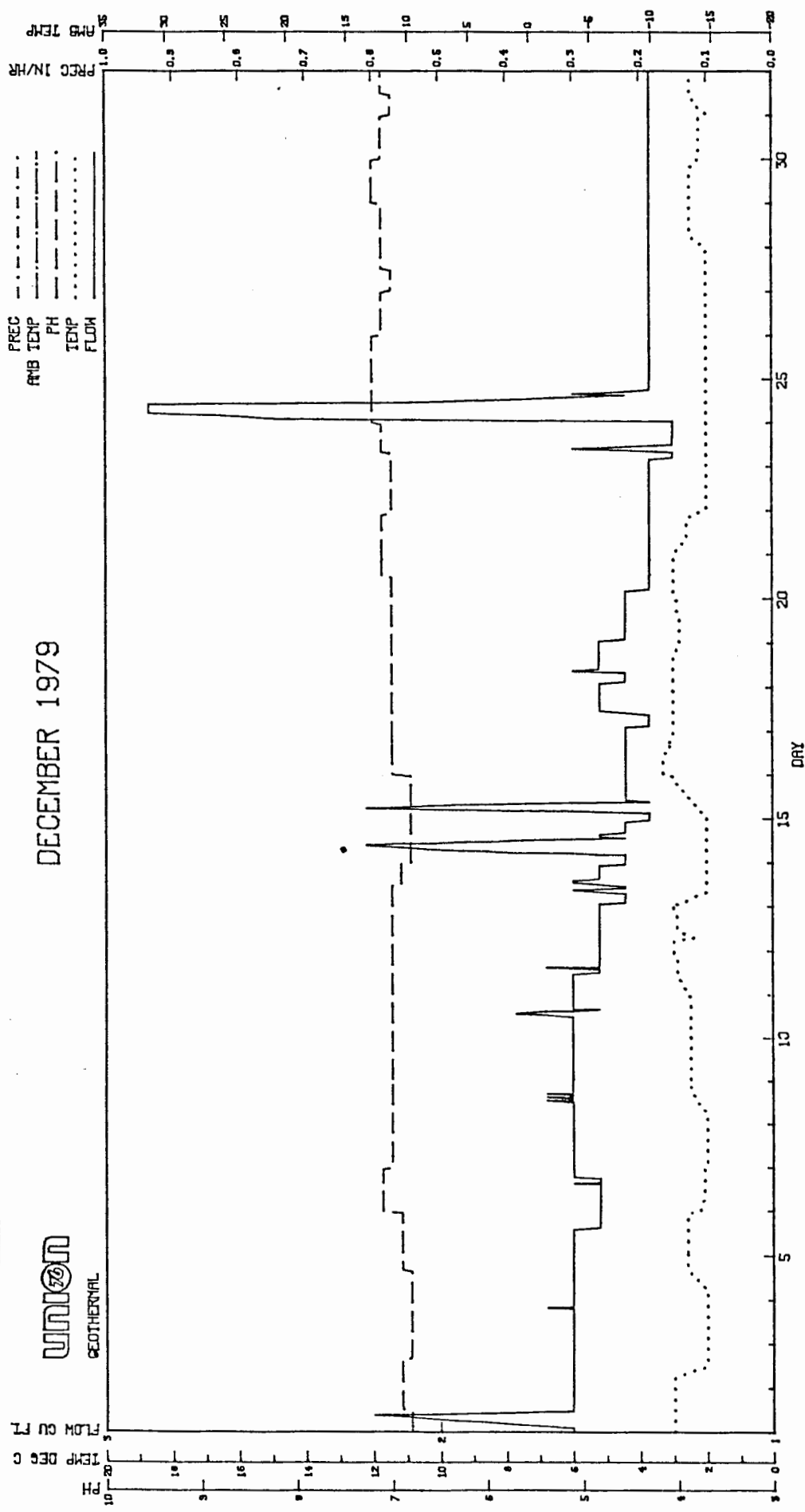


FIGURE 6

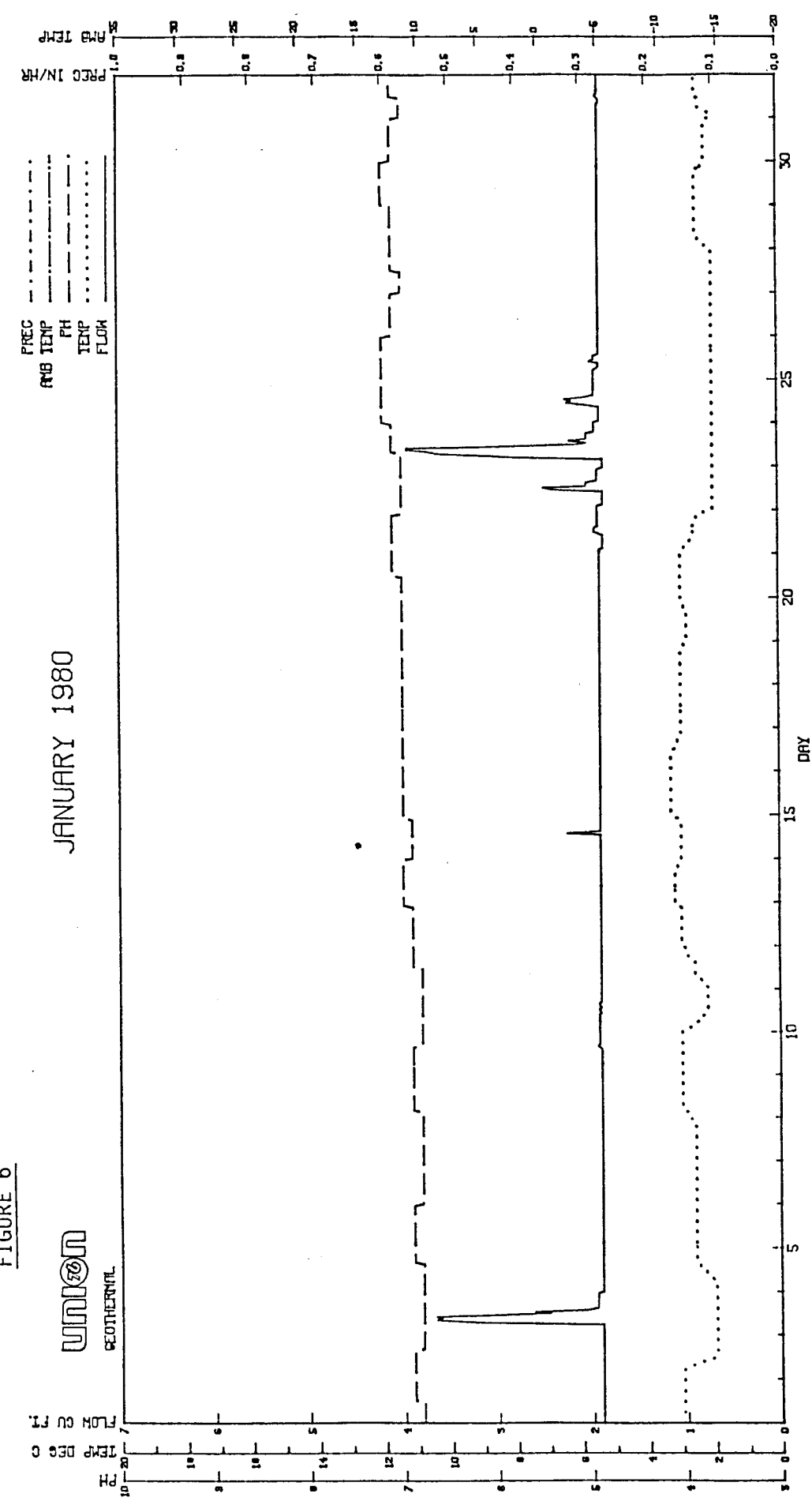


FIGURE 7

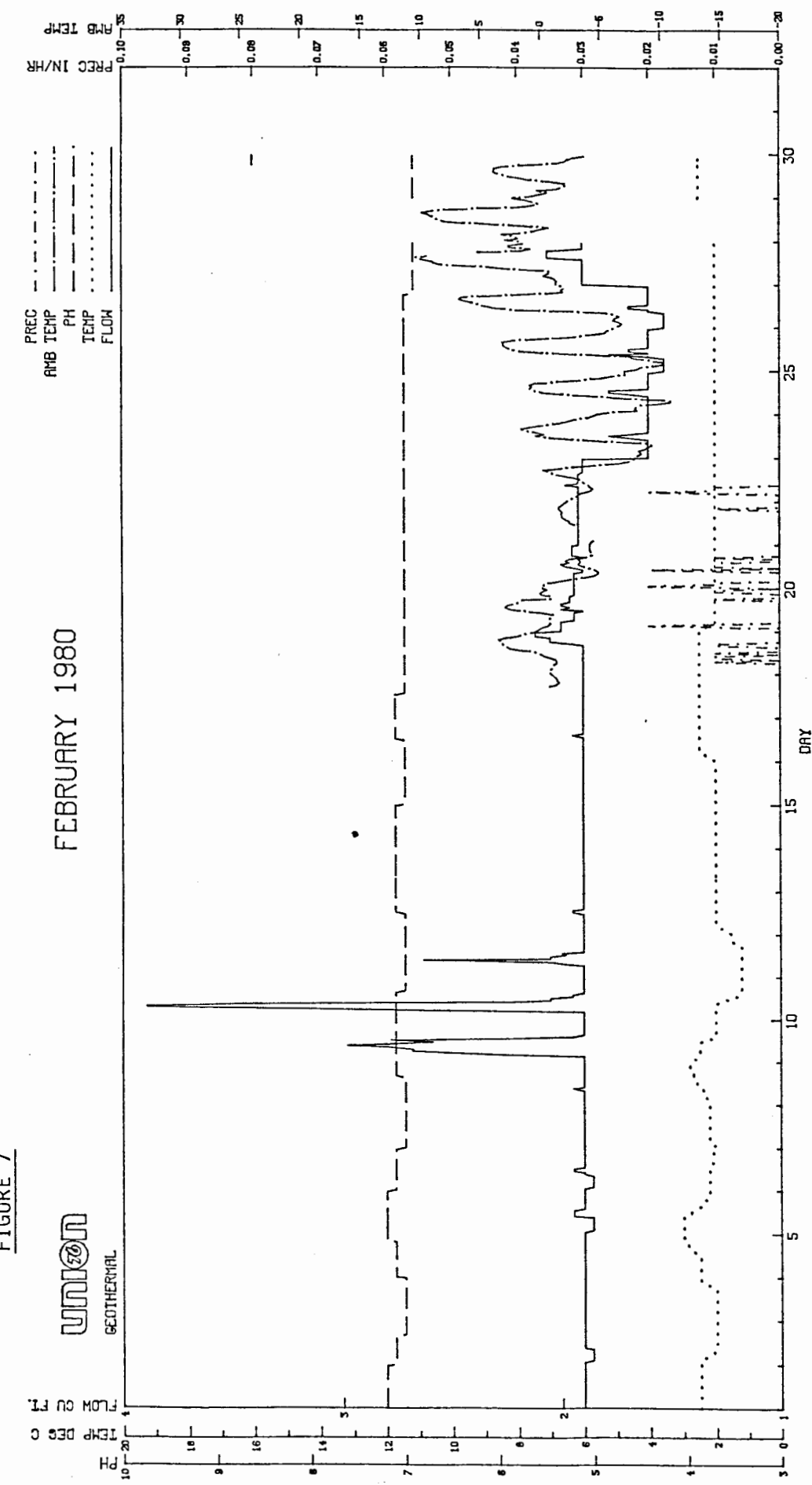


FIGURE 8

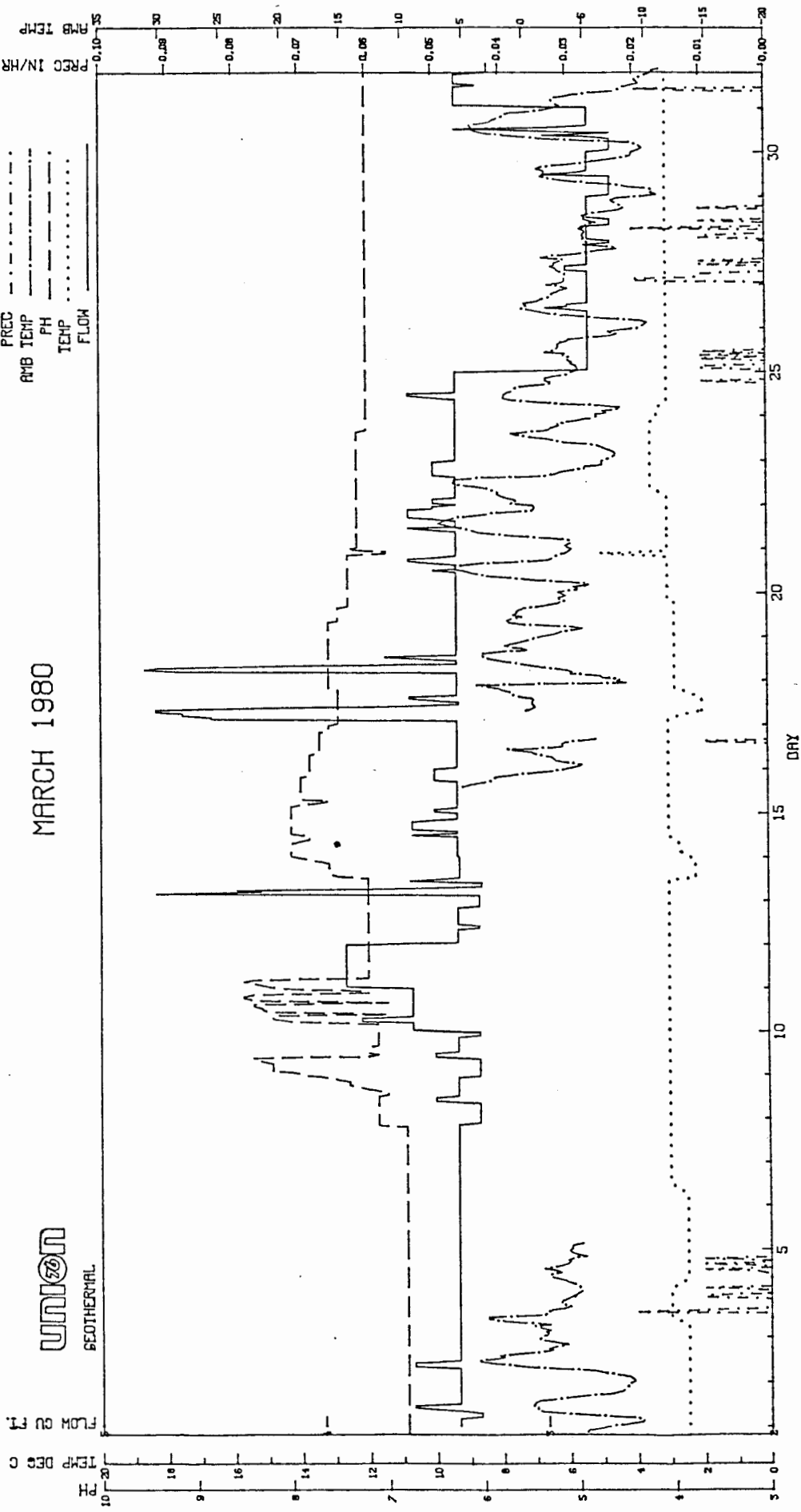


FIGURE 9

UNION
GEOHERMAL

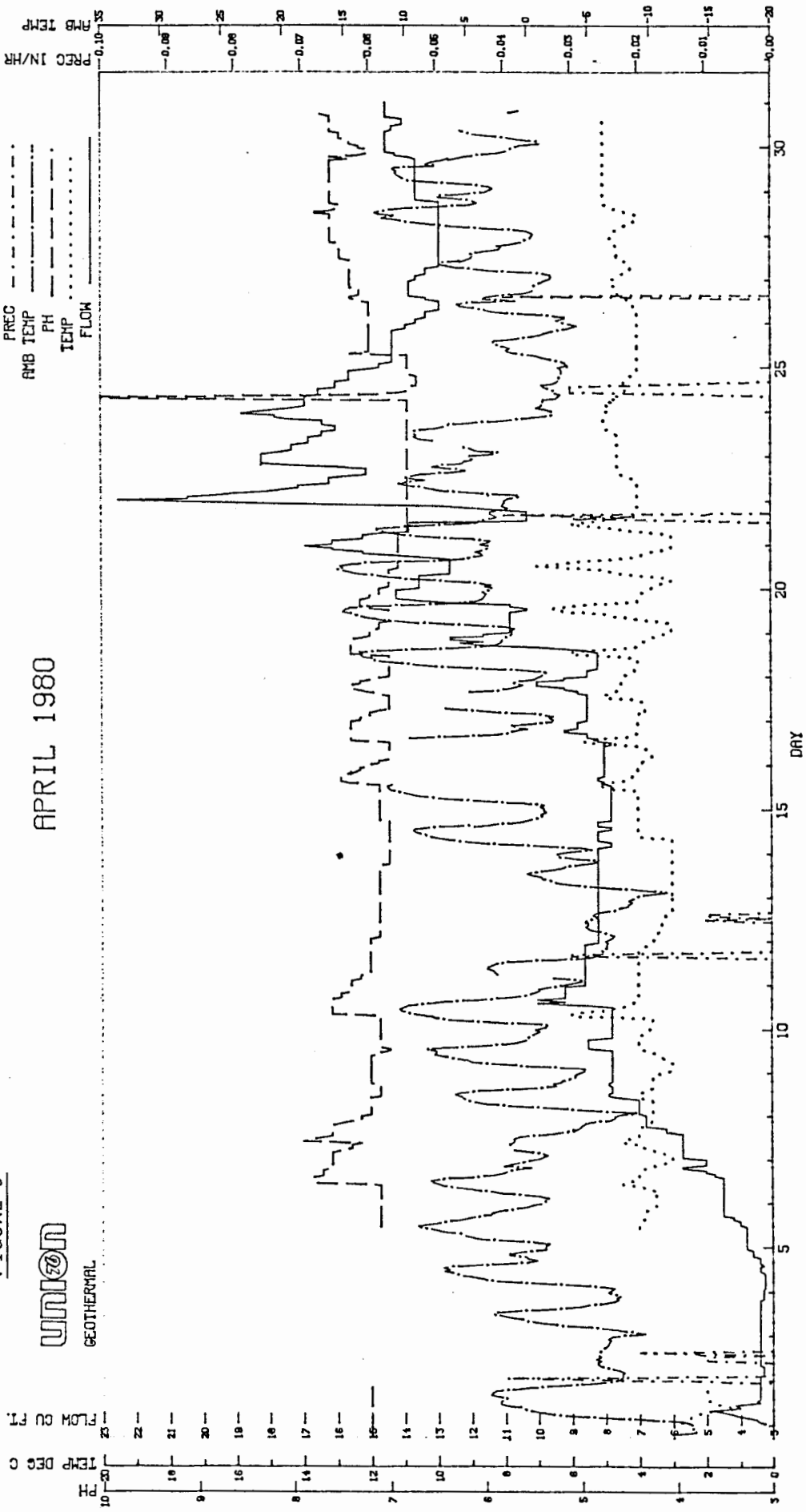


FIGURE 10

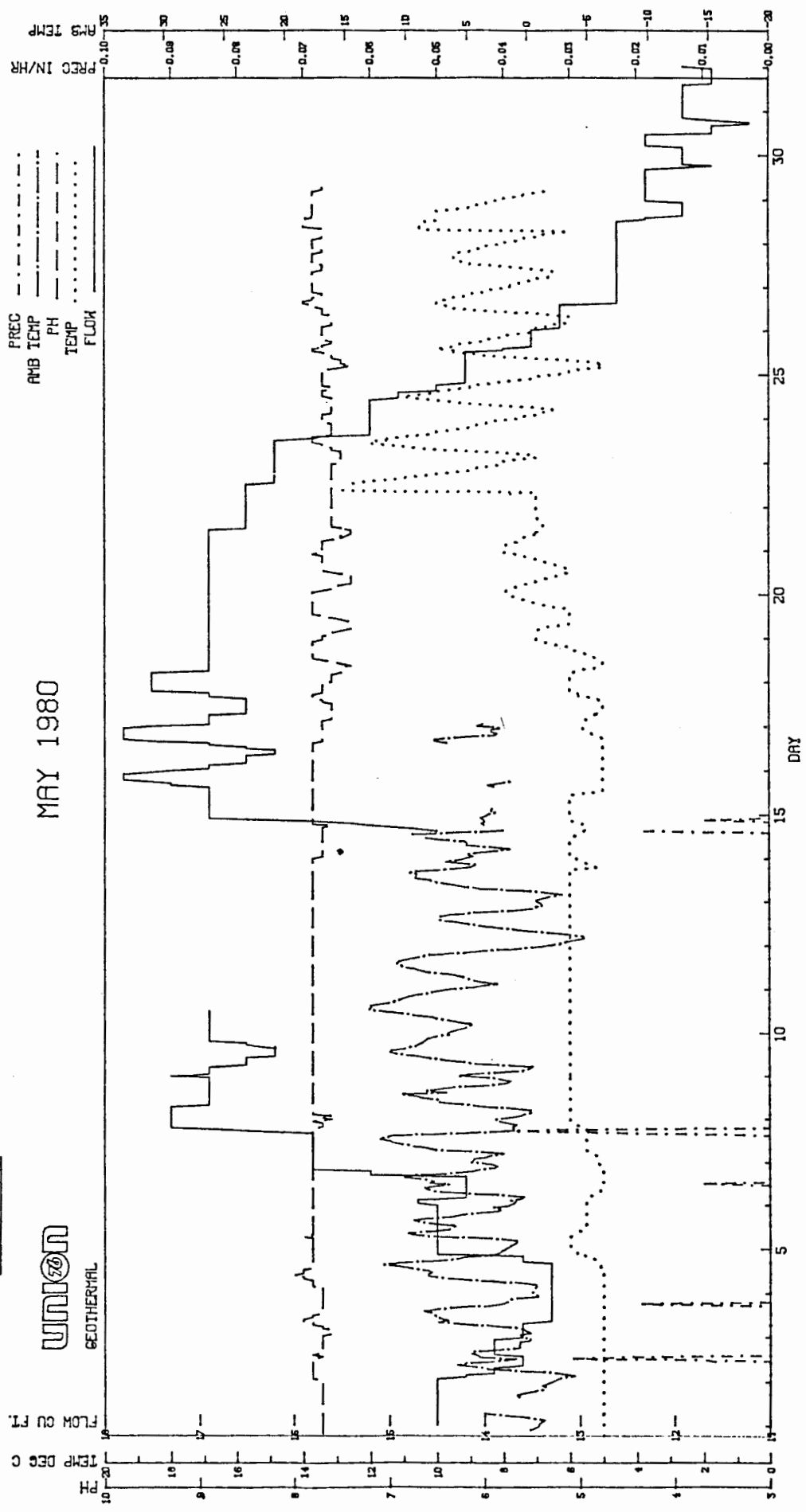
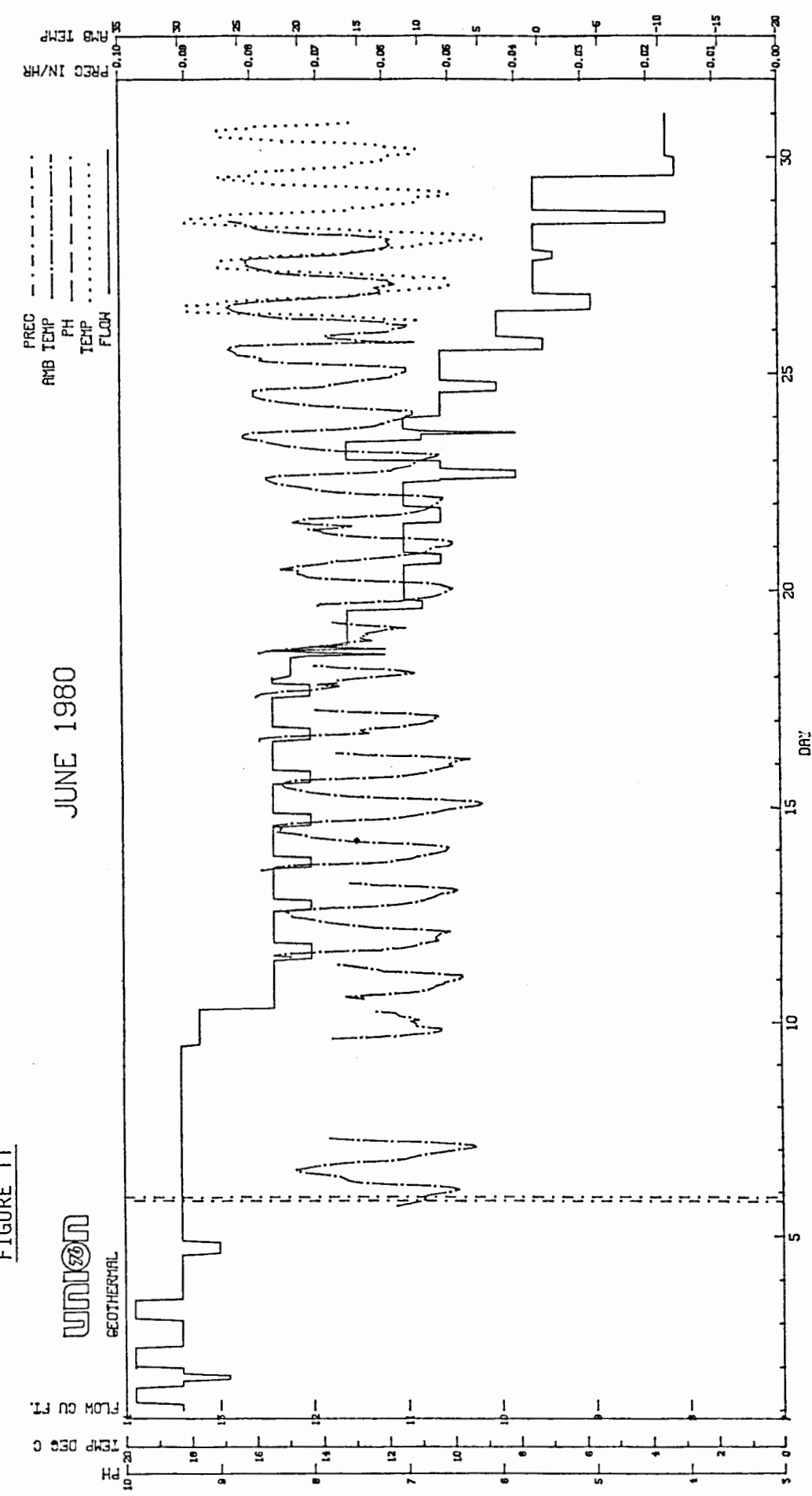


FIGURE 11



DATA LOGGED → 14:52 MT 13, 1980

FIGURE 12

union
GEO THERMAL

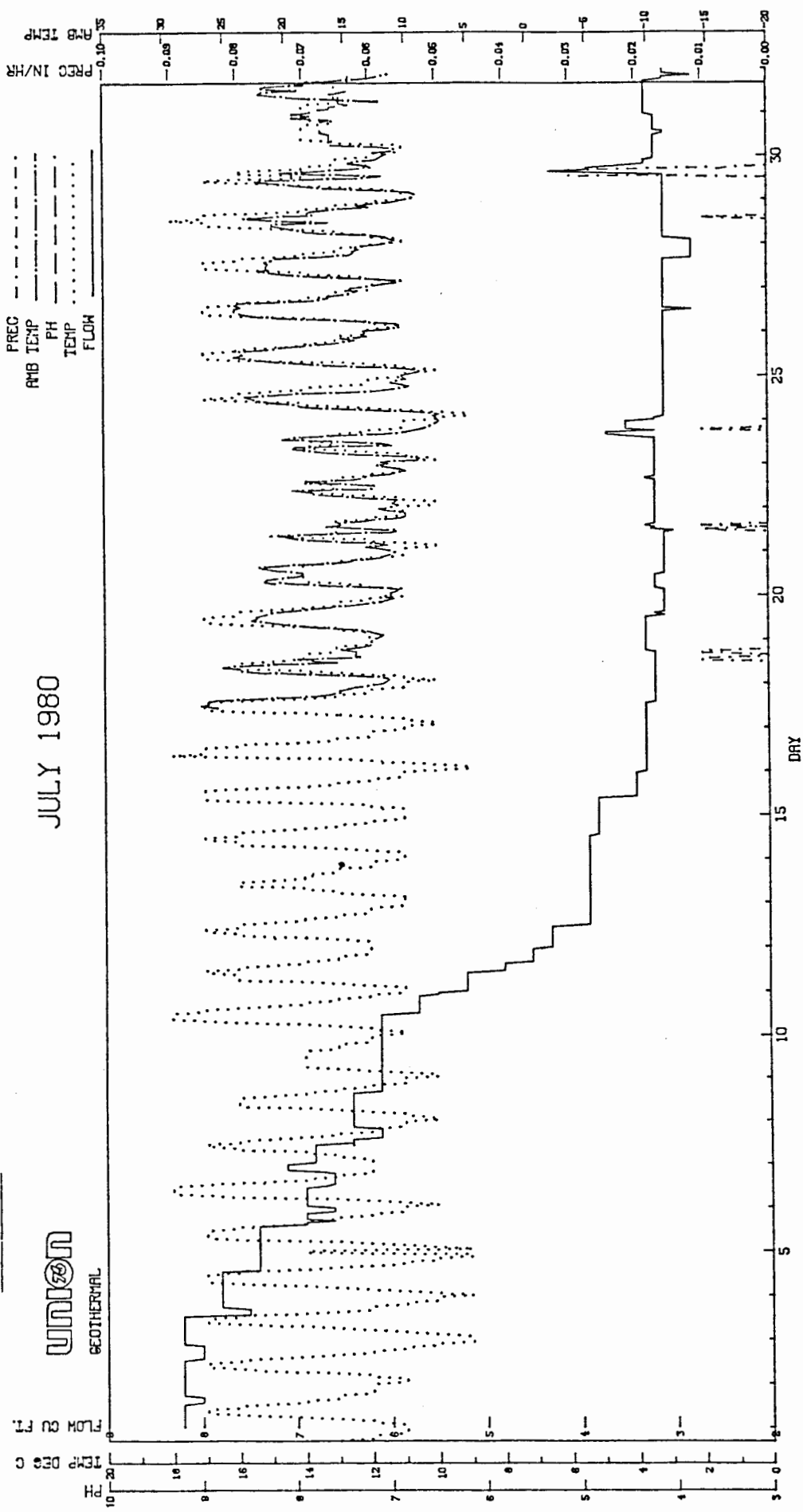


FIGURE 13

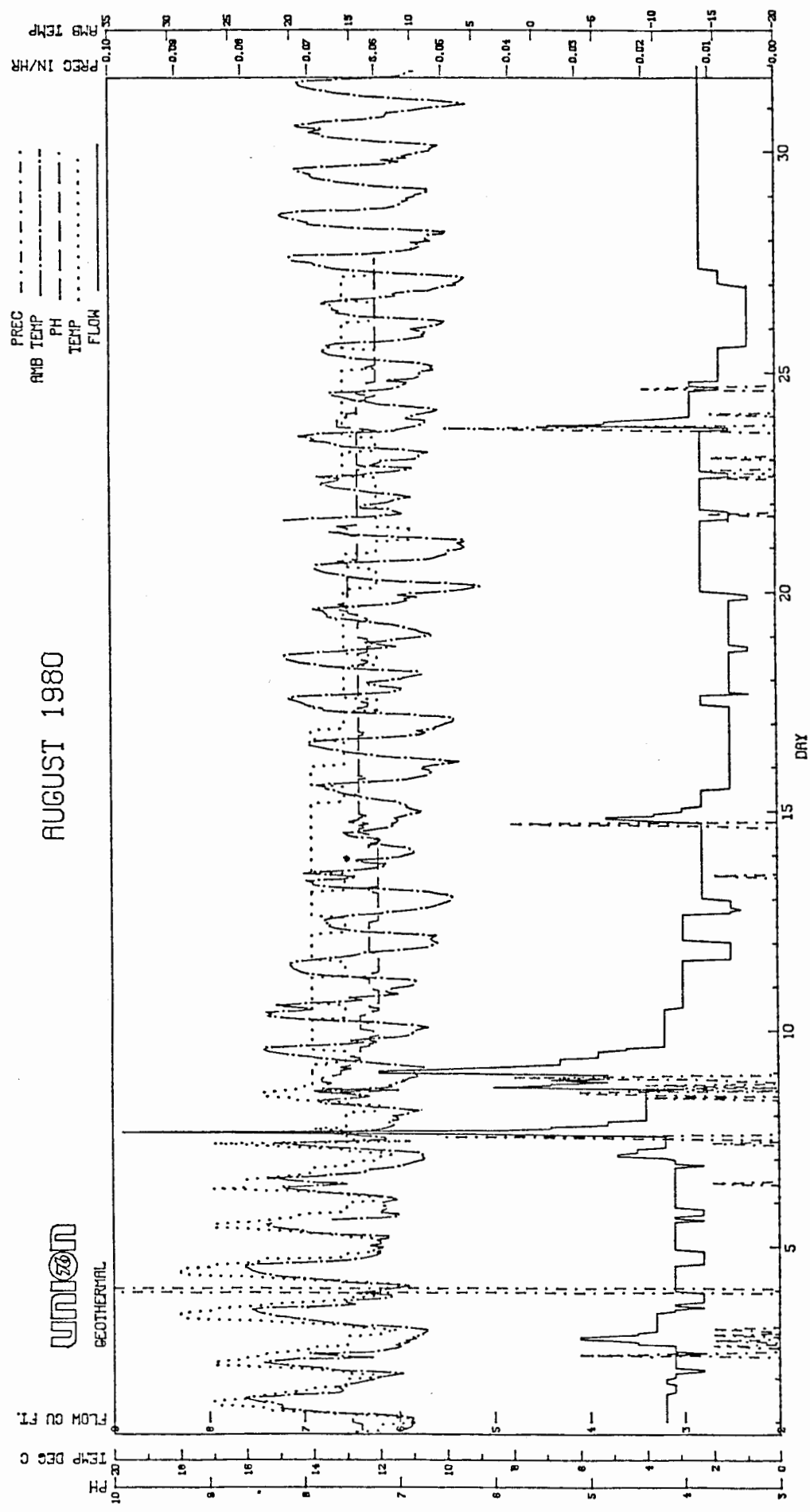


FIGURE 14

UNIL@N
GEOOTHERMAL

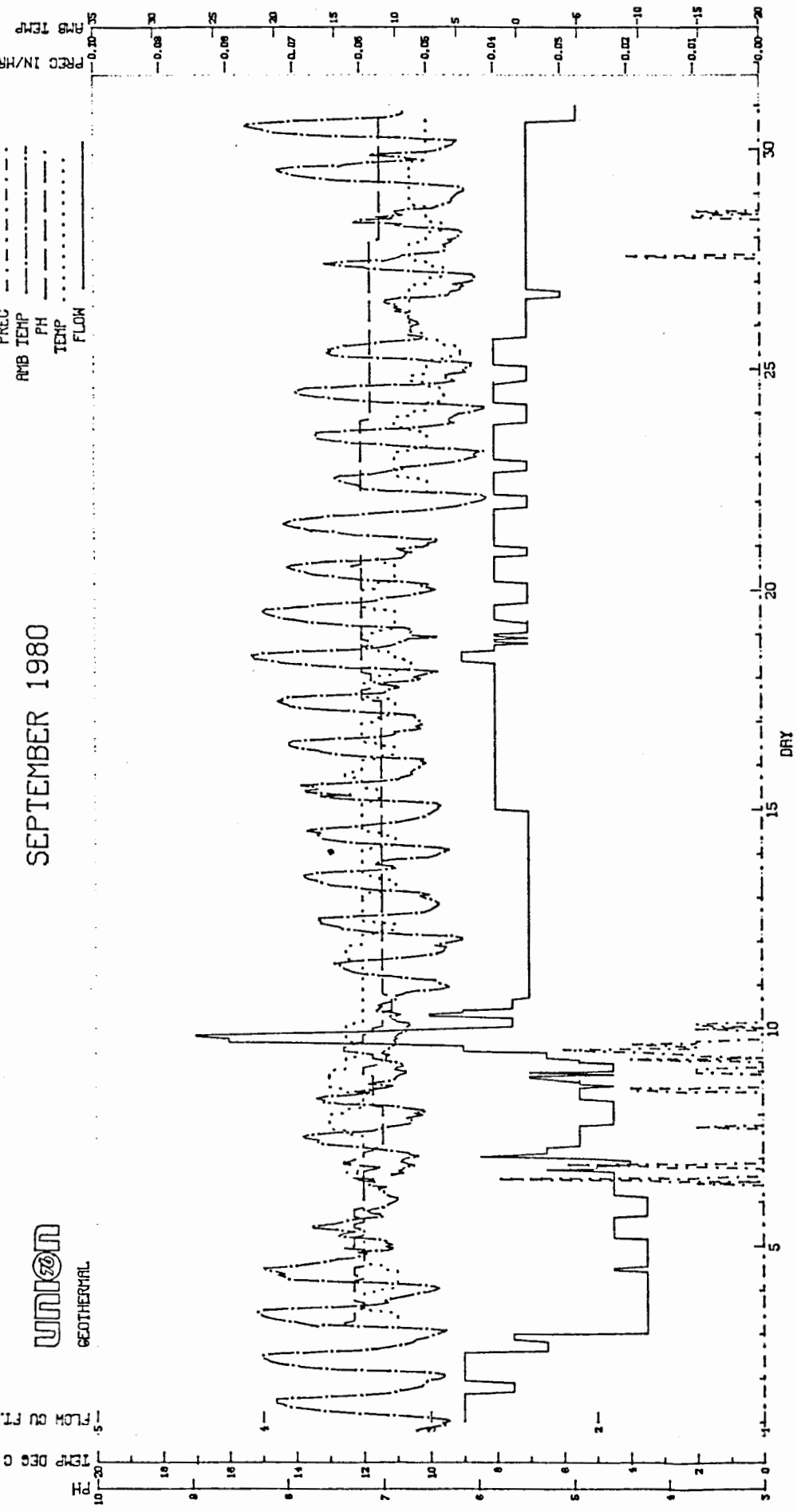


TABLE 5: REDONDO CREEK WATER QUALITY DATA

- data questionable - no known technique assures such accuracy
+ pH electrode questionable
pH, conductance and water temperature are field data

TABLE 6: SELECTED WATER SAMPLES COLLECTED FROM REDONDO CREEK
WATER YEAR 1979-1980

* IF NO ISCO / IS GIVEN WATER WAS COLLECTED BY HAND AT ISCO SITE.

TABLE 6 (cont'd)

TSS	18	25	21	22	2
TDS	179	109	141	105	117
I ¹³⁷ H	6.9	6.9	7.0	7.1	7.6
μ hos	103	103	102	101	86
B	.08	.08	.03	.03	.03
<i>8r</i>					
C1	73.5	14.9	11.9	14.9	4.0
S1	17	17	17	17	15
S0 ₄	8	8	8	11	3
A ₅	.02	.01	.02	.01	0.01
Hg	<.001	<.001	<.001	<.001	<.001
Date 1980					
* 1500 sample					
#1	#10	#10	#24	#28	
5/23					
5/23					
5/23					
5/23					

* * IF NO ISCO / 15 GIVEN, WATER WAS COLLECTED BY HAND AT ISCO SITE.

TABLE 6 (cont'd)

	TSS	Br	Cl	Si	SO₄	As	Hg	DATE 1980	Sample #	Power Surge?	T₃	T₄	T₅	T₆	T₇	T₈	T₉	T₁₀	T₁₁	T₁₂	T₁₃	T₁₄	T₁₅	T₁₆	T₁₇	T₁₈	T₁₉	T₂₀	T₂₁	T₂₂	T₂₃	T₂₄	T₂₅	T₂₆	T₂₇	T₂₈	T₂₉	T₃₀	T₃₁	T₃₂	T₃₃	T₃₄	T₃₅	T₃₆	T₃₇	T₃₈	T₃₉	T₄₀	T₄₁	T₄₂	T₄₃	T₄₄	T₄₅	T₄₆	T₄₇	T₄₈	T₄₉	T₅₀	T₅₁	T₅₂	T₅₃	T₅₄	T₅₅	T₅₆	T₅₇	T₅₈	T₅₉	T₆₀	T₆₁	T₆₂	T₆₃	T₆₄	T₆₅	T₆₆	T₆₇	T₆₈	T₆₉	T₇₀	T₇₁	T₇₂	T₇₃	T₇₄	T₇₅	T₇₆	T₇₇	T₇₈	T₇₉	T₈₀	T₈₁	T₈₂	T₈₃	T₈₄	T₈₅	T₈₆	T₈₇	T₈₈	T₈₉	T₉₀	T₉₁	T₉₂	T₉₃	T₉₄	T₉₅	T₉₆	T₉₇	T₉₈	T₉₉	T₁₀₀	T₁₀₁	T₁₀₂	T₁₀₃	T₁₀₄	T₁₀₅	T₁₀₆	T₁₀₇	T₁₀₈	T₁₀₉	T₁₁₀	T₁₁₁	T₁₁₂	T₁₁₃	T₁₁₄	T₁₁₅	T₁₁₆	T₁₁₇	T₁₁₈	T₁₁₉	T₁₂₀	T₁₂₁	T₁₂₂	T₁₂₃	T₁₂₄	T₁₂₅	T₁₂₆	T₁₂₇	T₁₂₈	T₁₂₉	T₁₃₀	T₁₃₁	T₁₃₂	T₁₃₃	T₁₃₄	T₁₃₅	T₁₃₆	T₁₃₇	T₁₃₈	T₁₃₉	T₁₄₀	T₁₄₁	T₁₄₂	T₁₄₃	T₁₄₄	T₁₄₅	T₁₄₆	T₁₄₇	T₁₄₈	T₁₄₉	T₁₅₀	T₁₅₁	T₁₅₂	T₁₅₃	T₁₅₄	T₁₅₅	T₁₅₆	T₁₅₇	T₁₅₈	T₁₅₉	T₁₆₀	T₁₆₁	T₁₆₂	T₁₆₃	T₁₆₄	T₁₆₅	T₁₆₆	T₁₆₇	T₁₆₈	T₁₆₉	T₁₇₀	T₁₇₁	T₁₇₂	T₁₇₃	T₁₇₄	T₁₇₅	T₁₇₆	T₁₇₇	T₁₇₈	T₁₇₉	T₁₈₀	T₁₈₁	T₁₈₂	T₁₈₃	T₁₈₄	T₁₈₅	T₁₈₆	T₁₈₇	T₁₈₈	T₁₈₉	T₁₉₀	T₁₉₁	T₁₉₂	T₁₉₃	T₁₉₄	T₁₉₅	T₁₉₆	T₁₉₇	T₁₉₈	T₁₉₉	T₂₀₀	T₂₀₁	T₂₀₂	T₂₀₃	T₂₀₄	T₂₀₅	T₂₀₆	T₂₀₇	T₂₀₈	T₂₀₉	T₂₁₀	T₂₁₁	T₂₁₂	T₂₁₃	T₂₁₄	T₂₁₅	T₂₁₆	T₂₁₇	T₂₁₈	T₂₁₉	T₂₂₀	T₂₂₁	T₂₂₂	T₂₂₃	T₂₂₄	T₂₂₅	T₂₂₆	T₂₂₇	T₂₂₈	T₂₂₉	T₂₃₀	T₂₃₁	T₂₃₂	T₂₃₃	T₂₃₄	T₂₃₅	T₂₃₆	T₂₃₇	T₂₃₈	T₂₃₉	T₂₄₀	T₂₄₁	T₂₄₂	T₂₄₃	T₂₄₄	T₂₄₅	T₂₄₆	T₂₄₇	T₂₄₈	T₂₄₉	T₂₅₀	T₂₅₁	T₂₅₂	T₂₅₃	T₂₅₄	T₂₅₅	T₂₅₆	T₂₅₇	T₂₅₈	T₂₅₉	T₂₆₀	T₂₆₁	T₂₆₂	T₂₆₃	T₂₆₄	T₂₆₅	T₂₆₆	T₂₆₇	T₂₆₈	T₂₆₉	T₂₇₀	T₂₇₁	T₂₇₂	T₂₇₃	T₂₇₄	T₂₇₅	T₂₇₆	T₂₇₇	T₂₇₈	T₂₇₉	T₂₈₀	T₂₈₁	T₂₈₂	T₂₈₃	T₂₈₄	T₂₈₅	T₂₈₆	T₂₈₇	T₂₈₈	T₂₈₉	T₂₉₀	T₂₉₁	T₂₉₂	T₂₉₃	T₂₉₄	T₂₉₅	T₂₉₆	T₂₉₇	T₂₉₈	T₂₉₉	T₃₀₀	T₃₀₁	T₃₀₂	T₃₀₃	T₃₀₄	T₃₀₅	T₃₀₆	T₃₀₇	T₃₀₈	T₃₀₉	T₃₁₀	T₃₁₁	T₃₁₂	T₃₁₃	T₃₁₄	T₃₁₅	T₃₁₆	T₃₁₇	T₃₁₈	T₃₁₉	T₃₂₀	T₃₂₁	T₃₂₂	T₃₂₃	T₃₂₄	T₃₂₅	T₃₂₆	T₃₂₇	T₃₂₈	T₃₂₉	T₃₃₀	T₃₃₁	T₃₃₂	T₃₃₃	T₃₃₄	T₃₃₅	T₃₃₆	T₃₃₇	T₃₃₈	T₃₃₉	T₃₄₀	T₃₄₁	T₃₄₂	T₃₄₃	T₃₄₄	T₃₄₅	T₃₄₆	T₃₄₇	T₃₄₈	T₃₄₉	T₃₅₀	T₃₅₁	T₃₅₂	T₃₅₃	T₃₅₄	T₃₅₅	T₃₅₆	T₃₅₇	T₃₅₈	T₃₅₉	T₃₆₀	T₃₆₁	T₃₆₂	T₃₆₃	T₃₆₄	T₃₆₅	T₃₆₆	T₃₆₇	T₃₆₈	T₃₆₉	T₃₇₀	T₃₇₁	T₃₇₂	T₃₇₃	T₃₇₄	T₃₇₅	T₃₇₆	T₃₇₇	T₃₇₈	T₃₇₉	T₃₈₀	T₃₈₁	T₃₈₂	T₃₈₃	T₃₈₄	T₃₈₅	T₃₈₆	T₃₈₇	T₃₈₈	T₃₈₉	T₃₉₀	T₃₉₁	T₃₉₂	T₃₉₃	T₃₉₄	T₃₉₅	T₃₉₆	T₃₉₇	T₃₉₈	T₃₉₉	T₄₀₀	T₄₀₁	T₄₀₂	T₄₀₃	T₄₀₄	T₄₀₅	T₄₀₆	T₄₀₇	T₄₀₈	T₄₀₉	T₄₁₀	T₄₁₁	T₄₁₂	T₄₁₃	T₄₁₄	T₄₁₅	T₄₁₆	T₄₁₇	T₄₁₈	T₄₁₉	T₄₂₀	T₄₂₁	T₄₂₂	T₄₂₃	T₄₂₄	T₄₂₅	T₄₂₆	T₄₂₇	T₄₂₈	T₄₂₉	T₄₃₀	T₄₃₁	T₄₃₂	T₄₃₃	T₄₃₄	T₄₃₅	T₄₃₆	T₄₃₇	T₄₃₈	T₄₃₉	T₄₄₀	T₄₄₁	T₄₄₂	T₄₄₃	T₄₄₄	T₄₄₅	T₄₄₆	T₄₄₇	T₄₄₈	T₄₄₉	T₄₅₀	T₄₅₁	T₄₅₂	T₄₅₃	T₄₅₄	T₄₅₅	T₄₅₆	T₄₅₇	T₄₅₈	T₄₅₉	T₄₆₀	T₄₆₁	T₄₆₂	T₄₆₃	T₄₆₄	T₄₆₅	T₄₆₆	T₄₆₇	T₄₆₈	T₄₆₉	T₄₇₀	T₄₇₁	T₄₇₂	T₄₇₃	T₄₇₄	T₄₇₅	T₄₇₆	T₄₇₇	T₄₇₈	T₄₇₉	T₄₈₀	T₄₈₁	T₄₈₂	T₄₈₃	T₄₈₄	T₄₈₅	T₄₈₆	T₄₈₇	T₄₈₈	T₄₈₉	T₄₉₀	T₄₉₁	T₄₉₂	T₄₉₃	T₄₉₄	T₄₉₅	T₄₉₆	T₄₉₇	T₄₉₈	T₄₉₉	T₅₀₀	T₅₀₁	T₅₀₂	T₅₀₃	T₅₀₄	T₅₀₅	T₅₀₆	T₅₀₇	T₅₀₈	T₅₀₉	T₅₁₀	T₅₁₁	T₅₁₂	T₅₁₃	T₅₁₄	T₅₁₅	T₅₁₆	T₅₁₇	T₅₁₈	T₅₁₉	T₅₂₀	T₅₂₁	T₅₂₂	T₅₂₃	T₅₂₄	T₅₂₅	T₅₂₆	T₅₂₇	T₅₂₈	T₅₂₉	T₅₃₀	T₅₃₁	T₅₃₂	T₅₃₃	T₅₃₄	T₅₃₅	T₅₃₆	T₅₃₇	T₅₃₈	T₅₃₉	T₅₄₀	T₅₄₁	T₅₄₂	T₅₄₃	T₅₄₄	T₅₄₅	T₅₄₆	T₅₄₇	T₅₄₈	T₅₄₉	T₅₅₀	T₅₅₁	T₅₅₂	T₅₅₃	T₅₅₄	T₅₅₅	T₅₅₆	T₅₅₇	T₅₅₈	T₅₅₉	T₅₆₀	T₅₆₁	T₅₆₂	T₅₆₃	T₅₆₄	T₅₆₅	T₅₆₆	T₅₆₇	T₅₆₈	T₅₆₉	T₅₇₀	T₅₇₁	T₅₇₂	T₅₇₃	T₅₇₄	T₅₇₅	T₅₇₆	T₅₇₇	T₅₇₈	T₅₇₉	T₅₈₀	T₅₈₁	T₅₈₂	T₅₈₃	T₅₈₄	T₅₈₅	T₅₈₆	T₅₈₇	T₅₈₈	T₅₈₉	T₅₉₀	T₅₉₁	T₅₉₂	T₅₉₃	T₅₉₄	T₅₉₅	T₅₉₆	T₅₉₇	T₅₉₈	T₅₉₉	T₆₀₀	T₆₀₁	T₆₀₂	T₆₀₃	T₆₀₄	T₆₀₅	T₆₀₆	T₆₀₇	T₆₀₈	T₆₀₉	T₆₁₀	T₆₁₁	T₆₁₂	T₆₁₃	T₆₁₄	T₆₁₅	T₆₁₆	T₆₁₇	T₆₁₈	T₆₁₉	T₆₂₀	T₆₂₁	T₆₂₂	T₆₂₃	T₆₂₄	T₆₂₅	T₆₂₆	T₆₂₇	T₆₂₈	T₆₂₉	T₆₃₀	T₆₃₁	T₆₃₂	T₆₃₃	T₆₃₄	T₆₃₅	T₆₃₆	T₆₃₇	T₆₃₈	T₆₃₉	T₆₄₀	T₆₄₁	T₆₄₂	T₆₄₃	T₆₄₄	T₆₄₅	T₆₄₆	T₆₄₇	T₆₄₈	T₆₄₉	T₆₅₀	T₆₅₁	T₆₅₂	T₆₅₃	T₆₅₄	T₆₅₅	T₆₅₆	T₆₅₇	T₆₅₈	T₆₅₉	T₆₆₀	T₆₆₁	T₆₆₂	T₆₆₃	T₆₆₄	T₆₆₅	T₆₆₆	T₆₆₇	T₆₆₈	T₆₆₉	T₆₇₀	T₆₇₁	T₆₇₂	T₆₇₃	T₆₇₄	T₆₇₅	T₆₇₆	T₆₇₇	T₆₇₈	T₆₇₉	T₆₈₀	T₆₈₁	T₆₈₂	T₆₈₃	T₆₈₄	T₆₈₅	T₆₈₆	T₆₈₇	T₆₈₈	T₆₈₉	T₆₉₀	T₆₉₁	T₆₉₂	T₆₉₃	T₆₉₄	T₆₉₅	T₆₉₆	T₆₉₇	T₆₉₈	T₆₉₉	T₇₀₀	T₇₀₁	T₇₀₂	T₇₀₃	T₇₀₄	T₇₀₅	T₇₀₆	T₇₀₇	T₇₀₈	T₇₀₉	T₇₁₀	T₇₁₁	T₇₁₂	T₇₁₃	T₇₁₄	T₇₁₅	T₇₁₆	T₇₁₇	T₇₁₈	T₇₁₉	T₇₂₀	T₇₂₁	T₇₂₂	T₇₂₃	T₇₂₄	T₇₂₅	T₇₂₆	T₇₂₇	T₇₂₈	T₇₂₉	T₇₃₀	T₇₃₁	T₇₃₂	T₇₃₃	T₇₃₄	T₇₃₅	T₇₃₆	T₇₃₇	T₇₃₈	T₇₃₉	T₇₄₀	T₇₄₁	T₇₄₂	T₇₄₃	T₇₄₄	T₇₄₅	T₇₄₆	T₇₄₇	T₇₄₈	T₇₄₉	T₇₅₀	T₇₅₁	T₇₅₂	T₇₅₃	T₇₅₄	T₇₅₅	T₇₅₆	T₇₅₇	T₇₅₈	T₇₅₉	T₇₆₀	T₇₆₁	T₇₆₂	T₇₆₃	T₇₆₄	T₇₆₅	T₇₆₆	T₇₆₇	T₇₆₈	T₇₆₉	T₇₇₀	T₇₇₁	T₇₇₂	T₇₇₃	T₇₇₄	T₇₇₅	T₇₇₆	T₇₇₇	T₇₇₈	T₇₇₉	T₇₈₀	T₇₈₁	T₇₈₂	T₇₈₃	T₇₈₄	T₇₈₅	T₇₈₆	T₇₈₇	T₇₈₈	T₇₈₉	T₇₉₀	T₇₉₁	T₇₉₂	T₇₉₃	T₇₉₄	T₇₉₅	T₇₉₆	T₇₉₇	T₇₉₈	T₇₉₉	T₈₀₀	T₈₀₁	T₈₀₂	T₈₀₃	T₈₀₄	T₈₀₅	T₈₀₆	T₈₀₇	T₈₀₈	T₈₀₉	T₈₁₀	T₈₁₁	T₈₁₂	T₈₁₃	T₈₁₄	T₈₁₅	T₈₁₆	T₈₁₇	T₈₁₈	T₈₁₉	T₈₂₀	T₈₂₁	T₈₂₂	T₈₂₃	T₈₂₄	T₈₂₅	T₈₂₆	T₈₂₇	T₈₂₈	T₈₂₉	T₈₃₀	T₈₃₁	T₈₃₂	T₈₃₃	T₈₃₄	T₈₃₅	T₈₃₆	T₈₃₇	T₈₃₈	T₈₃₉	T₈₄₀	T₈₄₁	T₈₄₂	T₈₄₃	T₈₄₄	T₈₄₅	T₈₄₆	T₈₄₇	T₈₄₈	T₈₄₉	T₈₅₀	T₈₅₁	T₈₅₂	T₈₅₃	T₈₅₄	T₈₅₅	T₈₅₆	T₈₅₇	T₈₅₈	T₈₅₉	T₈₆₀	T₈₆₁	T₈₆₂	T₈₆₃	T₈₆₄	T₈₆₅	T₈₆₆	T₈₆₇	T₈₆₈	T₈₆₉	T

PRESSURE TRANSIENT ANALYSIS

FOR HOT WATER AND TWO-PHASE GEOTHERMAL WELLS: SOME NUMERICAL RESULTS

Carl Uloog



BACA GEOTHERMAL DEMONSTRATION PROJECT

PREPARED BY:



SYSTEMS, SCIENCE
AND SOFTWARE

PUBLIC SERVICE COMPANY OF NEW MEXICO

UNION GEOTHERMAL COMPANY OF NEW MEXICO

UNITED STATES DEPARTMENT OF ENERGY

UNDER CONTRACT TO:



WESTEC Services, Inc.

Carl Uloog

Carl Wloog

DOE/ET/27163-5
Distribution Category UC-66f

BACA GEOTHERMAL DEMONSTRATION PROJECT

PRESSURE TRANSIENT ANALYSIS FOR HOT WATER AND
TWO-PHASE GEOTHERMAL WELLS: SOME NUMERICAL RESULTS

TOPICAL REPORT

Prepared By

S. K. Garg
J. W. Pritchett

Systems, Science and Software
P. O. Box 1620
La Jolla, California 92038

Date Published - October 1980

Prepared Under Subcontract to

WESTEC Services, Inc.

Prepared For

UNION GEOTHERMAL COMPANY OF NEW MEXICO

AND

PUBLIC SERVICE COMPANY OF NEW MEXICO

UNDER CONTRACT NO. GEO-CSL-25

Work Sponsored By

THE U.S. DEPARTMENT OF ENERGY

DIVISION OF GEOTHERMAL ENERGY

UNDER COOPERATIVE AGREEMENT NO. DE-FC03-78ET27163

DISCLAIMER

"This report was prepared as an account of work performed for Union Geothermal Company of New Mexico, Public Service Company of New Mexico, and the U.S. Department of Energy, an agency of the United States Government. Neither Union Geothermal Company of New Mexico, nor Public Service Company of New Mexico, nor the United States Government nor any agency thereof, nor any of their employees or subcontractors, makes any warranty, express or implied, or assumes any legal liability or responsibility for the accuracy, completeness, or usefulness of any information, apparatus, product, or process disclosed, or represents that its use would not infringe privately owned rights. Reference herein to any specific commercial product, process, or service by trade name, trademark, manufacturer, or otherwise, does not necessarily constitute or imply its endorsement, recommendation, or favoring by Union Geothermal Company of New Mexico, or Public Service Company of New Mexico, or the United States Government or any agency thereof. The views and opinions of authors expressed herein do not necessarily state or reflect those of Union Geothermal Company of New Mexico, or Public Service Company of New Mexico, or the United States Government or any agency thereof."

Printed in the United States of America

Available from:

WESTEC Services, Inc.
505 Marquette, N.W., Suite 1000
Albuquerque, NM 87102

ABSTRACT

A geothermal reservoir simulator has been employed in a series of calculations which describe the response of geothermal reservoirs to fluid production/injection from a single well. The numerical solutions were analyzed to generate interpretation techniques for pressure transient data from either single-phase or two-phase geothermal reservoirs. The investigations include (1) the drawdown/buildup response of hot water wells, (2) the drawdown/buildup behavior of initially two-phase (liquid water/steam) reservoirs, (3) the drawdown/buildup response of initially single-phase reservoirs which undergo flashing as a result of fluid production and (4) the effect of cold water injection into single-phase and two-phase reservoirs.

TABLE OF CONTENTS

	<u>Page</u>
SECTION 1: INTRODUCTION	1
1.1 Introduction	1
1.2 Scope of the Report	2
1.3 Summary and Conclusions	3
1.4 Recommendations for Future Study	3
SECTION 2: THEORETICAL PRODUCTION BEHAVIOR ANALYSES	5
2.1 Introduction	5
2.2 Summary	5
2.3 Production Behavior of Hot Water Reservoirs . .	5
2.3.1 Background of Theory	6
2.3.2 Single-Phase Reservoir Production Behavior	12
2.4 Production Behavior of Initially Two-Phase Geothermal Reservoirs	17
2.4.1 Background of Theory	17
2.4.2 Two-Phase Reservoir Production Behavior	19
2.5 Production Behavior of Hot Water Reservoirs which Flash on Fluid Withdrawal	30
2.5.1 Background of Theory	31
2.5.2 Hot Water Reservoirs which Undergo Flashing	31
Section 3: THEORETICAL INJECTION BEHAVIOR ANALYSES	43
3.1 Introduction	43
3.2 Summary	43
3.3 Cold Water Injection into a Hot Water Well . .	43
3.4 Cold Water Injection into Two-Phase Reservoirs	47
REFERENCES	63

LIST OF FIGURES

	<u>Page</u>
Figure 2.1. Drawdown data for hot water geothermal reservoir.	15
Figure 2.2. Buildup data for hot water geothermal reservoir.	16
Figure 2.3. Enthalpy variation as a function of $1/\eta^2$ for hot water reservoir.	18
Figure 2.4. Pressure drawdown and flowing enthalpy for case A.1.	22
Figure 2.5. Pressure drawdown and flowing enthalpy for case A.2.	23
Figure 2.6. Pressure and temperature buildup data for case A.1.	24
Figure 2.7. Pressure and temperature buildup data for case A.2.	25
Figure 2.8. Radial distribution of flowing kinematic viscosity ν_t at selected times for case A.1.	26
Figure 2.9. Radial distribution of flowing kinematic viscosity ν_t at selected times for case A.2.	27
Figure 2.10. Radial distribution of steam saturation S_g at selected times for case A.1.	28
Figure 2.11. Radial distribution of steam saturation S_g at selected times for case A.2.	29
Figure 2.12. Pressure drawdown and flowing enthalpy for case B.1.	32
Figure 2.13. Pressure drawdown for case B.2.	33
Figure 2.14. Pressure and temperature buildup data for case B.1.	34
Figure 2.15. Pressure and temperature buildup data for case B.2.	35
Figure 2.16. Radial distribution of flowing kinematic viscosity ν_t at selected times for case B.1.	36

LIST OF FIGURES (cont'd.)

	<u>Page</u>
Figure 2.17. Radial distribution of flowing kinematic viscosity v_t at selected times for case B.2.	37
Figure 2.18. Radial distribution of steam saturation S_g at selected times for case B.1.	38
Figure 2.19. Radial distribution of steam saturation S_g at selected times for case B.2.	40
Figure 3.1. Pressure buildup (Injection) data for cold water injection into a hot water well.	44
Figure 3.2. Radial distribution of flowing kinematic viscosity and temperature at $t \sim 5.868 \times 10^5$ s (end of injection period).	44
Figure 3.3. Pressure fall-off data for cold water injection into a hot water well.	45
Figure 3.4. Pressure buildup (Injection) data for case C.1.	49
Figure 3.5. Pressure buildup (Injection) data for case C.2.	50
Figure 3.6. Radial distribution of temperature and steam saturation at selected times for case C.1.	51
Figure 3.7. Radial distribution of temperature and steam saturation at selected times for case C.2.	52
Figure 3.8. Pressure fall-off data (Horner plot) for case C.1.	53
Figure 3.9. Pressure fall-off data (Horner plot) for case C.2.	54
Figure 3.10. Early pressure fall-off data for case C.1.	56
Figure 3.11. Early pressure fall-off data for case C.2.	57
Figure 3.12. Plot of $\log \Delta p$ versus $\log \Delta t$ for case C.1.	59
Figure 3.13. Plot of $\log \Delta p$ versus $\log \Delta t$ for case C.2.	60

SECTION 1: INTRODUCTION

1.1 Introduction

The line source solution (or Theis solution) has been traditionally used in hydrology and petroleum engineering to analyze pressure transient data from isothermal single-phase (water/oil/gas) and isothermal two-phase (oil with gas in solution, free gas) reservoir systems. For a constant flow rate well test, a plot of pressure drop versus logarithm of time asymptotes to a straight line after a short initial period. The slope and intercept of this line yield the mobility-thickness product and the total formation compressibility. The total formation compressibility depends upon, among other variables, fluid compressibility. Although very often it is not explicitly stated, the fluid compressibility in traditional applications is the one measured at constant temperature.

Extension of the Theis solution to analyze pressure transient data from geothermal reservoirs involves several difficulties. Geothermal reservoirs by their very nature contain fluid at elevated temperatures. Very often the in situ fluid is either boiling or near boiling. For single-phase hot liquid reservoirs, it is not self-evident whether or not the isothermal fluid compressibility is the appropriate one. (This question will be examined in detail in Section 2, and it will be shown that the isothermal fluid compressibility should be replaced by isenthalpic fluid compressibility at elevated temperatures.) In recent years, several investigators (Garg [1978], Grant [1978], Moench and Atkinson [1977]) have examined the production (or drawdown) behavior of two-phase geothermal reservoirs. The geothermal reservoir may be initially two-phase or may evolve into a two-phase reservoir as a result of fluid production. The plot of pressure drop versus logarithm of time asymptotes to a straight line after an initial non-linear period; the slope of the straight line can be used to calculate the kinematic mobility-thickness product. The intercept

of the straight line, however, provides a very poor approximation of the total formation compressibility which is primarily governed by phase change effects. Sorey, et al. [1980] have also numerically examined the buildup behavior in initially two-phase reservoirs; the plot of pressure versus $\log [(t+\Delta t)/\Delta t]$ (t = production time, Δt = shutin time) gives a straight line. The slope of this straight line again can be related to the kinematic mobility-thickness product; the kinematic mobility-thickness product calculated from buildup data is, however, different from that obtained from drawdown data due to nonlinear effects in two-phase non-isothermal flow. These nonlinear effects imply that the superposition principle does not apply in two-phase geothermal systems. As the present time, there exists little or no information in the literature on either the (1) buildup response of initially single-phase reservoirs which undergo flashing as a result of fluid production, or (2) the effect of cold water fluid injection into two-phase geothermal reservoirs.

The numerical results presented in the report form a theoretical framework which will be used in interpreting the flow data from the production/injection wells at the Baca Geothermal Demonstration Power Plant (GDPP) Project. The application of the techniques to the data from the Baca wells will be the subject of a separate topical report. The results contained herein, however, are of fundamental interest to geothermal reservoir engineers and applicable to other geothermal systems.

1.2 Scope of the Report

The main purpose of this report is to develop interpretation techniques for pressure transient data from either single-phase or two-phase geothermal reservoirs. More specifically, the Systems, Science and Software (³S) reservoir simulator CHARGR (Pritchett [1980]) will be employed in a series of one-dimensional radial flow problems to investigate (1) the drawdown/buildup response of hot water wells, (2) the drawdown/ buildup behavior of initially two-phase reservoirs, (3) the drawdown/buildup response of initially

single-phase reservoirs which undergo flashing as a result of fluid production and (4) the effect of fluid injection into single-phase and two-phase reservoirs. The numerical results are employed to generate guidelines for calculating mobility-thickness product from pressure transient data.

1.3 Summary and Conclusions

The numerical simulations presented herein demonstrate some of the difficulties associated with analyzing pressure transient data from hot water and two-phase geothermal reservoirs. It is demonstrated that production data (drawdown/buildup) from single-phase hot water and initially two-phase reservoirs may be analyzed in the usual manner to yield absolute permeability/kinematic mobility provided the total formation compressibility is defined differently from its conventional usage in petroleum engineering and hydrology. Drawdown data from initially single-phase reservoirs which undergo flashing during production can be made to give two-phase kinematic mobility; the buildup data from such reservoirs offers the possibility of determining absolute formation permeability. It is further shown that injection data for single-phase and two-phase reservoirs can be interpreted in a straightforward manner to give absolute formation permeability; the fall-off data (especially in two-phase systems) appear, however, to be of lesser utility.

1.4 Recommendations for Future Study

This report contains the results of theoretical calculations simulating transient production and injection testing of single-phase and two-phase reservoirs. The simulations provide a quantitative understanding of the phenomena which may be expected to occur during the pressure testing of wells in such a reservoir. The results are of direct relevance to the Baca reservoir system and will be used by S³ in evaluating the available flow test data for the Baca wells.

SECTION 2: THEORETICAL PRODUCTION BEHAVIOR ANALYSES

2.1 Introduction

In this section numerical simulations are presented which describe the production data (drawdown/buildup) for a single well producing fluid from a geothermal reservoir. The S³ geothermal reservoir simulation CHARGR is used to study all-liquid reservoirs, initially two-phase reservoirs and initially single-phase reservoirs which undergo flashing as a result of fluid production.

2.2 Summary

It is demonstrated that production data from single-phase hot water and initially two-phase reservoir may be analyzed, respectively, to yield absolute formation permeability and two-phase kinematic mobility. Drawdown data from initially single-phase reservoirs which undergo flashing during production can be made to give kinematic mobility; the buildup data may be used to determine absolute permeability.

2.3 Production Behavior of Hot Water Reservoirs

The classical methods of analyzing groundwater and petroleum fluid production data may be extended to interpret single-phase geothermal fluid production data. However, the extension requires a careful examination of the fluid compressibility factor which occurs in the classical solution. In this section it is shown that for hot water reservoir flow data it is necessary that the isoenthalpic fluid compressibility be used instead of the isoenergetic or isothermal fluid compressibility. Both drawdown and buildup flow tests are simulated.

2.3.1 Background of Theory

In groundwater hydrology and petroleum engineering, the line source solution to the linearized diffusivity equation is used to interpret pressure transient data. For constant rate of mass production M , the pressure at the bottom of the well $p_w(t)$ is given by

$$p_w(t) = p_i + \frac{Mv}{4\pi Hk} Ei \left[-\frac{r_w^2 \phi \rho C_T v}{Hkt} \right], \quad (2.1)$$

where

- p = initial reservoir pressure
- v = kinematic fluid viscosity
- H = formation thickness
- r_w = well radius
- ρ = fluid density
- k = absolute formation permeability
- ϕ = porosity
- t = time
- C_T = total formation compressibility
 $(= \frac{1-\phi}{\phi} C_m + C)$
- C_m = uniaxial formation compressibility
- C = fluid compressibility

If $\frac{4tk}{\phi r_w^2 \rho v C_T} > 100$, Equation (2.1) can be approximated as follows:

$$p_w(t) = p_i - \frac{1.15 v M}{2\pi H k} \left[\log \frac{kt}{\phi r_w^2 \rho v C_T} + 0.351 \right] \quad (2.2)$$

Equation (2.2) implies that a plot of p_w versus $\log t$ should be a straight line. If m denotes the slope of this straight line, then

$$k = \frac{1.15 v M}{2\pi H m} \quad (2.3)$$

$$C_T = \frac{kt}{\text{antilog} \left[\frac{p_i - p_w(t)}{m} - 0.351 \right]} \cdot \frac{1}{\phi r_w^2 v_p} \quad (2.4)$$

Superposition can be utilized to construct solutions for buildup (i.e., shutin after production for time t). The solution implies that a plot of p versus $\log(t+\Delta t/\Delta t)$ (Δt = shutin time) should be a straight line. The slope of the straight line can be used, together with Equation (2.3), to calculate formation permeability. (In the above, consideration of skin effect and well storage have been ignored. These effects, while important in practical well testing, are not germane to the present discussion.)

The fluid compressibility C can be defined in a number of ways (at constant internal energy C_E ; at constant temperature C_t ; at constant enthalpy C_h).

$$C_E = \frac{1}{\rho} \left(\frac{\partial \rho}{\partial p} \right)_E \quad (2.5)$$

$$C_t = \frac{1}{\rho} \left(\frac{\partial \rho}{\partial p} \right)_T \quad (2.6)$$

$$C_h = \frac{1}{\rho} \left(\frac{\partial \rho}{\partial p} \right)_h \quad (2.7)$$

Table 2.1 gives liquid water compressibilities as a function of pressure and temperature. (Note that the data in Table 2.1 are based on S³ CHARGR equation-of-state for water (Pritchett [1980]), and may be in error by a few percent. Nevertheless, it is believed that the relative values of C_E , C_t and C_h are approximately correct.) At 0°C, all three compressibilities are practically identical; thus for groundwater or petroleum reservoirs it is of little concern as to which fluid compressibility is used. However, at elevated temperatures characteristic of geothermal systems, substantial differences do exist between the different

Table 2.1
**CONSTANT ENERGY (c_E), ISOTHERMAL (c_t), AND ISENTHALPIC (c_h) COMPRESSIBILITIES FOR LIQUID WATER AS GIVEN
 BY THE S³ CHARGR EQUATION-OF-STATE.**
All compressibilities are in GPa⁻¹ (1GPa⁻¹ = 10⁻⁹ Pa⁻¹)

P(MPa)	T(0°C)						200						300					
	0	50	100	150	200	250	0	50	100	150	200	250	0	50	100	150	200	250
	c_E	c_t	c_h	c_E	c_t	c_h	c_E	c_t	c_h	c_E	c_t	c_h	c_E	c_t	c_h	c_E	c_t	c_h
0.1	0.491	0.495	0.411	0.424	0.512	-	-	-	-	-	-	-	-	-	-	-	-	-
2.5	0.490	0.490	0.497	0.411	0.424	0.512	0.416	0.465	0.597	0.499	0.602	0.753	0.624	0.820	0.970	-	-	-
5.0	0.490	0.490	0.498	0.410	0.423	0.512	0.415	0.464	0.595	0.490	0.600	0.750	0.622	0.815	0.964	0.831	1.27	1.32
7.5	0.489	0.489	0.498	0.410	0.423	0.512	0.415	0.463	0.594	0.497	0.598	0.747	0.620	0.810	0.959	0.826	1.25	1.31
10.0	0.488	0.488	0.499	0.409	0.422	0.512	0.414	0.462	0.592	0.496	0.596	0.744	0.618	0.806	0.954	0.821	1.24	1.30
12.5	0.488	0.488	0.500	0.409	0.422	0.512	0.413	0.461	0.590	0.495	0.594	0.741	0.616	0.801	0.948	0.817	1.23	1.28
15.0	0.487	0.487	0.501	0.409	0.422	0.512	0.413	0.460	0.589	0.493	0.592	0.738	0.614	0.797	0.943	0.812	1.21	1.27

compressibilities. One may speculate that for hot water reservoirs, isenthalpic fluid compressibility C_h is the appropriate one to use in the definition for total formation compressibility.

Hot water flow in geothermal reservoirs follows a complex thermodynamic path. Although the variations in internal energy, temperature, and enthalpy are small, they do nevertheless occur. The fluid flow cannot be simply treated as isoenergetic, isothermal or isenthalpic. The flowing enthalpy does, however, approach a definite limit as $r \rightarrow 0$ or $t \rightarrow \infty$. (It is worth emphasizing that the constancy of enthalpy means that internal energy and temperature must be varying.) The equations governing one-dimensional radial flow will now be considered to prove that

$$\lim_{\substack{r \rightarrow 0 \\ \text{or } t \rightarrow \infty}} h_f \rightarrow h_{fo} .$$

Assuming that (1) the rock porosity depends only on the fluid pressure, (2) the rock matrix and the fluid are in local thermal equilibrium (3) the global heat conduction is negligible, and (4) the fluid flow is governed by Darcy's law, the balance equations for mass and energy in radial geometry can be written as follows:

Mass (liquid)

$$\frac{\partial}{\partial t} (\phi p) - \frac{1}{r} \frac{\partial}{\partial r} \left[\frac{rk}{v} \frac{\partial p}{\partial r} \right] = 0 \quad (2.8)$$

Energy

$$\frac{\partial}{\partial t} \left[(1-\phi)\rho_r h_r + \phi p h - \phi p \right] - \frac{1}{r} \frac{\partial}{\partial r} \left[\frac{rk}{v} h \frac{\partial p}{\partial r} \right] = 0 \quad (2.9)$$

where

$$\begin{aligned} \rho_r &= \text{rock grain density,} \\ h_r &= \text{rock enthalpy.} \end{aligned}$$

The differential equations (2.8) and (2.9) are subject to the following boundary and intial conditions:

Boundary Conditions

$$\lim_{r \rightarrow 0} r \frac{\partial p}{\partial r} = - \frac{Mv}{2\pi H k} \quad (2.10)$$

$$\lim_{r \rightarrow \infty} p = p_i, h = h_i \quad (2.11)$$

Initial Conditions

$$t = 0: p = p_i, h = h_i \quad (2.12)$$

Following O'Sullivan [1980], the similarity variable η is introduced:

$$\eta = r^{0.5}/t \quad (2.13)$$

Substituting from (2.3) into (2.8)-(2.12), one obtains the following transformed equations:

Mass

$$\frac{d(\phi\rho)}{d\eta} + \frac{2}{\eta^2} \frac{d}{d\eta} \left[\frac{k}{v} \eta \frac{dp}{d\eta} \right] = 0 \quad (2.14)$$

Energy

$$\frac{d}{d\eta} \left[(1-\phi)\rho_r h_r + \phi\rho h \right] - \phi p + \frac{2}{\eta^2} \frac{d}{d\eta} \left[\frac{k}{v} h \eta \frac{dp}{d\eta} \right] = 0 \quad (2.15)$$

Boundary and Initial Conditions

$$\lim_{\eta \rightarrow 0} \eta \frac{dp}{d\eta} = - \frac{Mv}{2\pi H k} \quad (2.16)$$

$$\lim_{\eta \rightarrow \infty} p = p_i, h = h_i \quad (2.17)$$

Also, note that

$$\frac{d\phi}{dp} = (1-\phi)C_m, \quad (2.18)$$

$$h = c_r T \quad (2.19)$$

where T is the common local temperature of the rock matrix and the pore fluids, and c_r is the rock grain heat capacity.

Regarding p and h as independent thermodynamic variables and utilizing (2.18) and (2.19), Equations (2.14) and (2.15) may be algebraically manipulated to yield:

$$\begin{aligned} \phi_p \left\{ \frac{1-\phi}{\phi} C_m + C_h - \frac{1}{\rho} \left(\frac{\partial \phi}{\partial h} \right)_p p \frac{(1-\phi) \rho_r c_r \left(\frac{\partial T}{\partial p} \right)_h - (1-\phi) C_m (\rho_r h_r + p) - \phi}{(1-\phi) \rho_r c_r \left(\frac{\partial T}{\partial h} \right)_p p + \phi_p + \frac{2}{n} (k/v) \frac{dp}{dn}} \right\} \\ \cdot \frac{dp}{dn} + \frac{2}{n^2} \frac{d}{dn} \left[\left(\frac{k}{v} \right)_n \frac{dp}{dn} \right] = 0 \end{aligned} \quad (2.20)$$

$$\frac{dh}{dn} = - \frac{\left\{ (1-\phi) \rho_r c_r \left(\frac{\partial T}{\partial p} \right)_h - (1-\phi) C_m (\rho_r h_r + p) - \phi \right\}}{(1-\phi) \rho_r c_r \left(\frac{\partial T}{\partial h} \right)_p p + \phi_p + \frac{2}{n} \left(\frac{k}{v} \right) \frac{dp}{dn}} \cdot \frac{dp}{dn} \quad (2.21)$$

Equations (2.16) and (2.21) can be combined to give:

$$\lim_{n \rightarrow 0} \frac{dh}{dn} = 0 \quad (2.22)$$

Equation (2.22) demonstrates that the fluid enthalpy approaches a constant value in the limit $n \rightarrow 0$ (i.e., in the limit $r \rightarrow 0$ or $t \rightarrow \infty$). Since

$$\lim_{n \rightarrow 0} n \frac{dp}{dn} \neq 0 ,$$

Equation (2.22) also implies that internal energy E and temperature T are varying even as $t \rightarrow \infty$.

Although Equation (2.22) is only valid as $n \gg 0$, it is now assumed that $dh/dn = 0$ is a reasonable approximation to use in interpreting pressure transient data. With Equation (2.22) and taking k/v to be constant, Equation (2.21) leads to the usual diffusivity equation:

$$\phi \rho C_T \frac{dp}{dn} + \frac{2}{\eta^2} \frac{k}{v} \frac{d}{dn} \eta \frac{dp}{dn} = 0 \quad (2.23)$$

with

$$C_T = \frac{1-\phi}{\phi} C_m + C_h \quad (2.24)$$

The solution of Equation (2.23) subject to the boundary conditions, Equations (2.16 and (2.17), is identical with the classical Theis solution.

2.3.2 Single-Phase Reservoir Production Behavior

To test the validity of the preceding theory, the S³ reservoir simulator CHARGR was exercised in its one-dimensional radial mode. The radially infinite reservoir was simulated using a 60-zone [$\Delta r_1 = 0.11$ m; $\Delta r_2 = 1.2 \Delta r_1$; $\Delta r_3 = 1.2 \Delta r_2$, ..., $\Delta r_{60} = \Delta r_{59}$] radial grid. The outer radius of the grid is 25,825 m and is sufficiently large such that no signal reaches this boundary for production/shut-in periods. The formation thickness is $H = 250$ m. The well is assumed to be coincident with Zone 1. (In the CHARGR code, a well can be represented as an integral part of the grid by assigning to the well-block sufficiently high permeability and porosity.) The reservoir rock is assumed to be a typical sandstone. The relevant rock properties are given in Table 2.2. (Although the present problem is purely single-phase, Table 2.2 also lists relative permeabilities, and residual liquid and

Table 2.2
ROCK PROPERTIES EMPLOYED IN NUMERICAL SIMULATION

	<u>Well-Block</u> ($i = 1$)	<u>Rock Matrix</u> ($2 \leq i \leq 60$)
Porosity, ϕ	0.9999	0.1
Permeability, $k(m^2)$	50×10^{-12}	5×10^{-14}
Uniaxial Formation Compressibility, $C_m(MPa^{-1})$	0	0
Rock Grain Density, $\rho_r(kg/m^3)$	1	2650
Grain Thermal Conductivity, $K_r(W/m \cdot ^\circ C)$	0	5.25
Heat Capacity, $c_r(kJ/kg \cdot ^\circ C)$	0.001	1
Relative Permeability (k_{rl}, k_{rg})	Straight Line*	Corey**
Residual Liquid Saturation, S_{lr}	0	0.3
Residual Gas Saturation, S_{gr}	0	0.05

* $k_{rl} = S_l, k_{rg} = S_g = 1 - S_l, S_l(S_g) = \text{liquid (gas) volume fraction.}$

** $k_{rl} = \frac{(S_l^*)^4}{(S_l - S_{lr})/(1 - S_{lr} - S_{gr})}, k_{rg} = (1 - S_l^{*2})(1 - S_l^*)^2, S_l^* =$

vapor saturations for later use in sections on two-phase flow.) The mixture (rock/fluid) thermal conductivity is approximated by Budiansky's formula (Pritchett [1980]).

The initial formation pressure and temperature are 9.3917 MPa and 300°C respectively. The reservoir is produced at a constant rate of 35 kg/s for $t = 5.868 \times 10^5$ s, and is then shutin for $\Delta t = 1.3932 \times 10^6$ s⁺. Figures 2.1 and 2.2 show the calculated drawdown and buildup response of the well. The drawdown curve has a slope m of 0.0644×10^6 Pa/~. With $v = 1.244 \times 10^{-7}$ m²/s (= kinematic viscosity of fluid at initial reservoir pressure and temperature), we obtain for formation permeability k

$$k = \frac{1.15 v M}{2\pi H m} = \frac{1.15 \times 1.244 \times 35 \times 10^{-7}}{2\pi \times 250 \times 0.0644 \times 10^6} \sim 4.95 \times 10^{-14} \text{ m}^2$$

The slope of the buildup curve ($\sim 0.0653 \times 10^6$ Pa/~) yields $k = 4.88 \times 10^{-14} \text{ m}^2$. Both drawdown and buildup data thus yield permeability values in close agreement with the actual permeability of $5.00 \times 10^{-14} \text{ m}^2$. With $\rho = 713.9 \text{ kg/m}^3$ (fluid density at initial reservoir conditions), the following is obtained for total formation compressibility C_T (= fluid compressibility C since $C_m = 0$):

$$\begin{aligned} C_T &= \frac{1}{\phi r_w^2 v \rho} \frac{kt}{\text{antilog} \left[\frac{p_i - p_w(t)}{m} \right] - 0.351} \\ &= \frac{1}{0.1 (0.11)^2 1.244 \times 10^{-7} \times 713.9} \frac{4.95 \times 10^{-14} \times 5 \times 10^5}{\text{antilog} \left[\frac{9.3917 - 8.8490}{0.0644} \right] - 0.351} \\ &= 1.93 \text{ GPa}^{-1} \end{aligned}$$

⁺ For the various cases discussed in the following sections, the grid, formation properties, production (injection) rate, drawdown (injection) time and shutin (falloff) time specified in this section will be used. The initial fluid state will, however, vary from case to case.

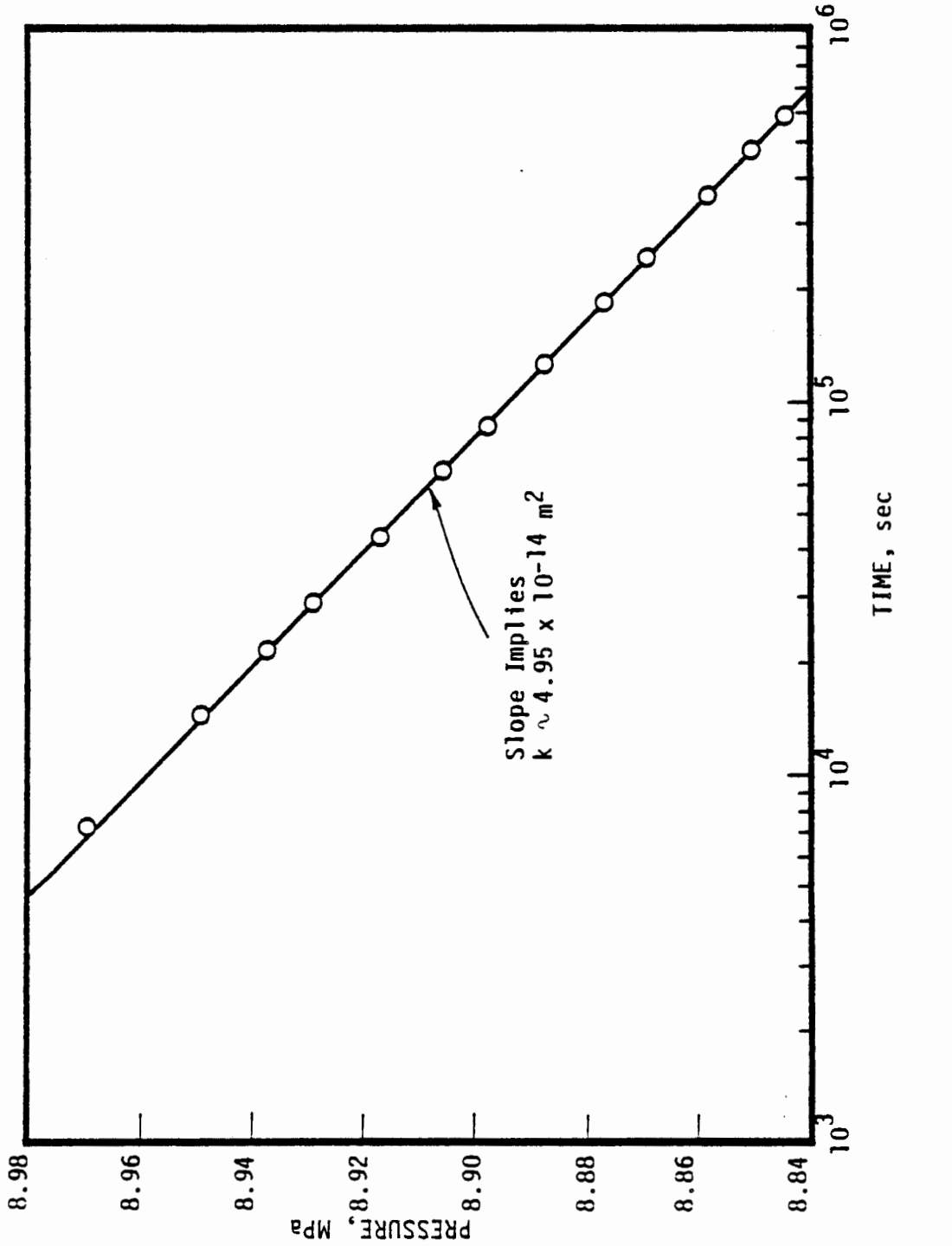


Figure 2.1. Drawdown data for hot water geothermal reservoir ($p_i = 9.3917 \text{ MPa}$, $T_i = 300^\circ\text{C}$).

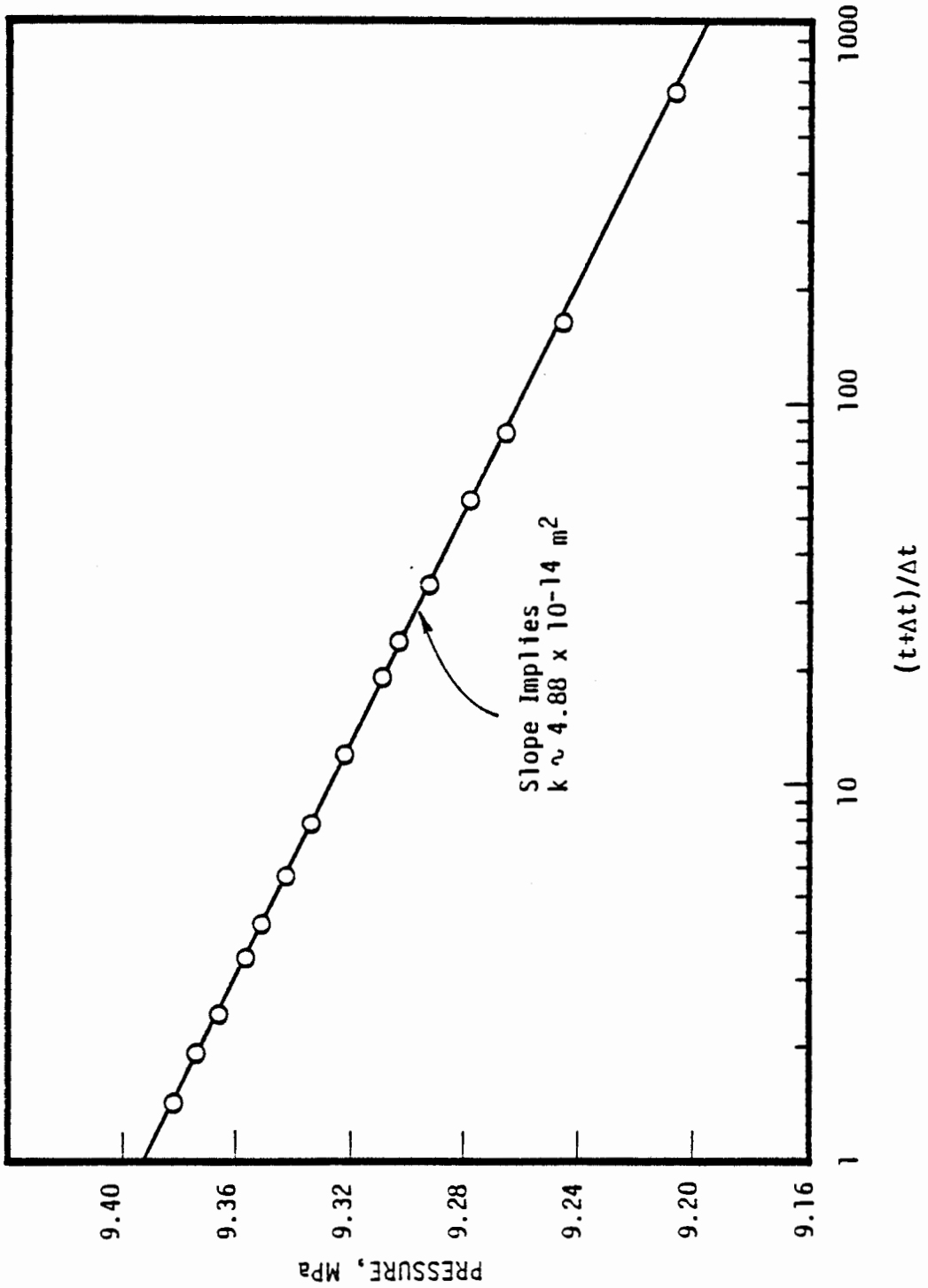


Figure 2.2. Buildup data for hot water geothermal reservoir ($p_i = 9.3917 \text{ MPa}$, $T_i = 300^\circ\text{C}$).

The calculated fluid compressibility value is in reasonable agreement with the isenthalpic fluid compressibility ($\sim 2.01 \text{ GPa}^{-1}$) but is considerably different from the isoenergetic ($\sim 1.24 \text{ GPa}^{-1}$) and isothermal ($\sim 2.49 \text{ GPa}^{-1}$) compressibilities. This verifies the speculation that the isenthalpic fluid compressibility should be used in the definition for total formation compressibility. Finally, for the sake of completeness, Figure 2.3 shows the enthalpy variation with $1/n^2$. Although $\max |\Delta h/h| (0.20/1344 \sim 1.5 \times 10^{-4})$ is very small, the fluid does undergo enthalpy changes. Furthermore, Δh (and hence h) approaches a constant value for $1/n^2 > 10^4$ (or $n < 10^{-2}$).

2.4 Production Behavior of Initially Two-Phase Geothermal Reservoirs

Approximate analytical solutions of limited applicability have been presented for cases in which a geothermal reservoir, initially boiling everywhere is produced at a constant rate. In this section detailed numerical results are presented for two cases simulating the response of such two-phase geothermal reservoirs. The bottomhole fluid pressure and temperature variations with time are examined as well as the radial distributions of flowing kinematic viscosity and steam saturation at selected times. Both drawdown and buildup flow tests are simulated.

2.4.1 Background of Theory

Recently Garg [1978], Grant [1978] and Moench and Atkinson [1977] have examined the drawdown response of initially two-phase geothermal reservoirs. The plot of pressure drop versus logarithm of time asymptotes to a straight line after an initial nonlinear period; the slope m of the straight line is related to the kinematic mobility as follows:

$$(k/v)_t = \frac{1.15 M}{2\pi H m} \quad (2.25)$$

where

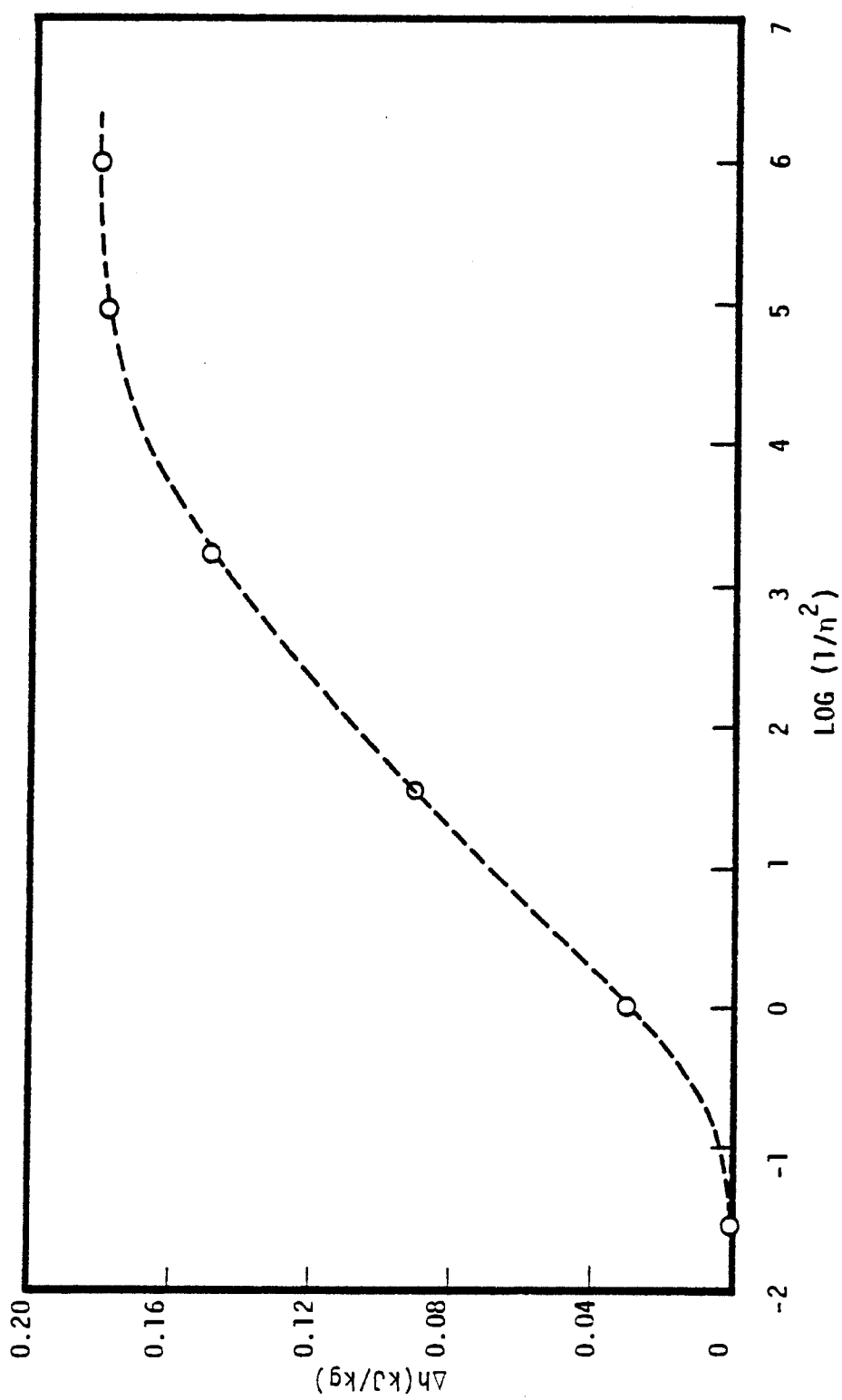


Figure 2.3. Enthalpy variation as a function of $1/n^2$ for hot water reservoir.

$$(k/v)_t = k/v_t \quad (2.26)$$

$$\frac{1}{v_t} = \frac{k_{rl}}{v_l} + \frac{k_{rg}}{v_g} \quad (2.27)$$

Given flowing enthalpy h_f , it also is possible to obtain the separate liquid- and vapor-phase kinematic mobilities.

$$\frac{kk_{rl}}{v_l} = (k/v)_t \left[\frac{h_g - h_f}{h_g - h_l} \right]; \quad \frac{kk_{rg}}{v_g} = (k/v)_t \left[\frac{h_f - h_l}{h_g - h_l} \right] \quad (2.28)$$

The intercept of the straight line can be used to calculate an effective total formation compressibility C_T ; however, as noted by Garg [1978] and Sorey, et al. [1980], the inferred value often provides a very poor approximation to the actual value.

Sorey, et al. [1980] have numerically investigated the buildup behavior in initially two-phase reservoirs; the plot of pressure versus logarithm of time gives a straight line. The slope of the straight line can be used to calculate total kinematic mobility from Equation (2.25). The kinematic mobility inferred from the buildup data is, however, different from the one given by drawdown data; this illustrates the nonlinear nature of two-phase flow in porous media. Sorey, et al. also observed over-recovery of liquid saturation near the wellbore during buildup.

2.4.2 Two-Phase Reservoir Production Behavior

In the following, two cases will be considered in which the reservoir, initially boiling everywhere, is produced at a constant rate. The initial fluid state is given in Table 2.3.

Table 2.3
INITIAL FLUID STATE FOR TWO-PHASE CASES

<u>Case No.</u>	<u>Pressure, MPa</u>	<u>Steam Sat.</u>	<u>Enthalpy (kJ/kg)</u>
A.1	8.5917	0.28	1466
A.2	8.5917	0.05	1345

Figures 2.4 and 2.5 show the drawdown and the flowing enthalpy data. The drawdown data closely fit a straight line; the slope of the straight line m yields the flowing kinematic viscosity v_t .

$$v_t = \frac{2\pi H m}{1.15 M} k \quad (2.29)$$

The inferred values of v_t (Figures 2.4 and 2.5) are representative of a large region surrounding the producing well (see Figures 2.8 and 2.9) wherein $\alpha S_g/\partial r$ is small (Figures 2.10 and 2.11). After an initial nonlinear period, the flowing enthalpy approaches a more or less constant value (Figures 2.4 and 2.5) as predicted by the linear theory of Grant [1979a]; the flowing enthalpy does, however, undergo small fluctuations even at late times. With $h_l = 1345 \text{ kJ/kg}$ and $h_g = 2749 \text{ kJ/kg}$ (values corresponding to 8.5917 MPa), the separate liquid- and vapor-phase relative permeabilities as calculated from Equation (2.28) are given in Table 2.4.

The calculated relative permeability values are representative of the reservoir region wherein $\alpha S_g/\partial r$ is small. Agreement between the calculated and inferred values (especially gas) could be improved by evaluating v_l and v_g at actual bottom-hole conditions.

The pressure and temperature buildup data are given in Figures 2.6 and 2.7. For the high saturation case (case A.1), pressure buildup data fit a straight line; the inferred v_t from the straight line is characteristic of the two-phase region (see Figure 2.8). In the low-saturation case (case A.2), more than one straight line can be fit to the pressure buildup data indicating a nonlinear buildup response; the calculated v_t 's can, however, still be identified with those obtained in the two-phase region (Figure 2.9). Figures 2.10 and 2.11 show the vapor saturation distribution at different times; during buildup substantial liquid over-recovery is seen. The condensation front (Figures 10 and 11) eventually engulfs most of the reservoir region affected during the

Table 2.4
CALCULATION OF LIQUID- AND VAPOR-PHASE RELATIVE PERMEABILITIES

<u>Case</u>	<u>h_f (kJ/kg)</u>	<u>h_l (kJ/kg)</u>	<u>h_g (kJ/kg)</u>	<u>$\frac{kk_{rl}}{v_l}$ (s)</u>	<u>$\frac{kk_{rg}}{v_g}$ (s)</u>
A.1	2158	1346	2749	1.41×10^{-8}	1.95×10^{-8}
A.2	1414	1345	2749	7.70×10^{-8}	0.40×10^{-8}
<u>Case</u>	<u>v_l (m^2/s)*</u>	<u>v_g (m^2/s)*</u>	<u>k_{rl}</u>	<u>k_{rl} (actual)</u>	<u>k_{rg} (actual)</u>
A.1	1.245×10^{-7}	4.283×10^{-7}	0.035	0.167	0.033 - 0.056
A.2	1.245×10^{-7}	4.283×10^{-7}	0.192	0.034	0.18 - 0.25

* Values at $P \sim 8.5917$ MPa, $T \sim 300^\circ C$

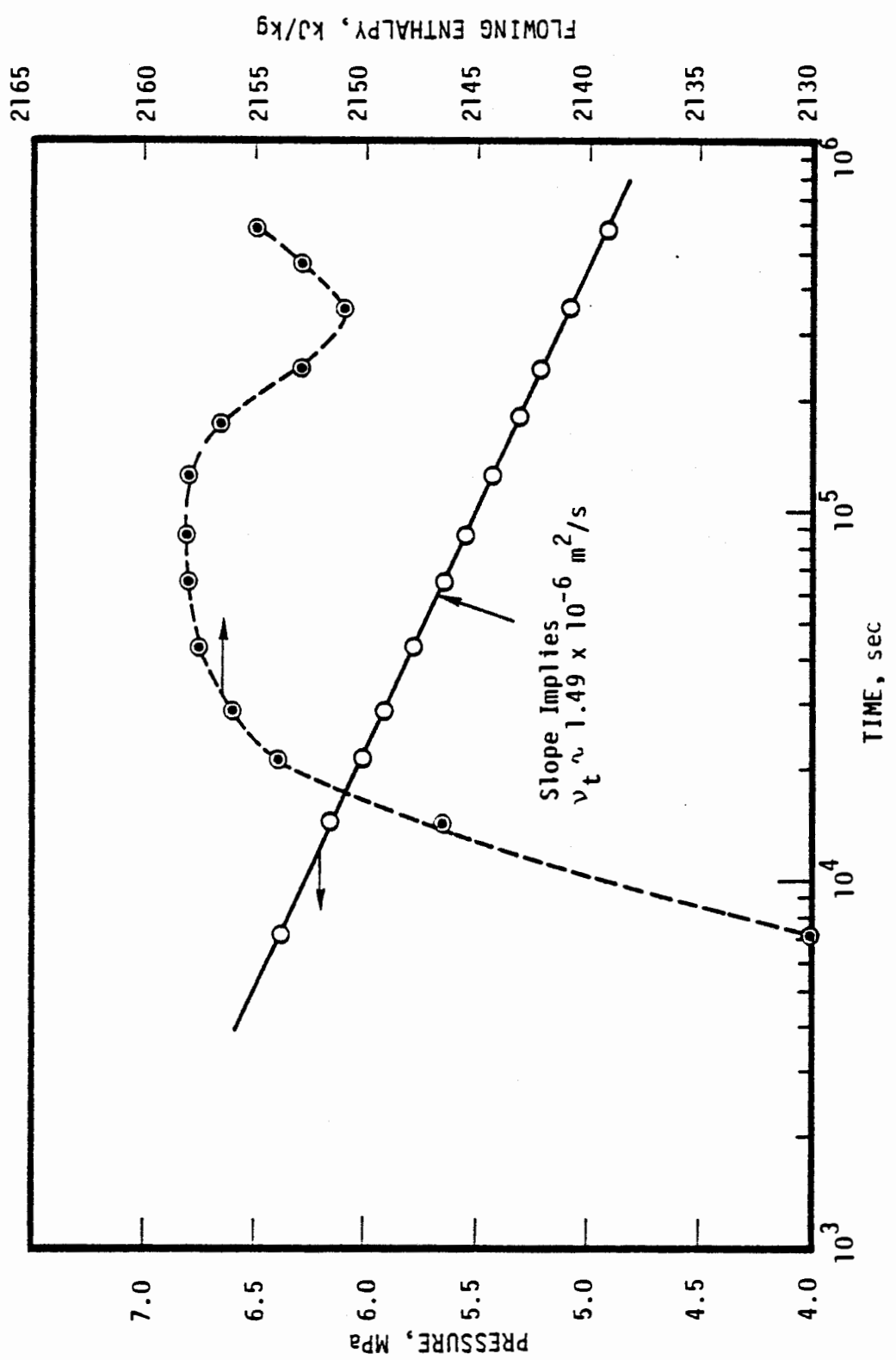


Figure 2.4. Pressure drawdown and flowing enthalpy for case A.1 ($p_i = 8.5917 \text{ MPa}$, $s_{gi} = 0.28$, $h_i = 1466 \text{ kJ/kg}$).

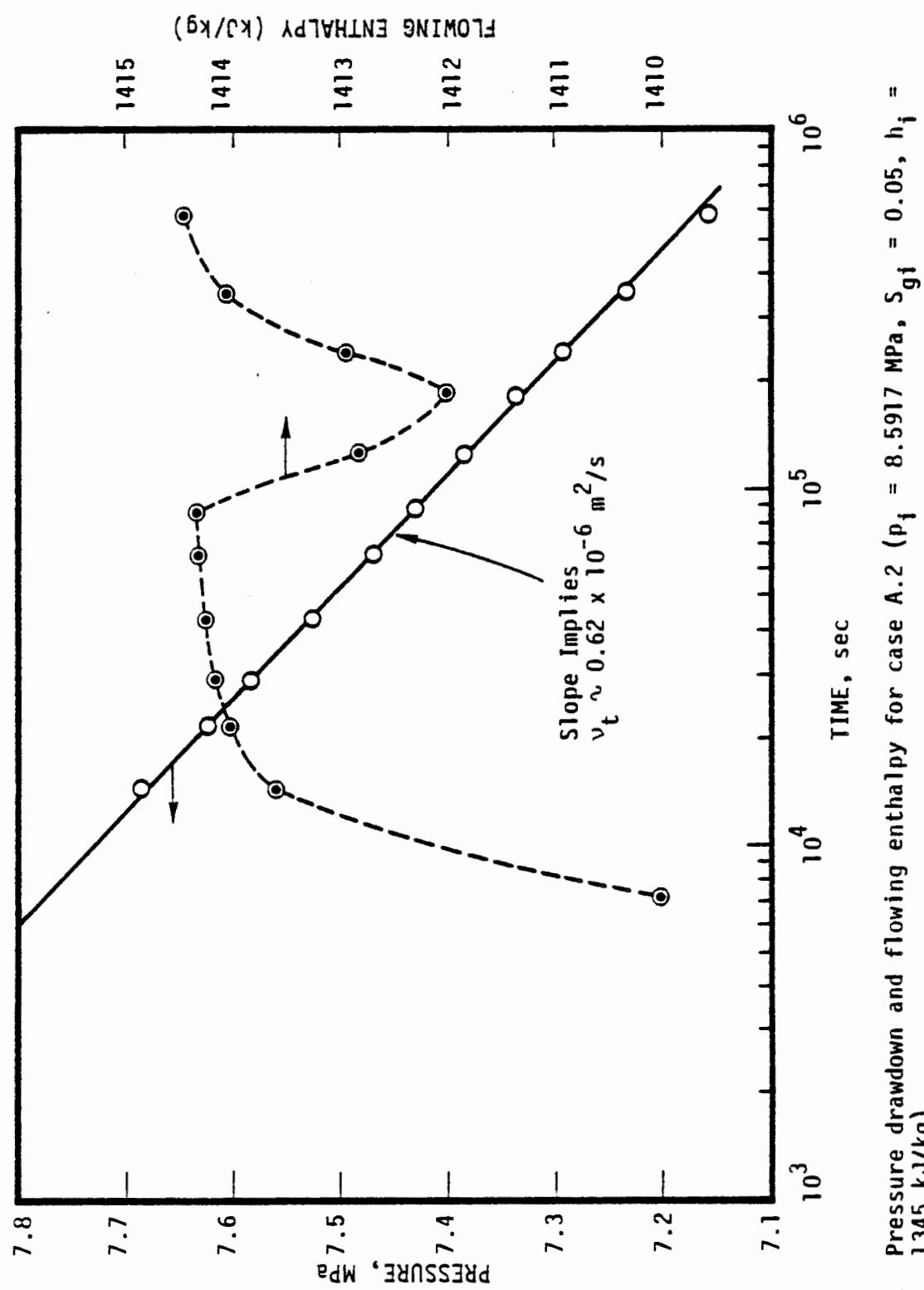


Figure 2.5. Pressure drawdown and flowing enthalpy for case A.2 ($p_i = 8.5917 \text{ MPa}$, $s_{gi} = 0.05$, $h_i = 1345 \text{ kJ/kg}$).

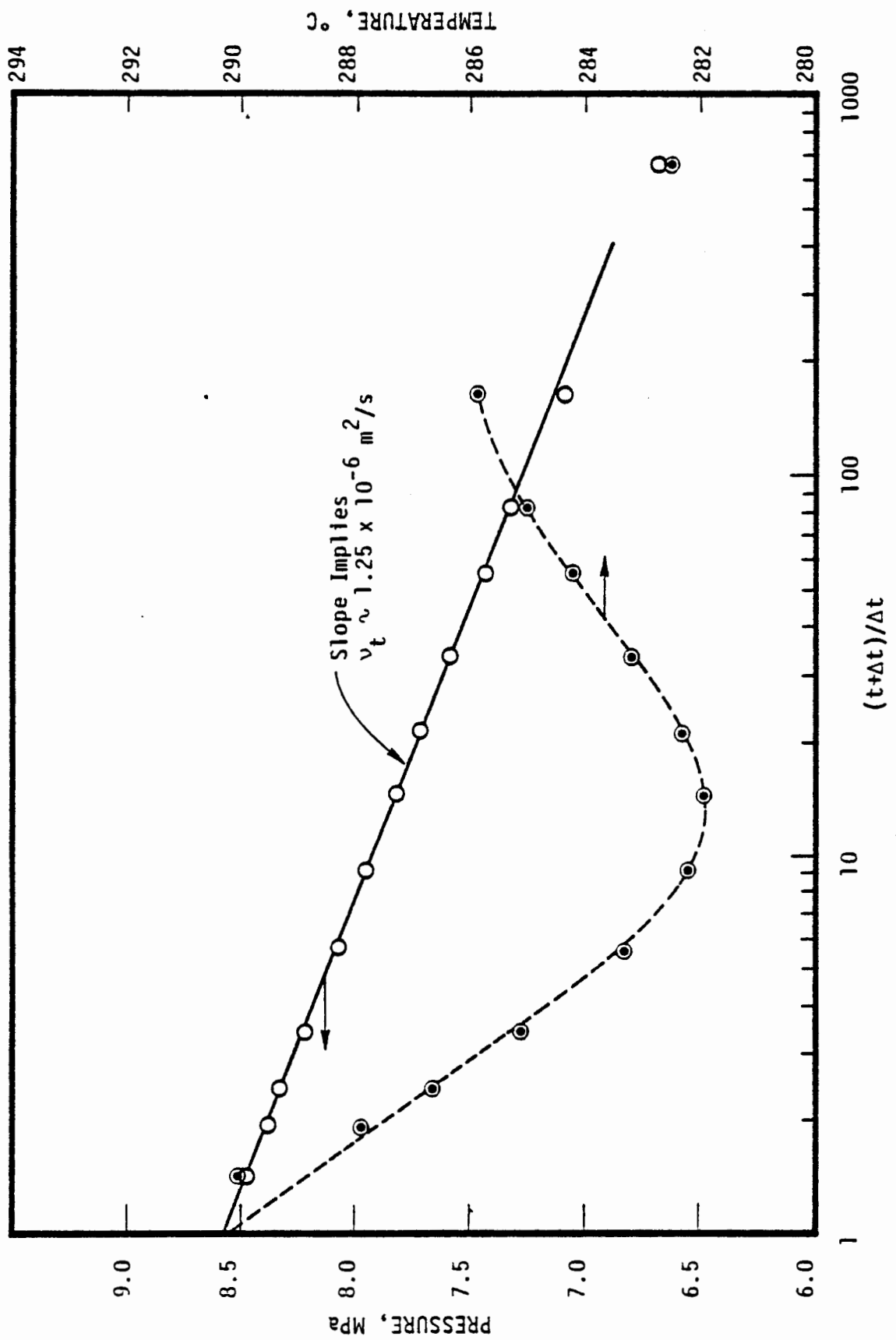


Figure 2.6. Pressure and temperature buildup data for case A.1.

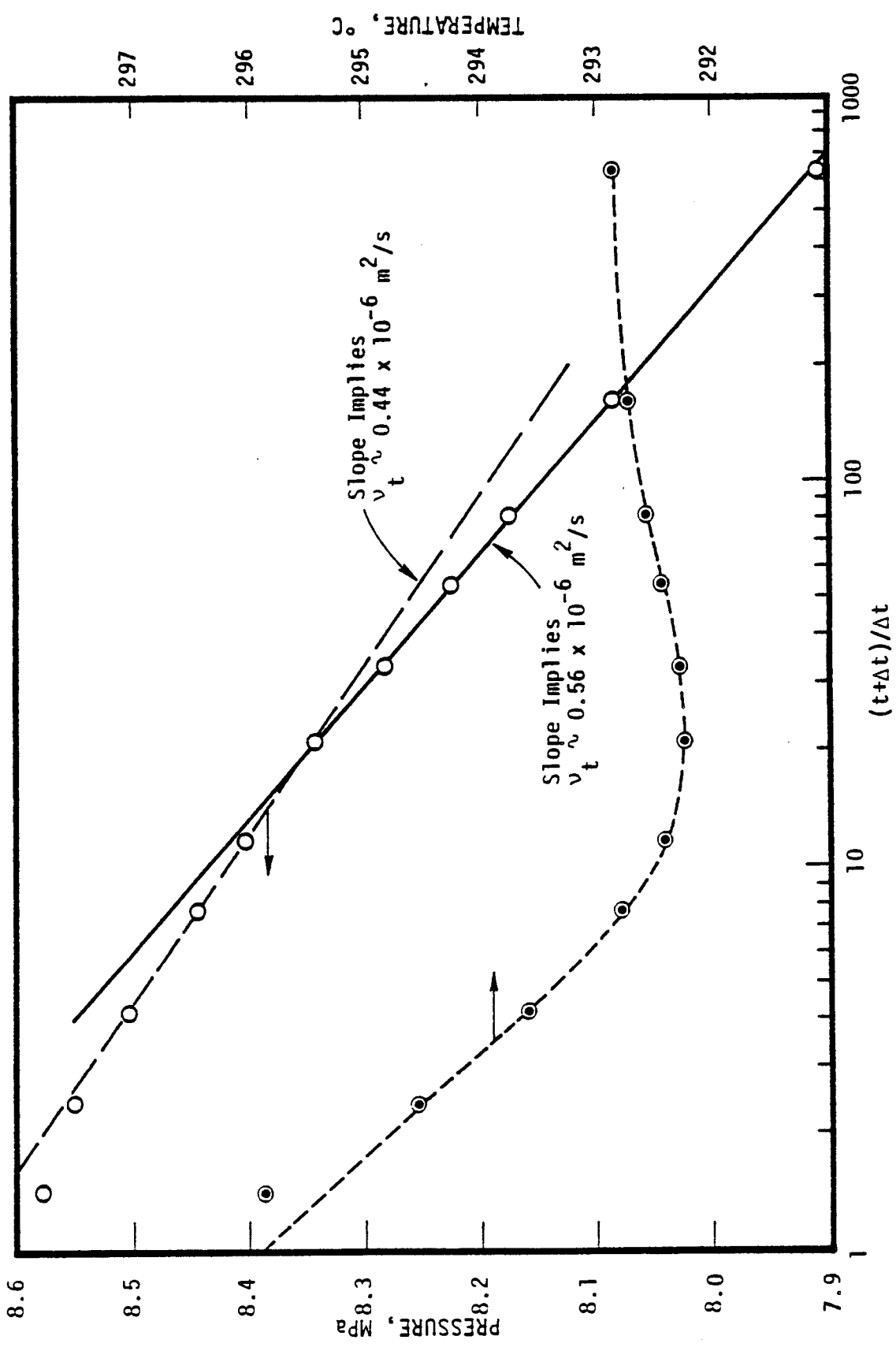


Figure 2.7. Pressure and temperature buildup data for case A.2.

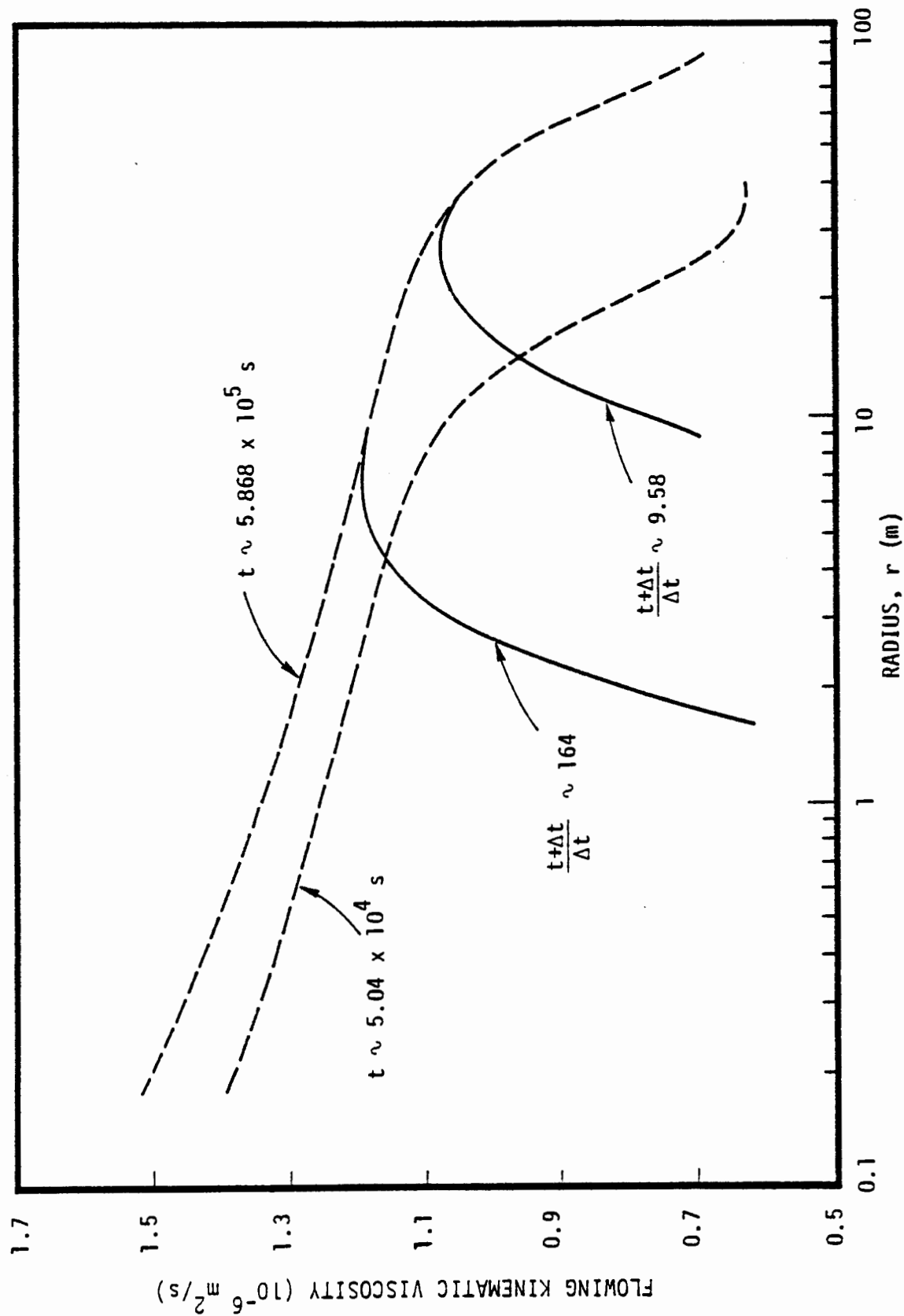


Figure 2.8. Radial distribution of flowing kinematic viscosity v_t at selected times for case A.1.

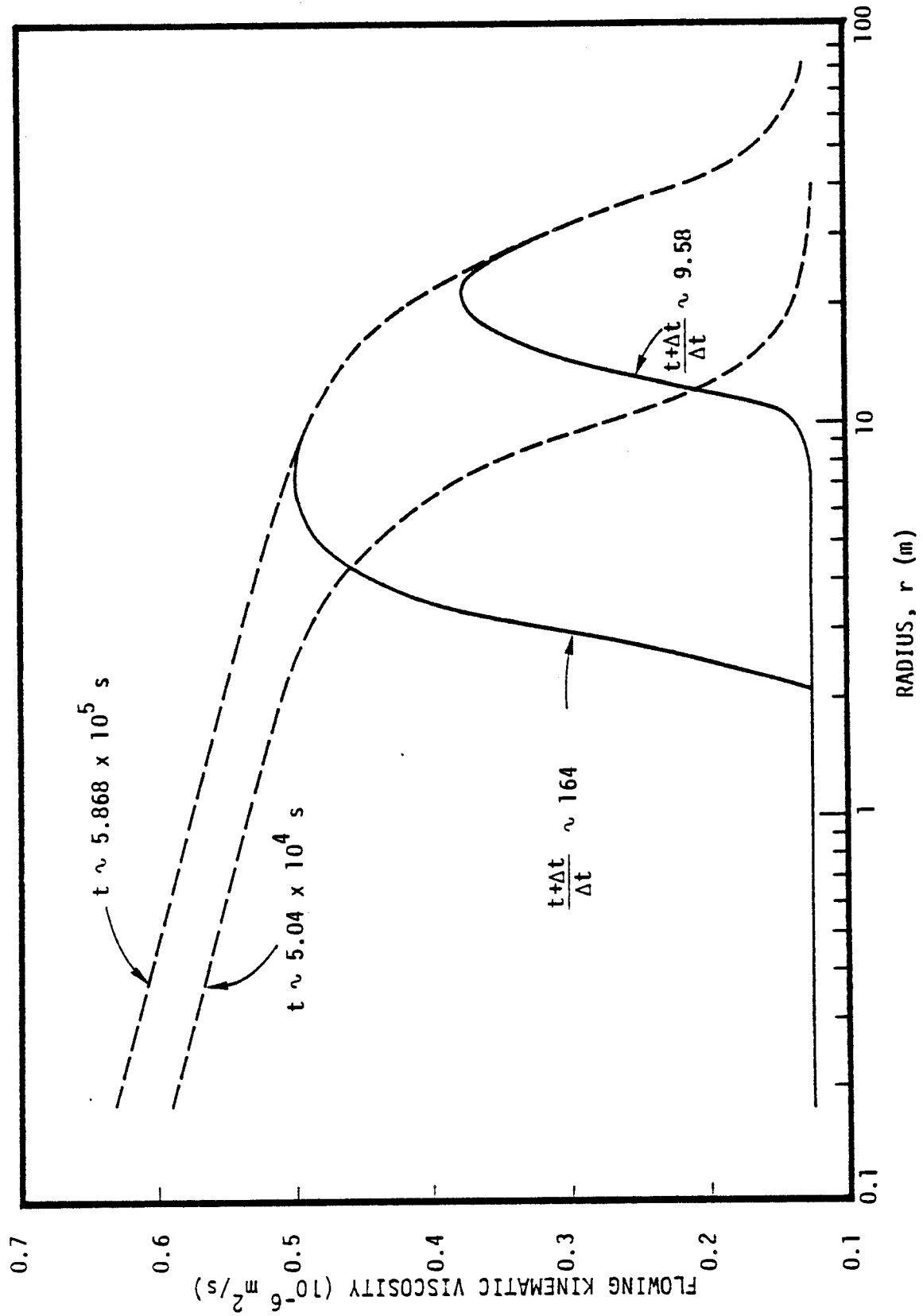


Figure 2.9. Radial distribution of flowing kinematic viscosity v_t at selected times for case A.2.

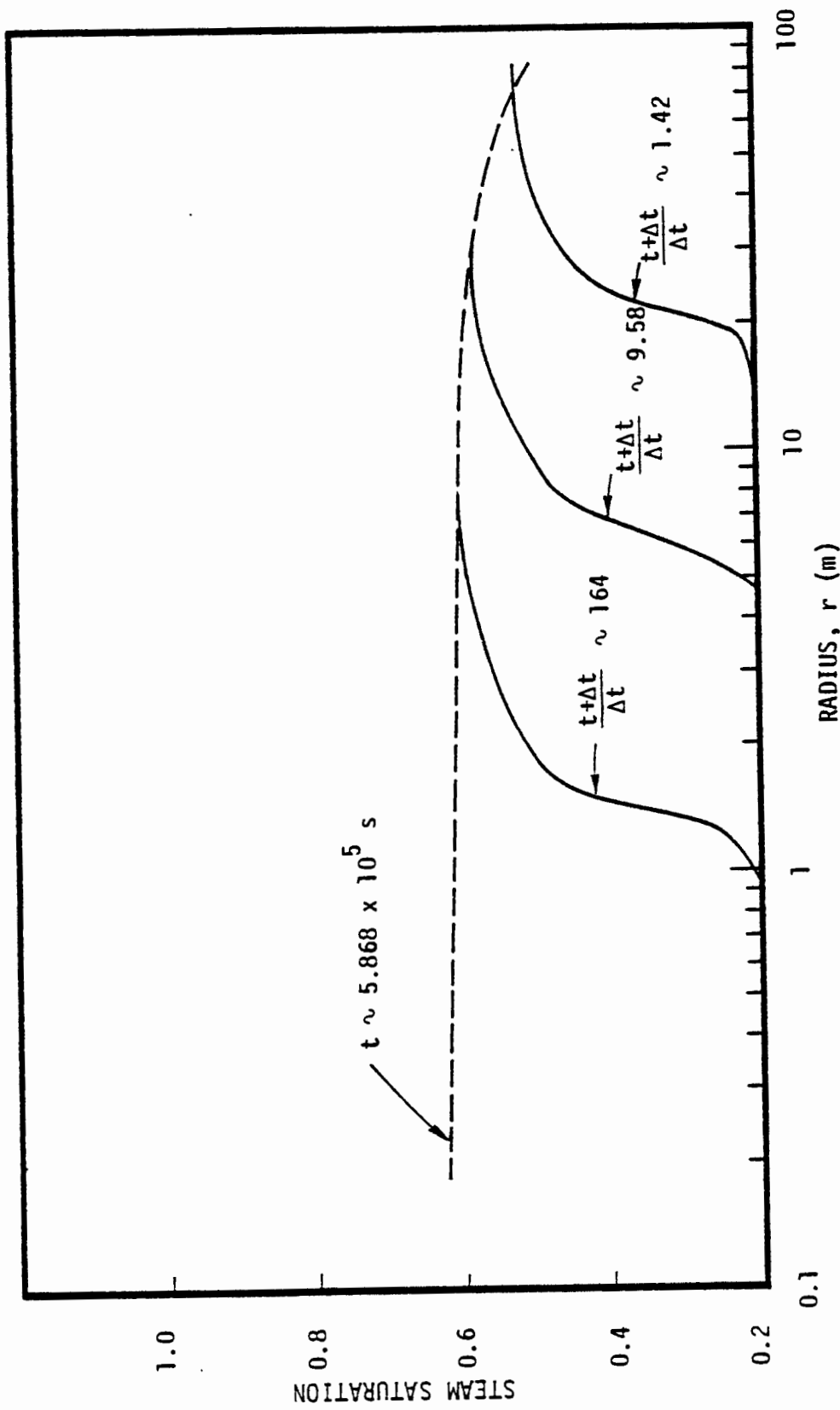


Figure 2.10. Radial distribution of steam saturation S_g at selected times for case A.1.

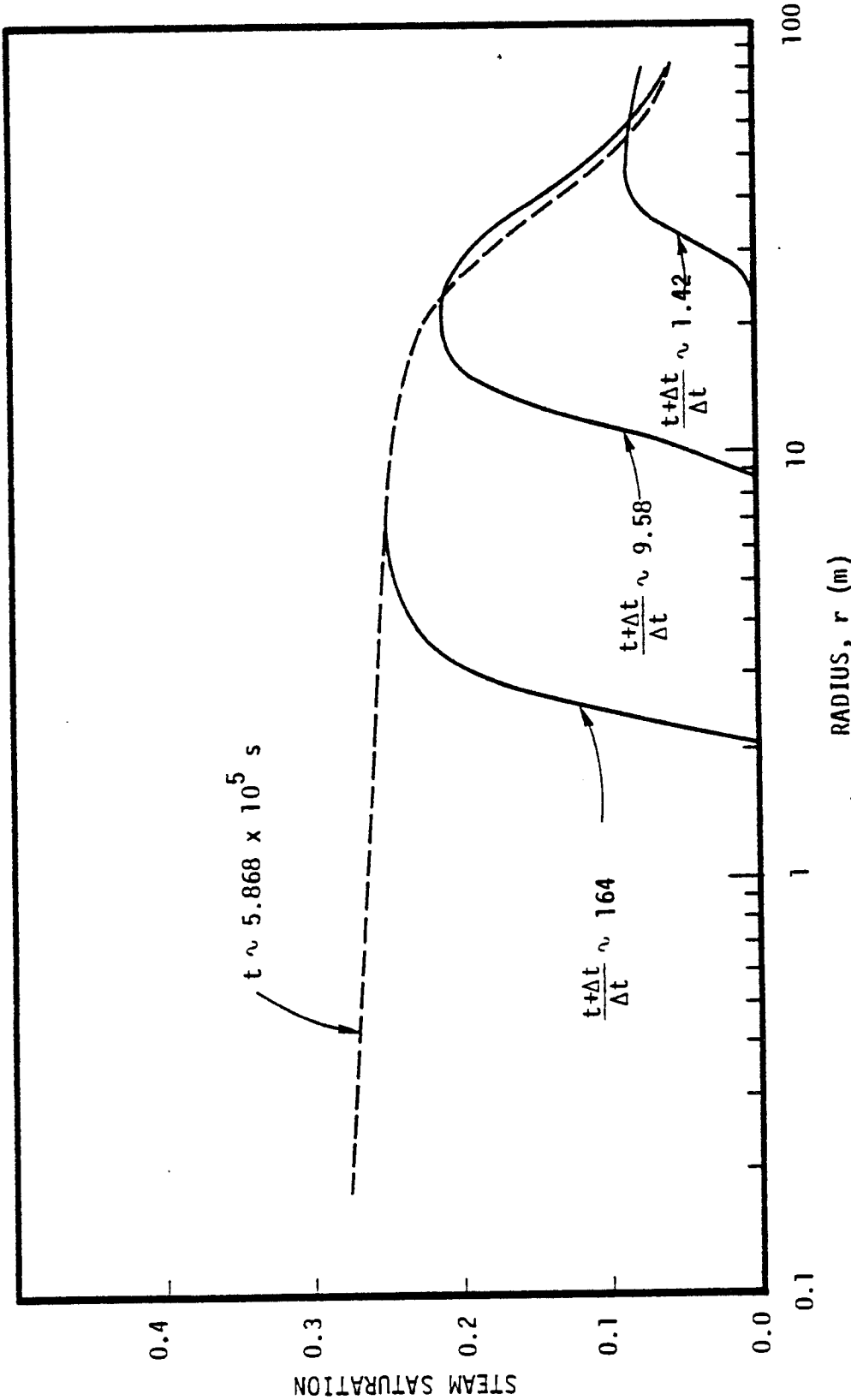


Figure 2.11. Radial distribution of steam saturation S_g at selected times for case A.2.

drawdown period. The reason for liquid-phase over-recovery during buildup is fairly straightforward. During drawdown, a decrease in pressure is accompanied by a corresponding reduction in temperature. (Note that pressure and temperature in two-phase flow are not independent.) On shutin, the pressure tends to recover to the initial formation pressure. The temperature recovery beyond the saturation point at local reservoir conditions occurs on a much longer time scale than the one for pressure recovery. (Temperature recovery is mainly governed by heat conduction.) A puzzling aspect of pressure recovery is that it appears to be essentially governed by the two-phase region in the reservoir. The reason for the latter behavior must be sought in the great difference between the liquid- and two-phase compressibilities. Since the liquid compressibility is much smaller (by 2 to 3 orders of magnitude) than the two-phase compressibility, the liquid-phase will reach pressure equilibrium (i.e., zero pressure gradient) on a much faster time scale than the two-phase region. Numerical calculations show that the liquid-region pressure gradients are essentially zero for the entire buildup period. Finally, it is noted that the condensation front does not obey the law ($R \propto t^{1/2}$); this demonstrates that the similarity solution (see e.g., O'Sullivan [1980]) does not apply to buildup in two-phase reservoirs.

2.5 Production Behavior of Hot Water Reservoirs which Flash on Fluid Withdrawal

In this section the response of an initially single-phase reservoir which undergoes flashing on fluid production is considered. Detailed numerical results are presented which simulate both the propagation of the flash front during production and the propagation of a condensation front, during buildup. The presence of these fronts is shown to greatly complicate the interpretation of the well test data.

2.5.1 Background of Theory

Garg [1978] has considered the drawdown response of an initially single-phase reservoir which undergoes flashing on fluid production. In this case, the reservoir exhibits single-phase response until some time t_f when the well pressure falls below the saturation pressure at the local reservoir temperature; for $t > t_f$, a flash front starts propagating into the formation. The reservoir (for $t > t_f$) is two-phase for $r < R$ [$R = R(t)$ denotes the location of the flash front], and is single-phase for $r > R$. The drawdown curve ($t > t_f$) asymptotes to a straight line; the slope of the straight line yields the total kinematic mobility $(k/v)_t$ (c.f., Equation (2.25)). The buildup behavior of such reservoirs has apparently not been previously investigated.

2.5.2 Hot Water Reservoirs which Undergo Flashing

To study the drawdown/buildup behavior of hot water reservoirs which undergo flashing on production, two cases will be considered. The initial fluid-state for these cases is given in Table 2.5.

Table 2.5
INITIAL FLUID-STATE FOR HOT-WATER RESERVOIRS WHICH UNDERGO
FLASHING ON PRODUCTION

<u>Case No.</u>	<u>Pressure, MPa</u>	<u>Temperature, °C</u>
B.1	8.7917	300
B.2	8.9917	300

Figures 2.12 and 2.13 show the simulated drawdown histories for the two cases; these figures show only the two-phase part of the drawdown response. In case B.1 (low pressure case), the flash front propagates to approximately 20 m at the end of the drawdown period (Figure 2.18); for the high-pressure case (B.2), the flash front

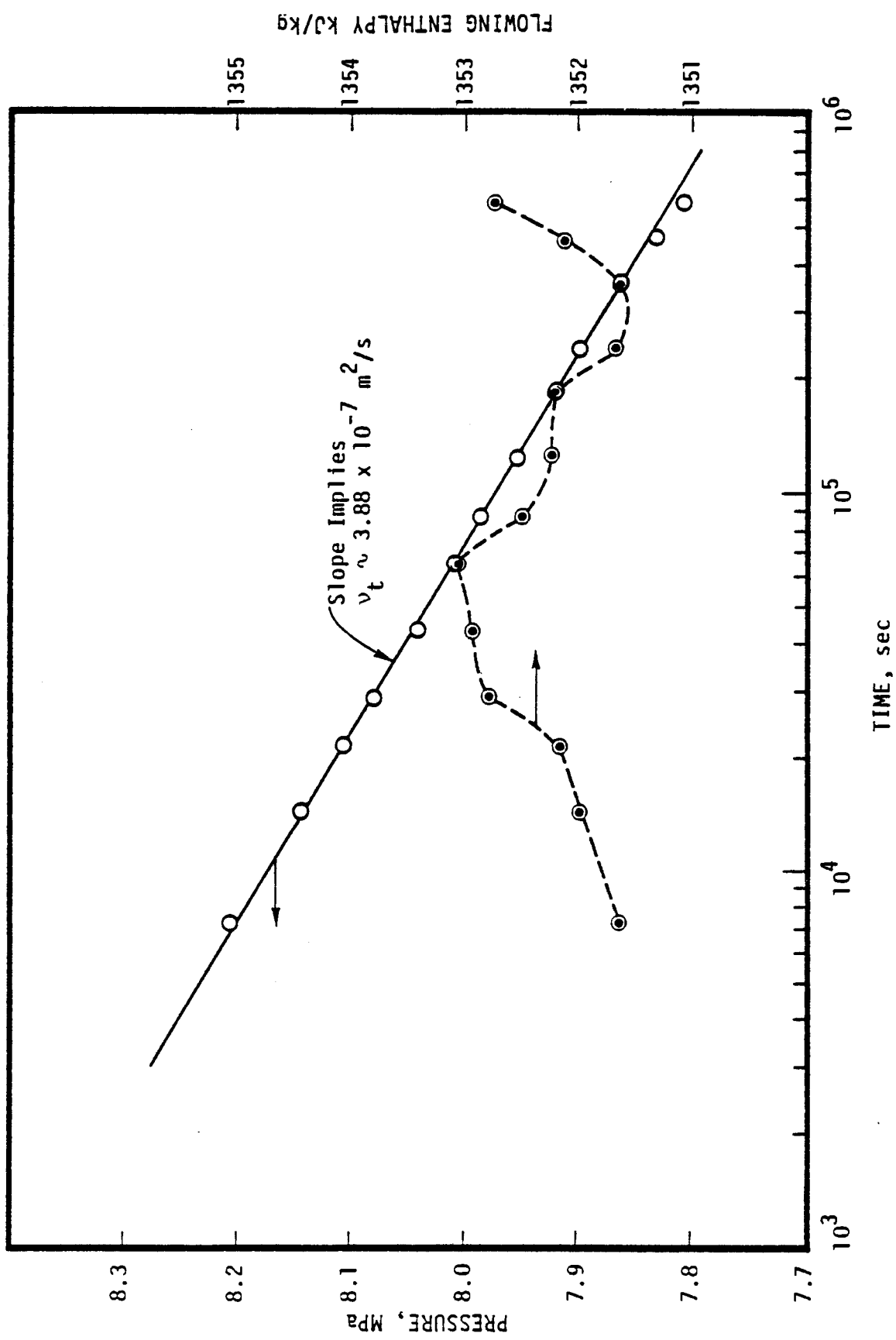


Figure 2.12. Pressure drawdown and flowing enthalpy for case B.1 ($p_i = 8.7917 \text{ MPa}$, $T_i = 300^\circ\text{C}$)

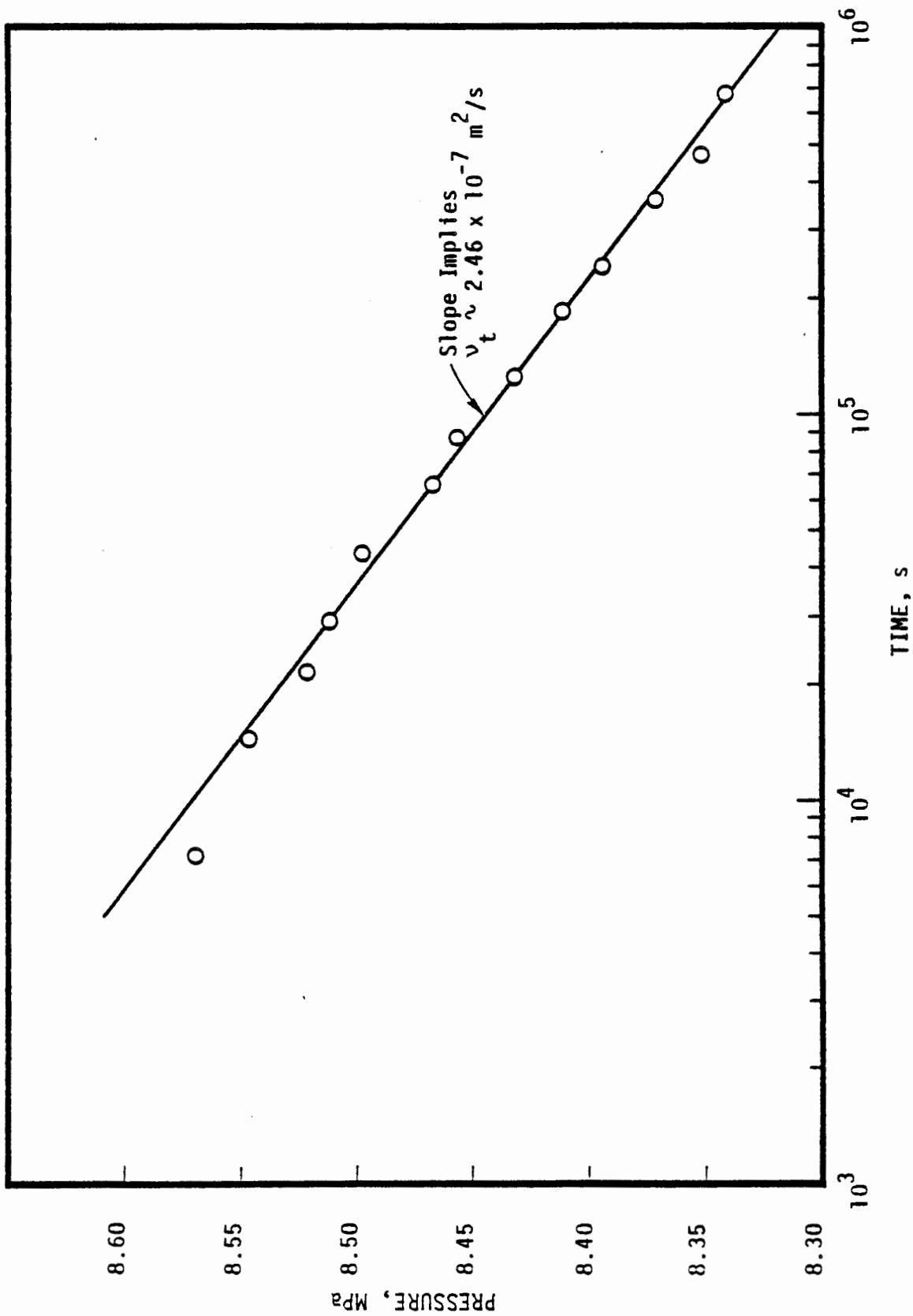


Figure 2.13. Pressure drawdown for case B.2 ($p_i = 8.9917 \text{ MPa}$, $T_i = 300^\circ\text{C}$)

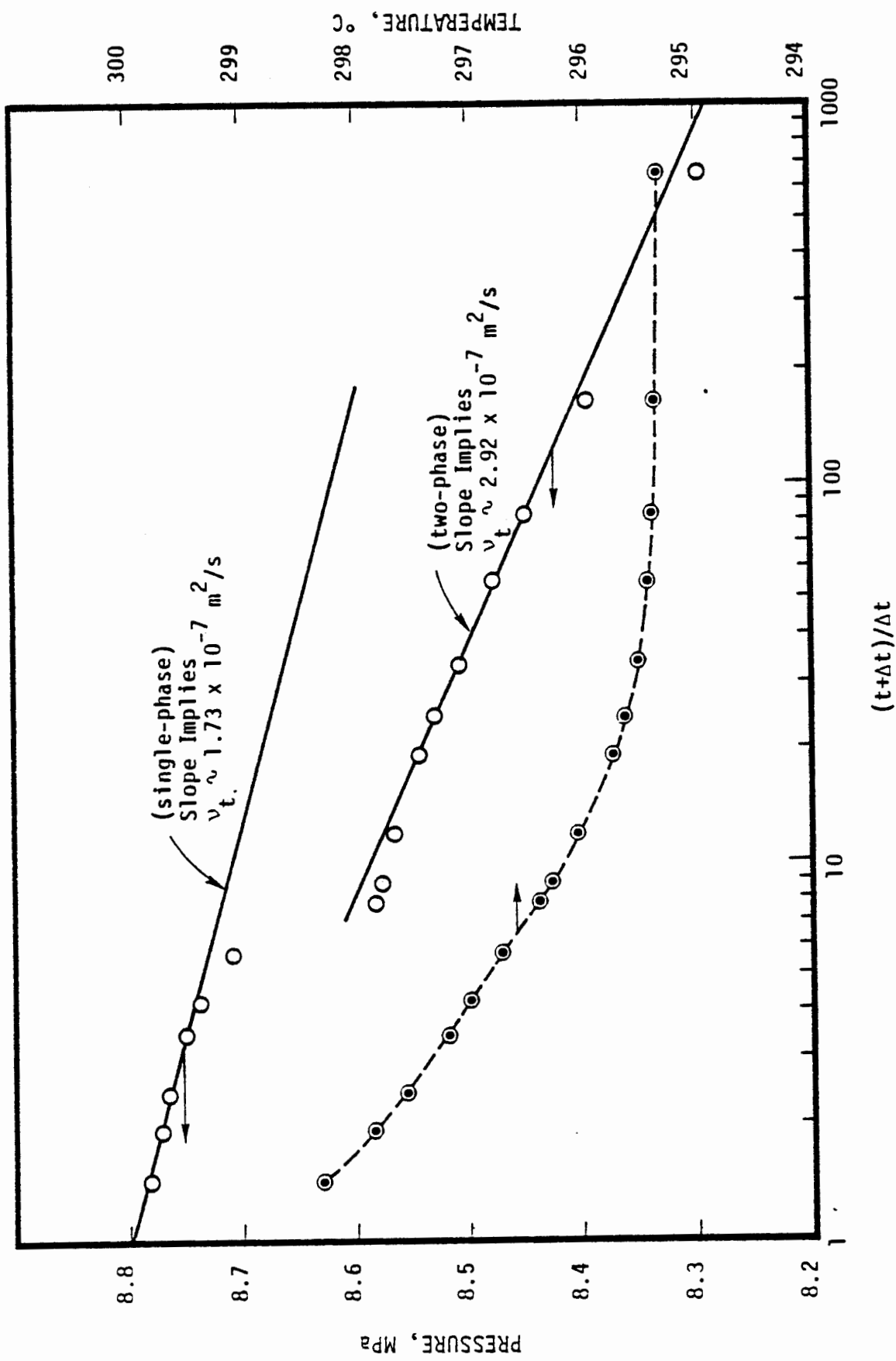


Figure 2.14. Pressure and temperature buildup data for case B.1.

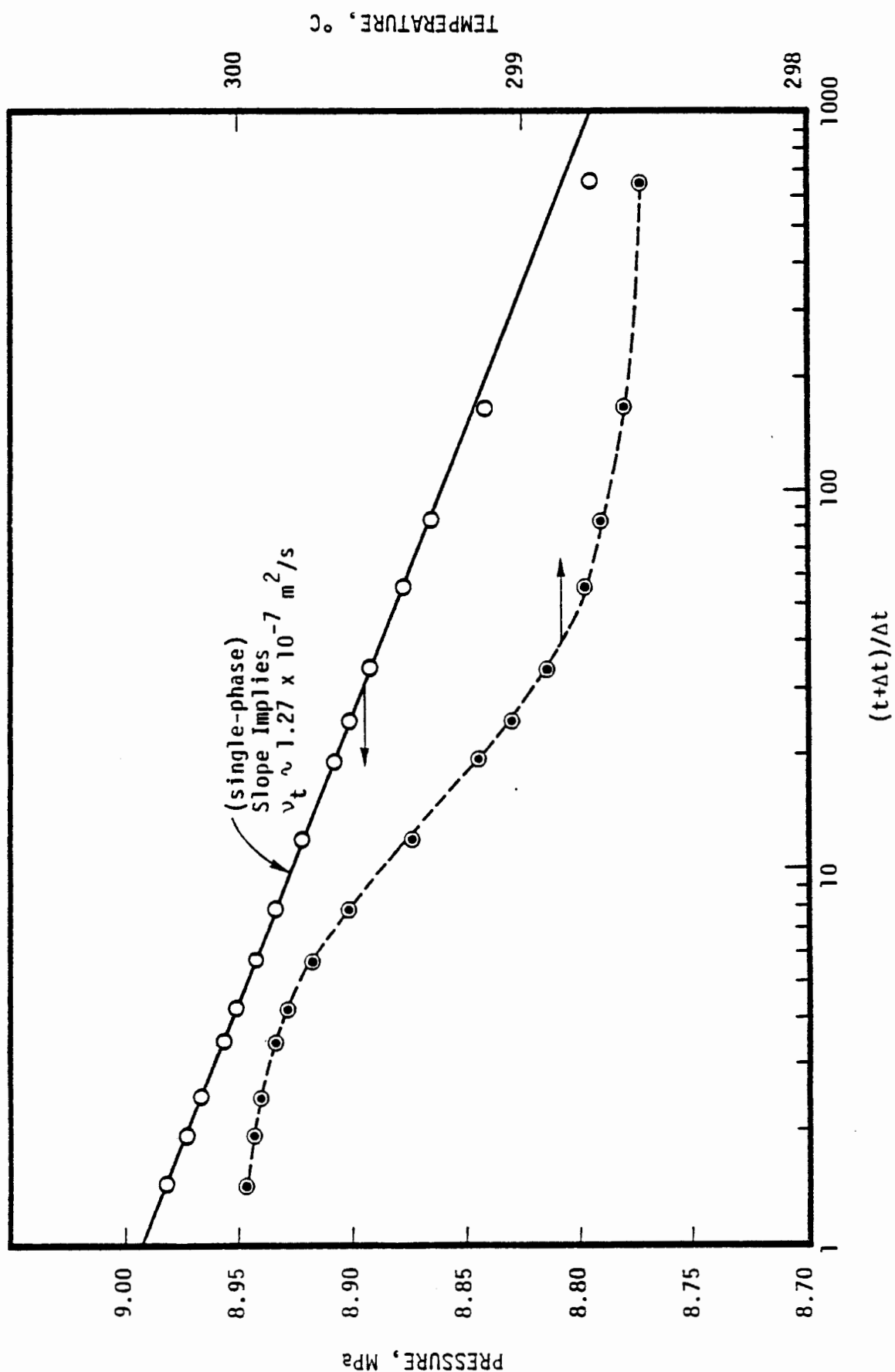


Figure 2.15. Pressure and temperature buildup data for case B.2.

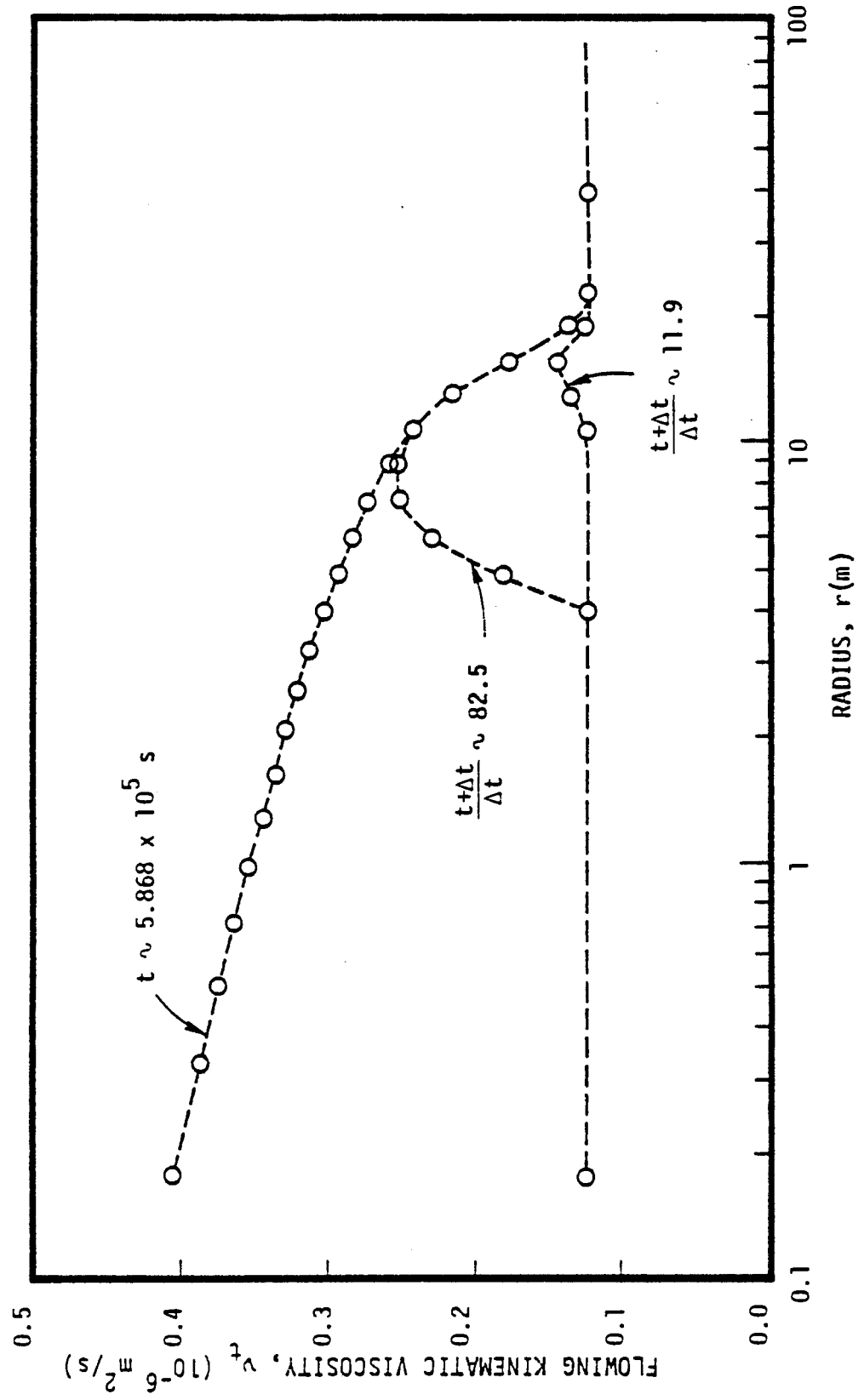


Figure 2.16. Radial distribution of flowing kinematic viscosity v_t at selected times for Case B.1.

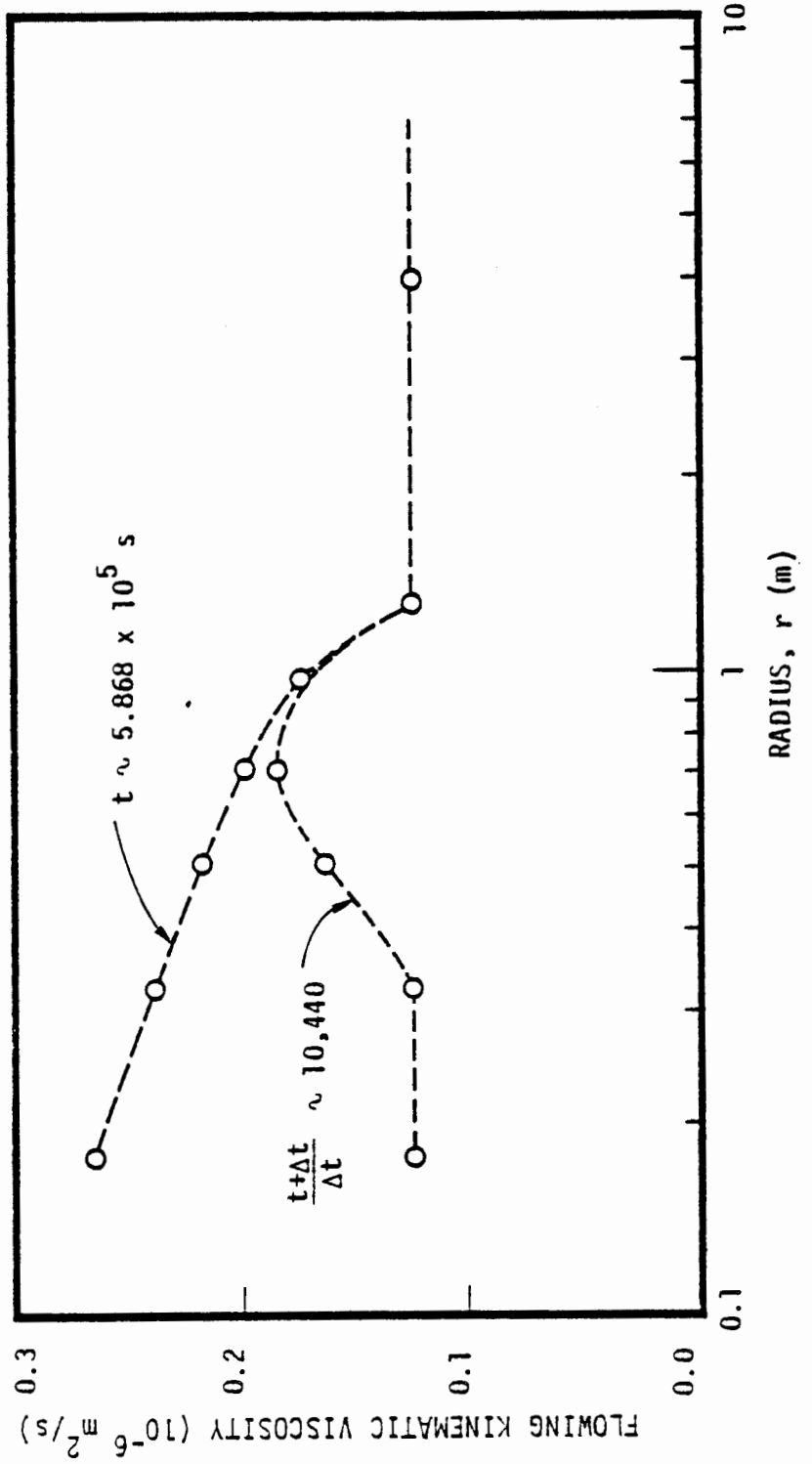


Figure 2.17. Radial distribution of flowing kinematic viscosity v_t at selected times for case B.2.

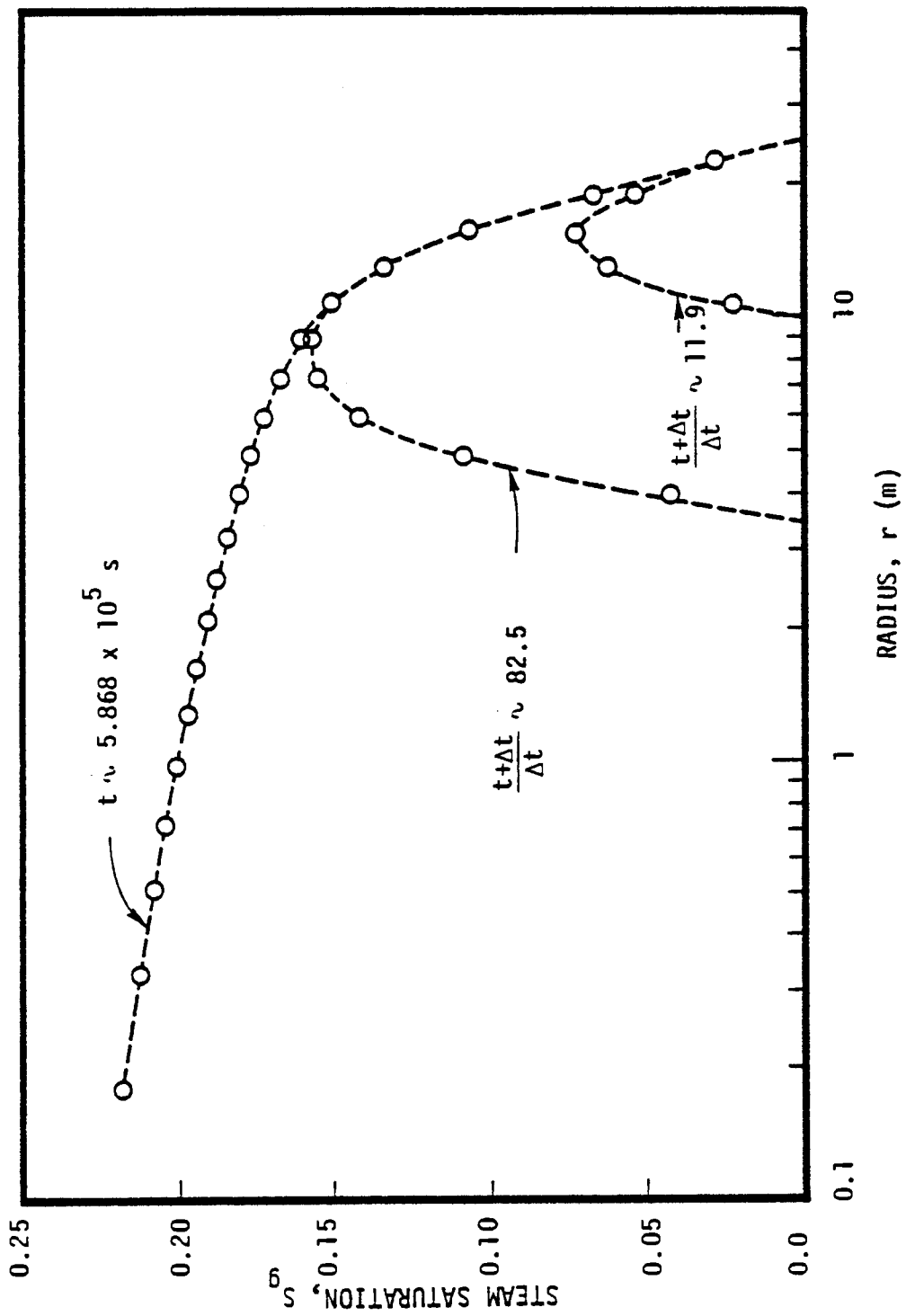


Figure 2.18. Radial distribution of steam saturation S_g at selected times for case B.1.

advances to only 1 m (Figure 2.19). The drawdown data closely fit straight lines; the slopes of the straight lines yield flowing kinematic viscosities which are representative of the two-phase part of the reservoir wherein $\partial S_g / \partial r$ is small (see Figures 2.12, 2.13, 2.16 and 2.17).

The buildup behavior is shown in Figures 2.14 and 2.15. Referring to Figure 2.14, it may be seen that in the low pressure case, the initial buildup behavior is governed by the two-phase region of the reservoir; the slope of this curve yields v_t which is characteristic of the two-phase region created during drawdown (see Figure 2.14 and 2.16). The pressure buildup is accompanied by the propagation of a condensation front, originating at the well, into the formation (Figure 2.18); the condensation front eventually engulfs the entire two-phase region after which the buildup behavior is essentially that of a single-phase fluid. The two-buildup segments (single-phase and two-phase) are separated by approximately one log cycle (Figure 2.14). The single-phase buildup behavior (Figure 2.14) extends over less than one-half cycle; the slope of this straight line yields a kinematic viscosity $v_t \sim 1.73 \times 10^{-7} \text{ m}^2/\text{s}$ which is approximately 40 percent larger than the actual value of $1.245 \times 10^{-7} \text{ m}^2/\text{s}$. The divergence between the inferred and actual values of v_t is really not surprising in view of the fact that single-phase buildup response in this particular instance is observed for less than one-half log cycle. In the high pressure case (B.2), the two-phase buildup behavior lasts for only a very brief period (at most a few minutes, see Figures 2.17 and 2.19); the single-phase buildup, however, lasts for approximately two-log cycles (Figure 2.15). The slope of the straight line in case B.2 yields a v_t in good agreement with the actual value of $1.245 \times 10^{-7} \text{ m}^2/\text{s}$.

The above discussion of buildup behavior illustrates the importance of selecting the correct straight line. If sufficiently long (at least one-log cycle) straight line segments can be identified, then the buildup data may be interpreted to give both

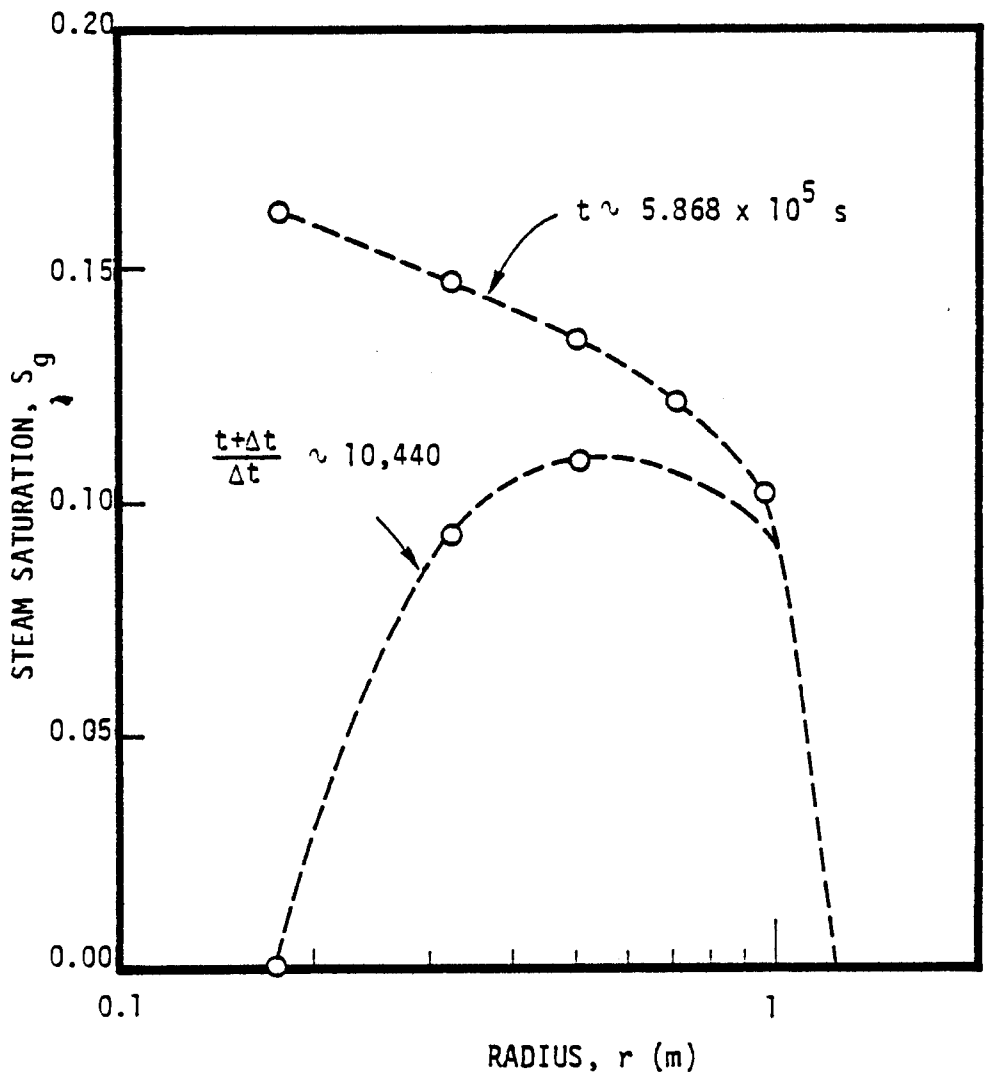


Figure 2.19. Radial distribution of steam saturation S_g at selected times for case B.2.

single- and two-phase kinematic mobilities. In many practical situations, however, it is likely that the buildup data will not be such as to make possible the unambiguous determination of both single- and two-phase mobilities.

SECTION 3: THEORETICAL INJECTION BEHAVIOR ANALYSES

3.1 Introduction

In this section numerical simulations are presented which describe the injection data for a single well injecting into a geothermal reservoir. The S³ geothermal reservoir simulator CHARGR is used to analyze single-phase and two-phase reservoirs.

3.2 Summary

It is demonstrated that injection data for single-phase and two-phase geothermal reservoirs can be interpreted to yield absolute formation permeability. The pressure fall-off data subsequent to injection are of lesser utility.

3.3 Cold Water Injection into a Hot Water Well

In this section, a case is considered wherein cold water is injected into a single-phase (all liquid) hot water well. The initial formation pressure and temperature are 8.7917 MPa and 300°C respectively; the temperature of the injected fluid (injection rate = 35 kg/s) is approximately 151°C. The pressure buildup (Injection) data are seen to fit a straight line (Figure 3.1); the slope of this straight line yields $v_t \sim 1.985 \times 10^{-7} \text{ m}^2/\text{s}$ which is in good agreement with the kinematic viscosity of the injected fluid ($\sim 1.955 \times 10^{-7} \text{ m}^2/\text{s}$). Figure 3.2 shows the radial distribution of v_t and temperature T at the end of the injection period ($\sim 5.868 \times 10^5 \text{ s}$); the thermal front is seen to have propagated approximately 6 m into the formation. The fall-off (shutin) data are plotted in Figure 3.3; the fall-off data asymptote to a straight line whose slope yields a value of $v_t \sim 1.20 \times 10^{-7} \text{ m}^2/\text{s}$ which is in good agreement with the kinematic viscosity of hot water ($\sim 1.25 \times 10^{-7} \text{ m}^2/\text{s}$). No straight line corresponding to cold water pressure fall-off can, however, be identified on Figure 3.3; the reason for this is tied to the relatively small radius ($\sim 6 \text{ m}$) affected by cold

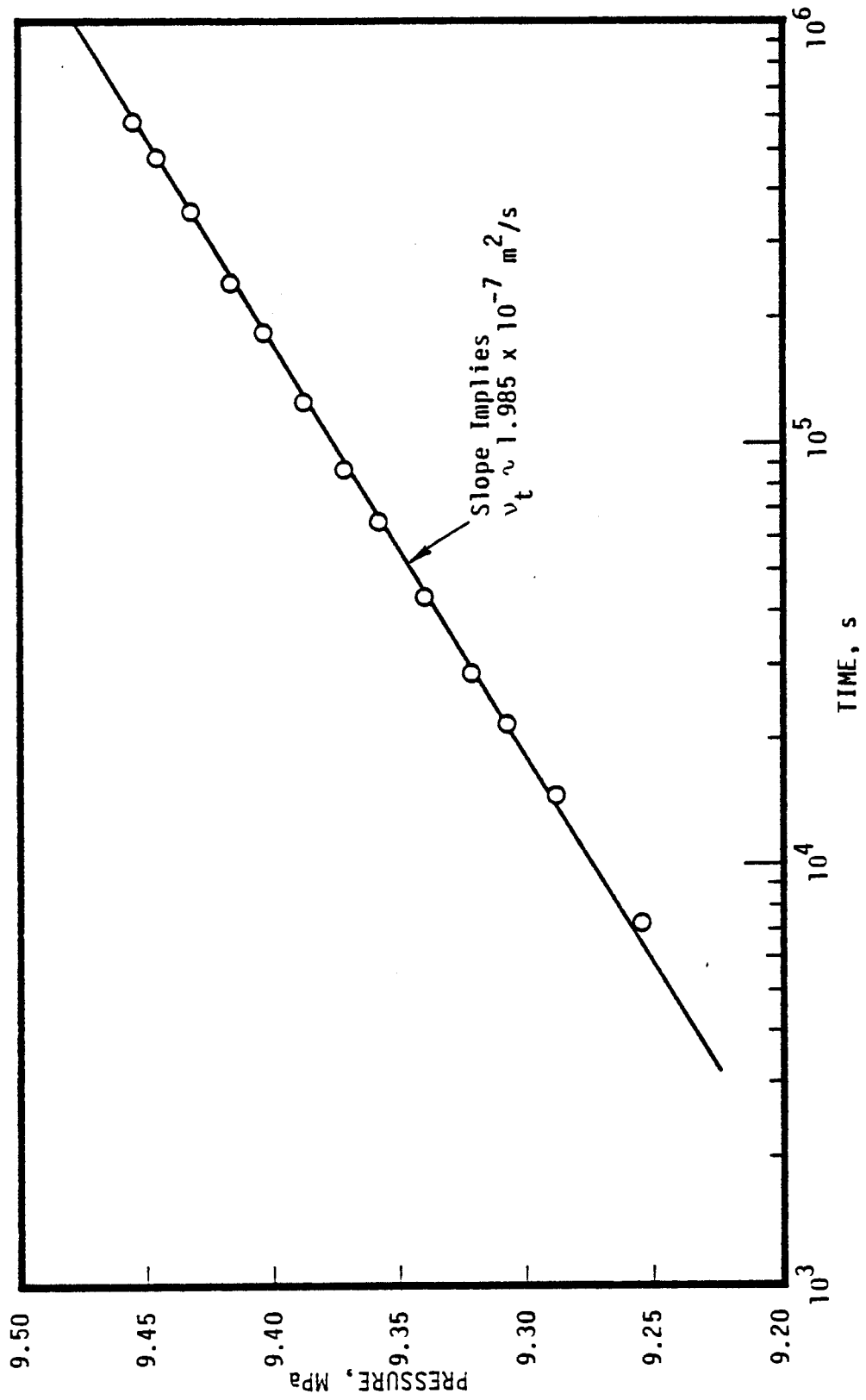


Figure 3.1. Pressure buildup (Injection) data for cold water injection into a hot water well ($p_1 = 8.9917 \text{ MPa}$, $T_1 = 300^\circ\text{C}$, $T_{injection} \sim 151^\circ\text{C}$).

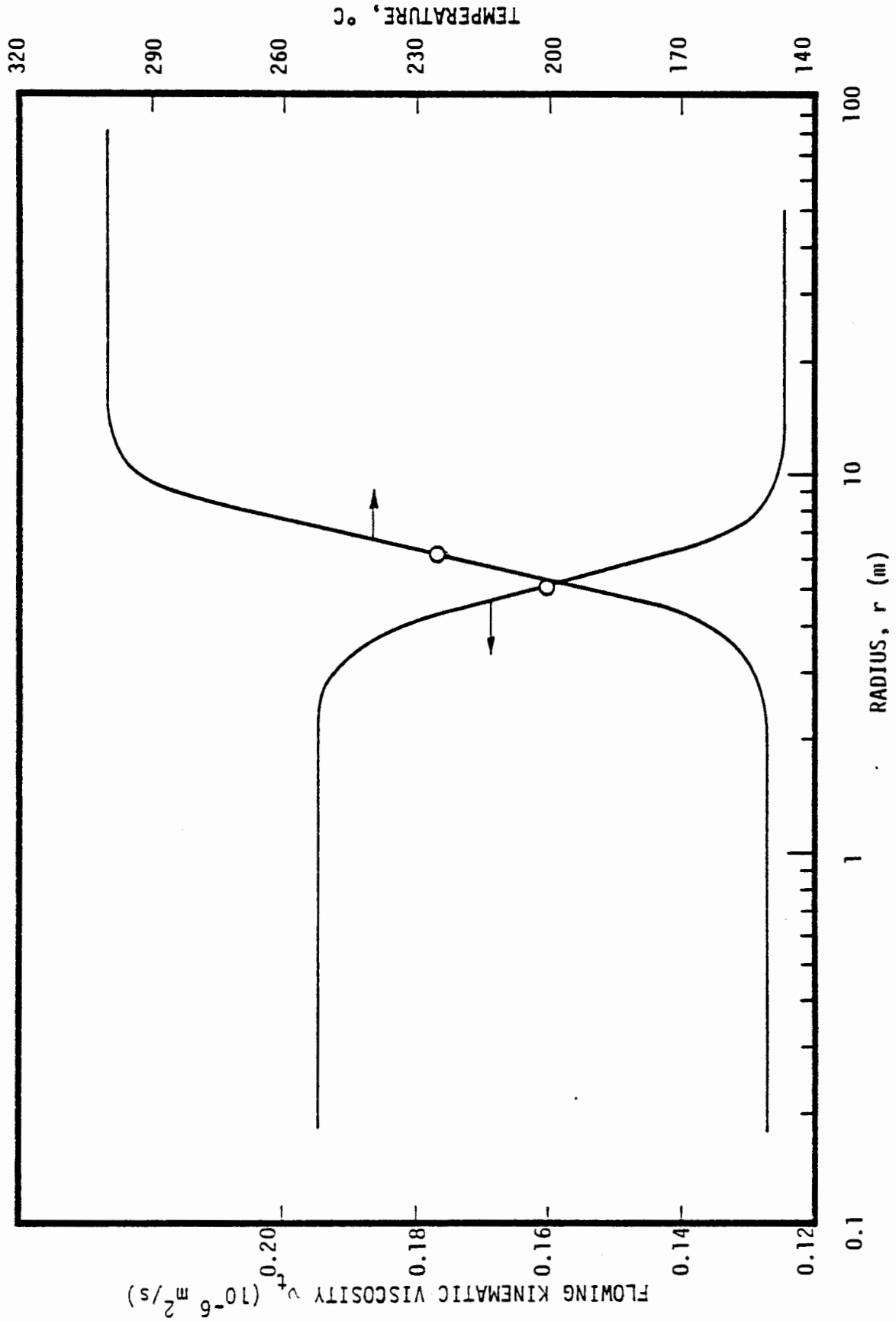


Figure 3.2. Radial distribution of flowing kinematic viscosity and temperature at $t \sim 5.868 \times 10^5$ s (end of injection period). O denotes the location of the front (defined as the mid point).

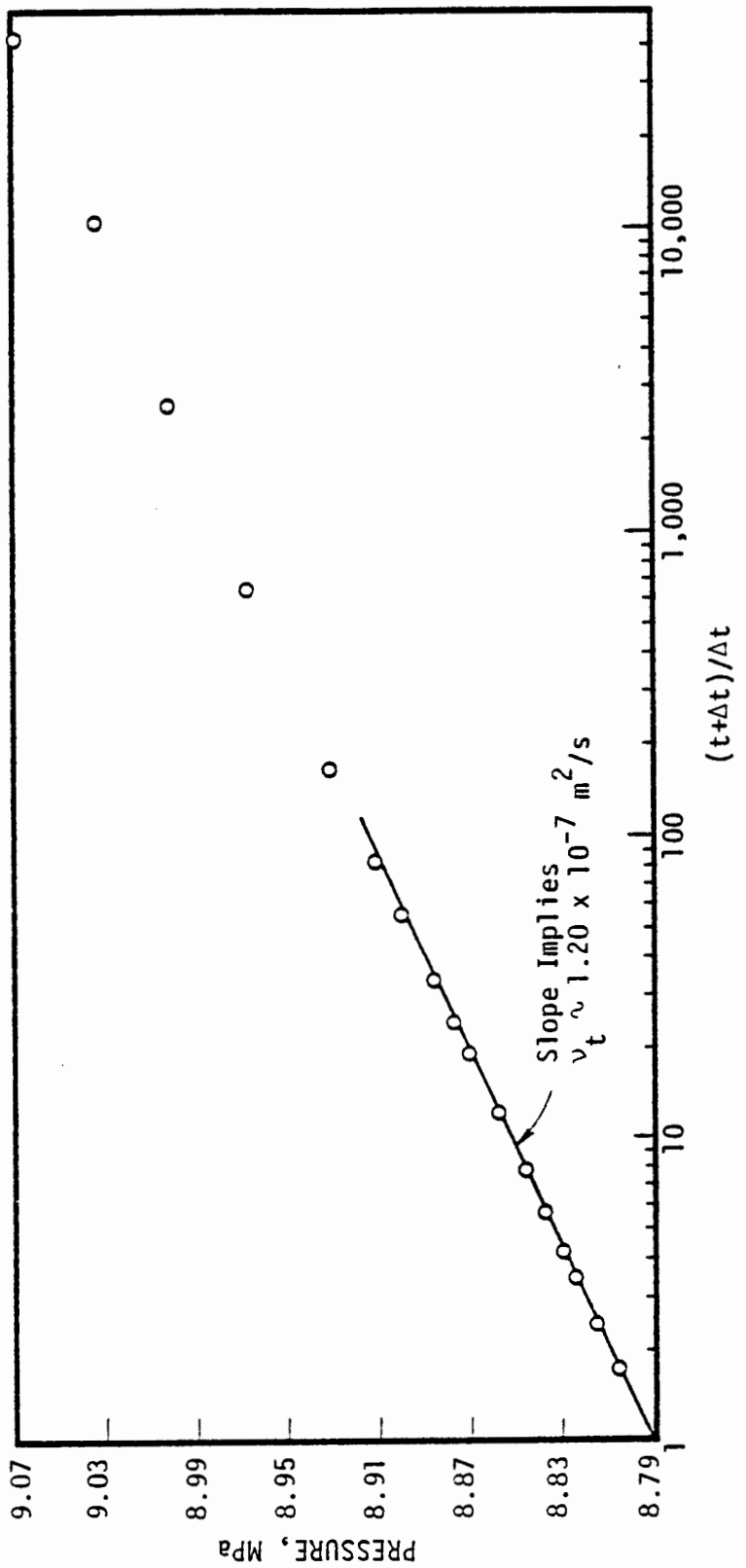


Figure 3.3. Pressure fall-off data for cold water injection into a hot water well.

water injection. The time to investigate a particular radius r during fall-off is approximately given by (see e.g., Matthews and Russell [1977]):

$$\Delta t = \frac{r_{inv}^2}{4} \frac{\phi \mu C_T}{k} \quad (3.1)$$

where

- Δt = Fall off time in sec
- r_{inv} = Radius of investigation in meters
- μ = Dynamic fluid viscosity in Pa-s
- C_T = Total formation compressibility in Pa^{-1}
- k = Formation permeability in m^2

with $r_{inv} = 6 \text{ m}$, $\phi = 0.1$, $\mu \sim 1.8 \times 10^{-4} \text{ Pa-s}$, $C_T \sim 0.075 \times 10^{-8} \text{ Pa}^{-1}$ (μ and $C_T = C_h$ are evaluated at 151°C), we have $\Delta t \sim 2.4 \text{ s}$. The first point on the fall-off curve corresponds to a Δt of 14 s.

3.4 Cold Water Injection into Two-Phase Reservoirs

Although cold water injection into two-phase reservoirs has been suggested by several investigators for evaluating formation properties (see e.g., Grant [1979b]), yet theoretical analyses of pressure buildup/fall-off data are currently unavailable in the published literature. In order to investigate the effects of cold water injection into two-phase reservoirs, two cases will be considered. The initial fluid state for these cases is given in Table 3.1; the fluid injection rate (35 kg/s) and the injected fluid temperature, are identical with those employed in the preceding section.

Table 3.1
INITIAL FLUID STATE FOR COLD WATER INJECTION INTO
TWO-PHASE RESERVOIRS

<u>Case No.</u>	<u>Pressure, MPa</u>	<u>Temperature, °C</u>	<u>Steam Sat.</u>
C.1	8.5917 MPa	300	0.28
C.2	8.5917 MPa	300	0.05

The pressure buildup (injection) data (Figures 3.4 and 3.5) closely fit straight lines with identical slopes. The slope implies a flowing kinematic viscosity of $2.02 \times 10^{-7} \text{ m}^2/\text{s}$ which is in good agreement with the kinematic viscosity of the cold injected water ($\nu \sim 1.96 \times 10^7 \text{ m}^2/\text{s}$). Figures 3.6 and 3.7 show the radial distribution of steam saturation and temperature at the end of the injection period ($t \sim 5.868 \times 10^5 \text{ s}$). The condensation front (especially in the low steam saturation case C.2) is seen to have advanced further into the formation than the edge of the thermal front. The latter effect is due to the fact that pressure changes are experienced over a much larger portion of the reservoir than the one undergoing cooling as a result of cold fluid injection.

Horner plots of pressure fall-off data are given in Figures 3.8 and 3.9. Three regions can be identified on these plots:

- (i) for large $(t + \Delta t)/\Delta t$ (i.e., small shut-in times), pressure falls off relatively rapidly
- (ii) for moderate values of $(t + \Delta t)/\Delta t$, pressure is essentially constant
- (iii) for small values of $(t + \Delta t)/\Delta t$ (i.e., large buildup times), pressure again starts to fall rather rapidly.

The first region (i.e., $(t + \Delta t)/\Delta t$ large) of the fall-off curve is governed by the pressure response of the condensed fluid region. Due to the large contrast in single-phase and two-phase compressibilities, the two-phase region remains practically unaffected during this time period (see e.g., steam saturation

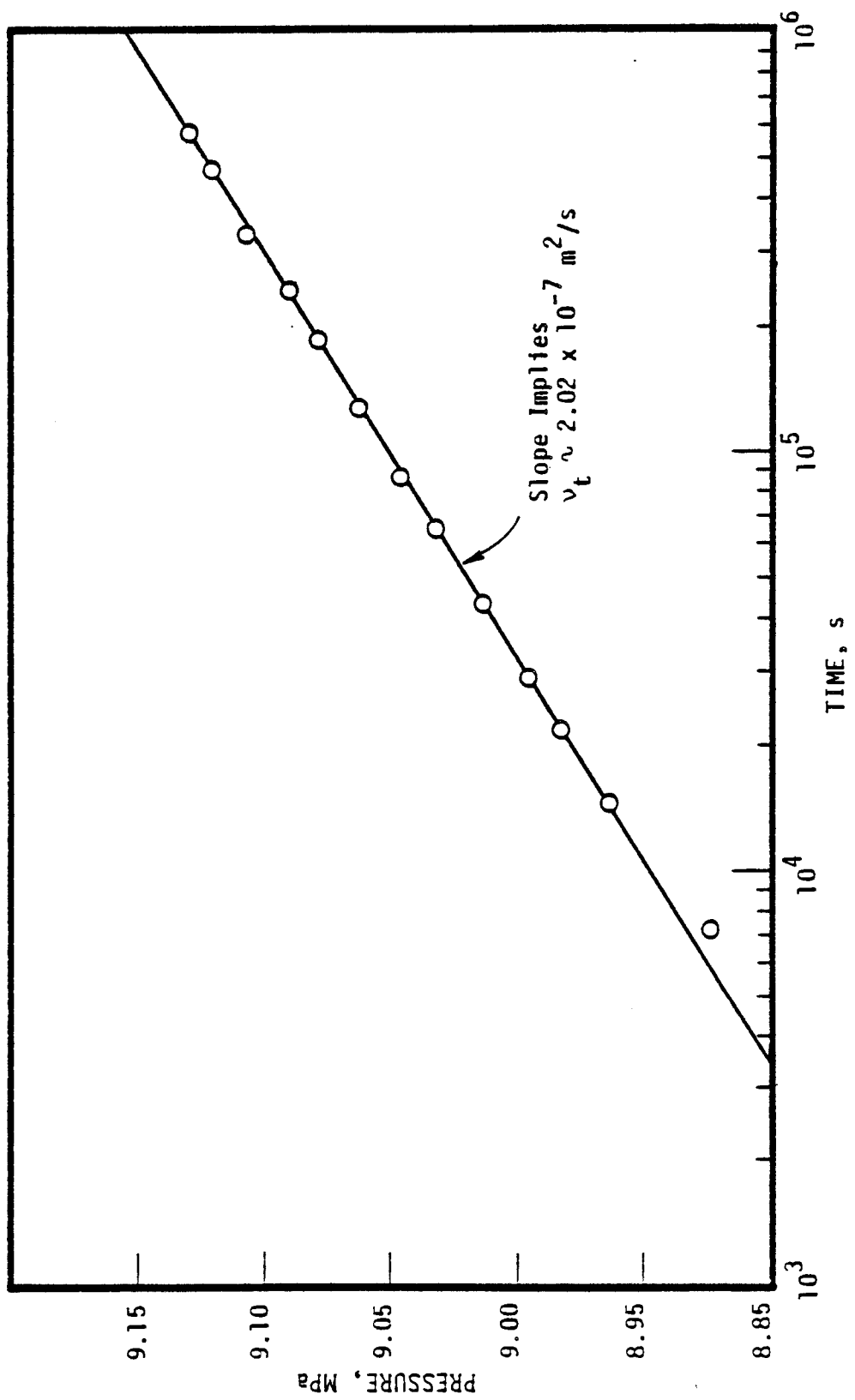


Figure 3.4. Pressure buildup (Injection) data for case C.1.

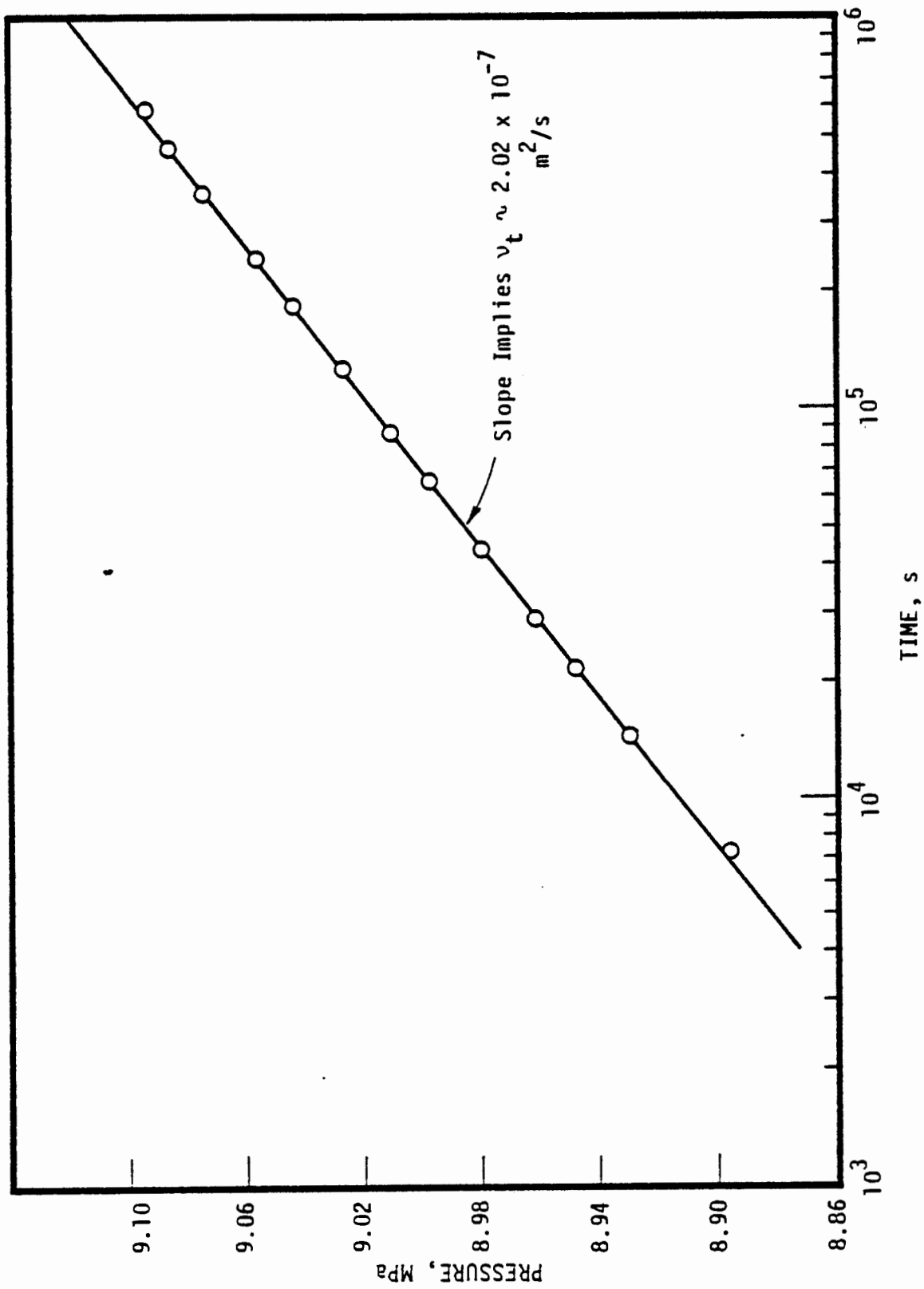


Figure 3.5. Pressure buildup (Injection) data for case C.2.

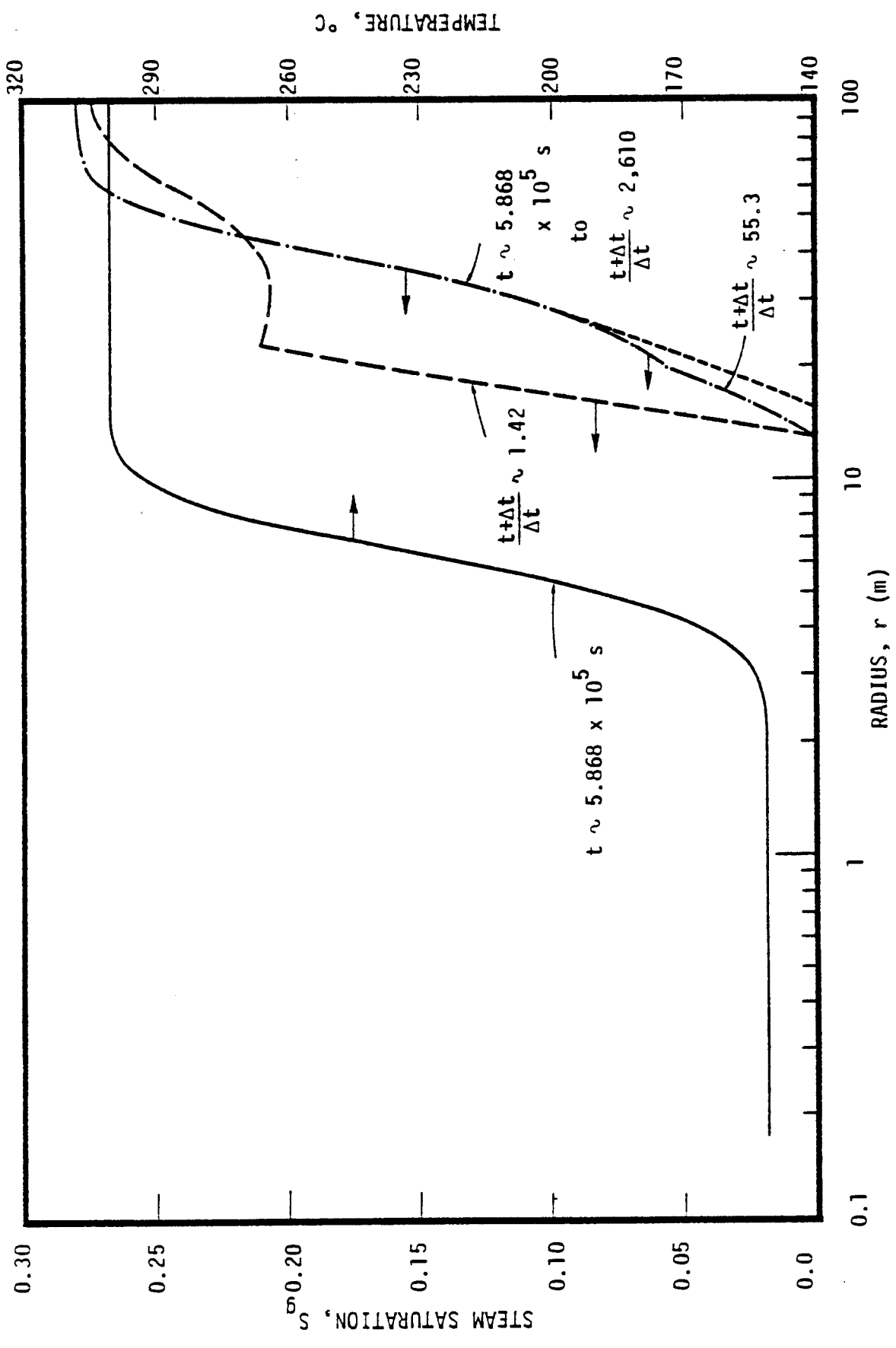


Figure 3.6. Radial distribution of temperature and steam saturation at selected times for case C.1.

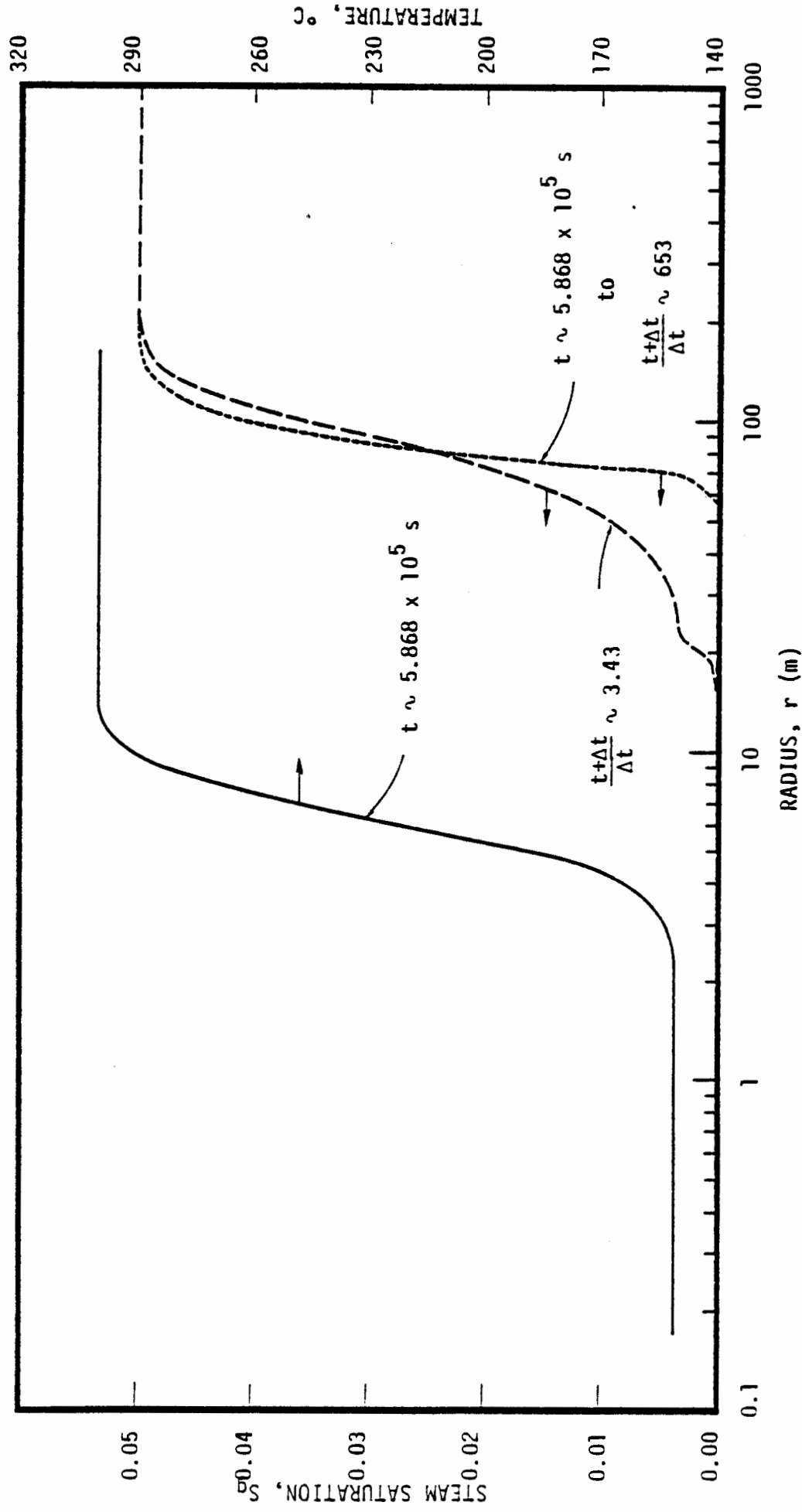


Figure 3.7. Radial distribution of temperature and steam saturation at selected times for case C.2.

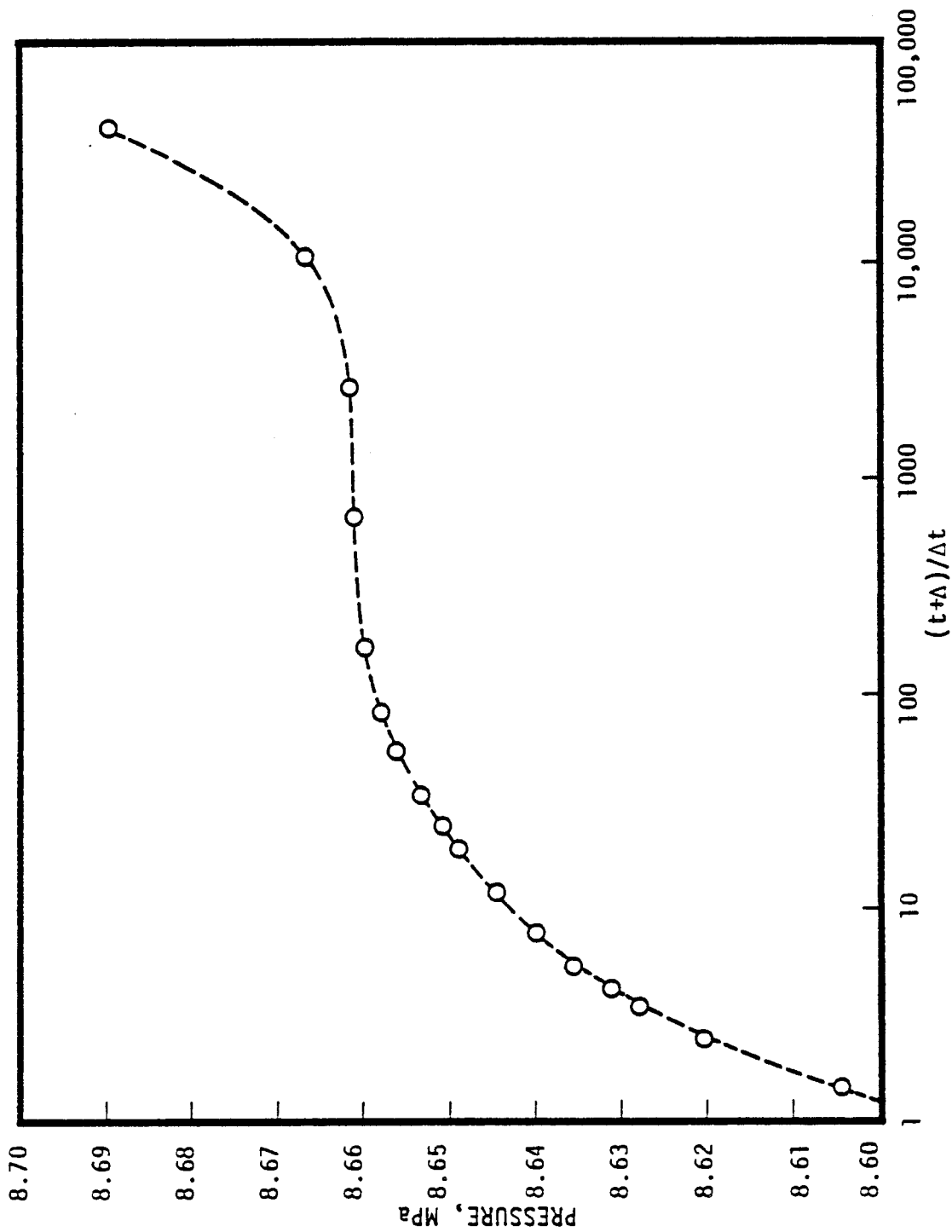


Figure 3.8. Pressure fall-off data (Horner plot) for case C.1.

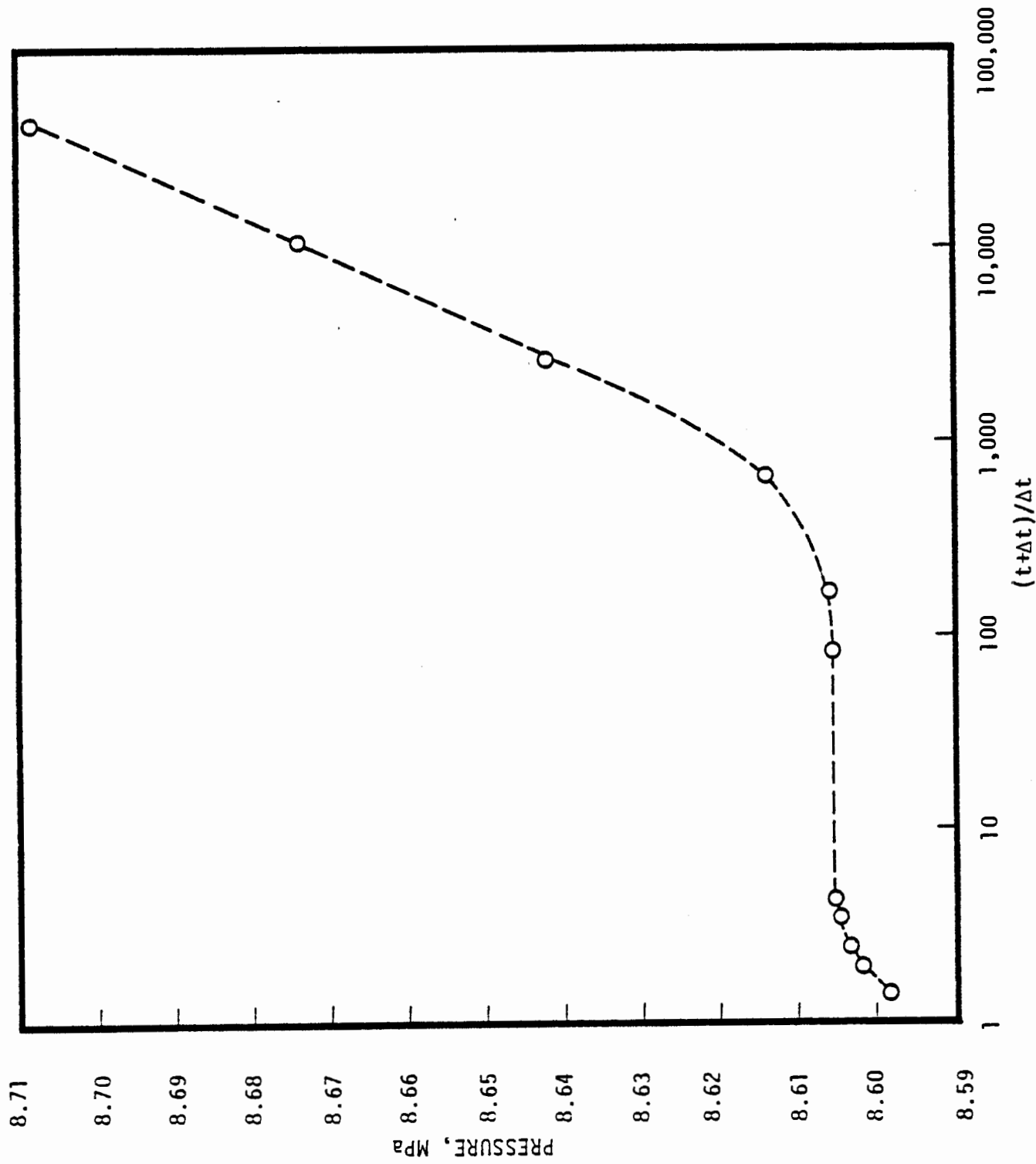


Figure 3.9. Pressure fall-off data (Horner plot) for case C.2

profiles in Figures 3.6 and 3.7). The condensed fluid region behaves like a reservoir with a constant pressure (= pressure at the edge of the condensation front) boundary. These early pressure fall-off data are replotted in Figures 3.10 and 3.11; these figures clearly demonstrate that the early fall-off behavior in the present cases resembles that of a reservoir with a constant pressure boundary. The condensation front radius, r_e , can, therefore, be calculated from the formula (Earlougher [1977]):

$$r_e = \left(\frac{k \Delta t_s}{1.25 \phi \mu C_T} \right)^{0.5} \quad (3.2)$$

where

- k = formation permeability
- Δt_s = time to startup of semi-steady reservoir behavior
(time at which pressure curve bends over)
- μ = viscosity of injected liquid water
- C_T = Total formation compressibility in the condensed region.

The condensation front radii inferred from Equation (3.2) and data of Figures 3.10 and 3.11 are compared with the actual values in Table 3.2.

Table 3.2
CONDENSATION FRONT RADII

$(\mu = 1.8 \times 10^{-4} \text{ Pa-s}; C_T = 0.075 \times 10^{-8} \text{ Pa}^{-1})$

<u>Case No.</u>	<u>Δt_s</u>	<u>r_e (inferred)</u>	<u>r_e (actual)</u>
C.1	72 s	14.6 m	(15.5 ± 1.5) m
C.2	753 s	47.2 m	(57.1 ± 5.2) m

Although the inferred values for r_e are in reasonable agreement with the actual values, a note of caution is in order here. In practical situations, the early fall-off data (such as that utilized

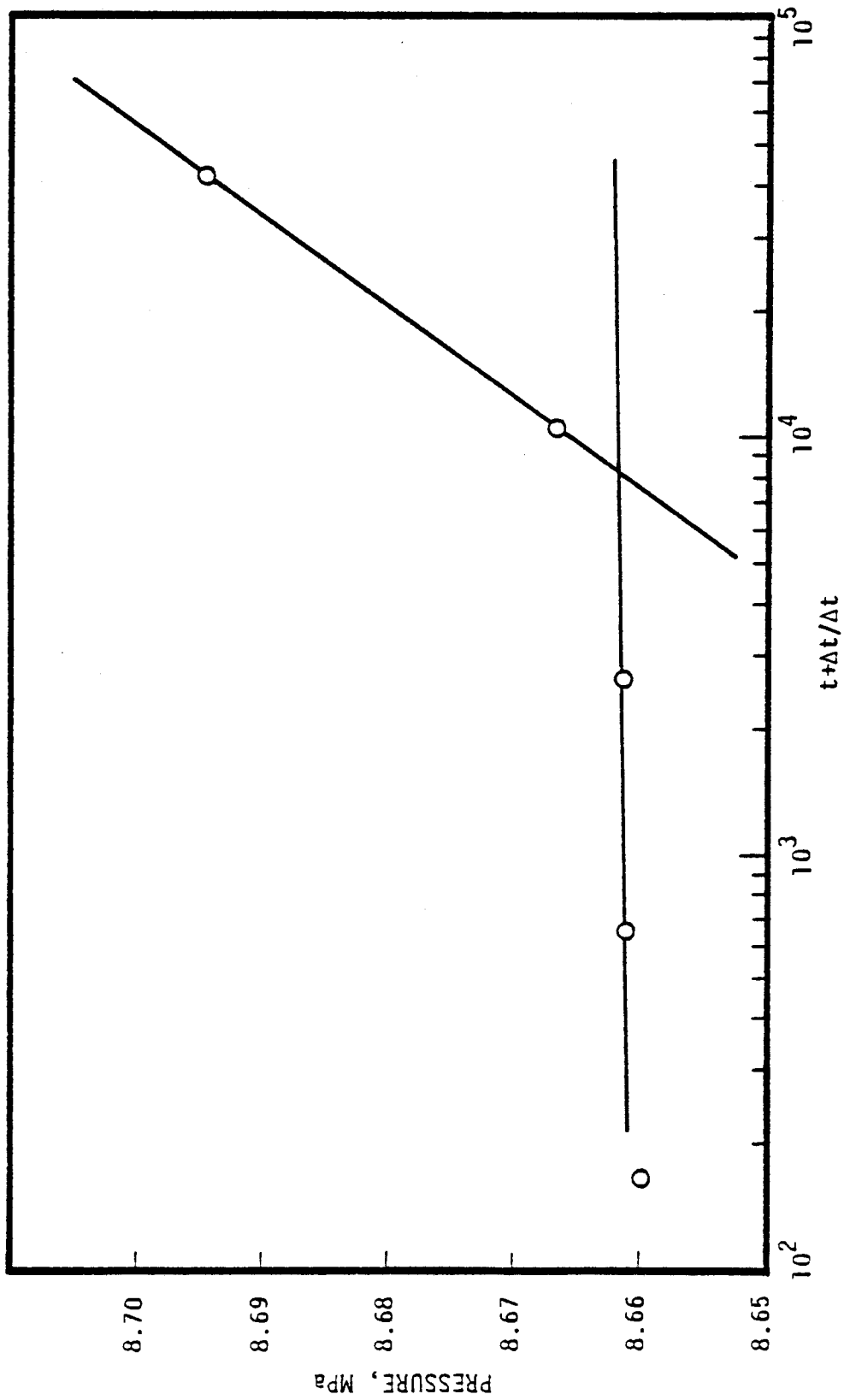


Figure 3.10. Early pressure fall-off data for case C.1.

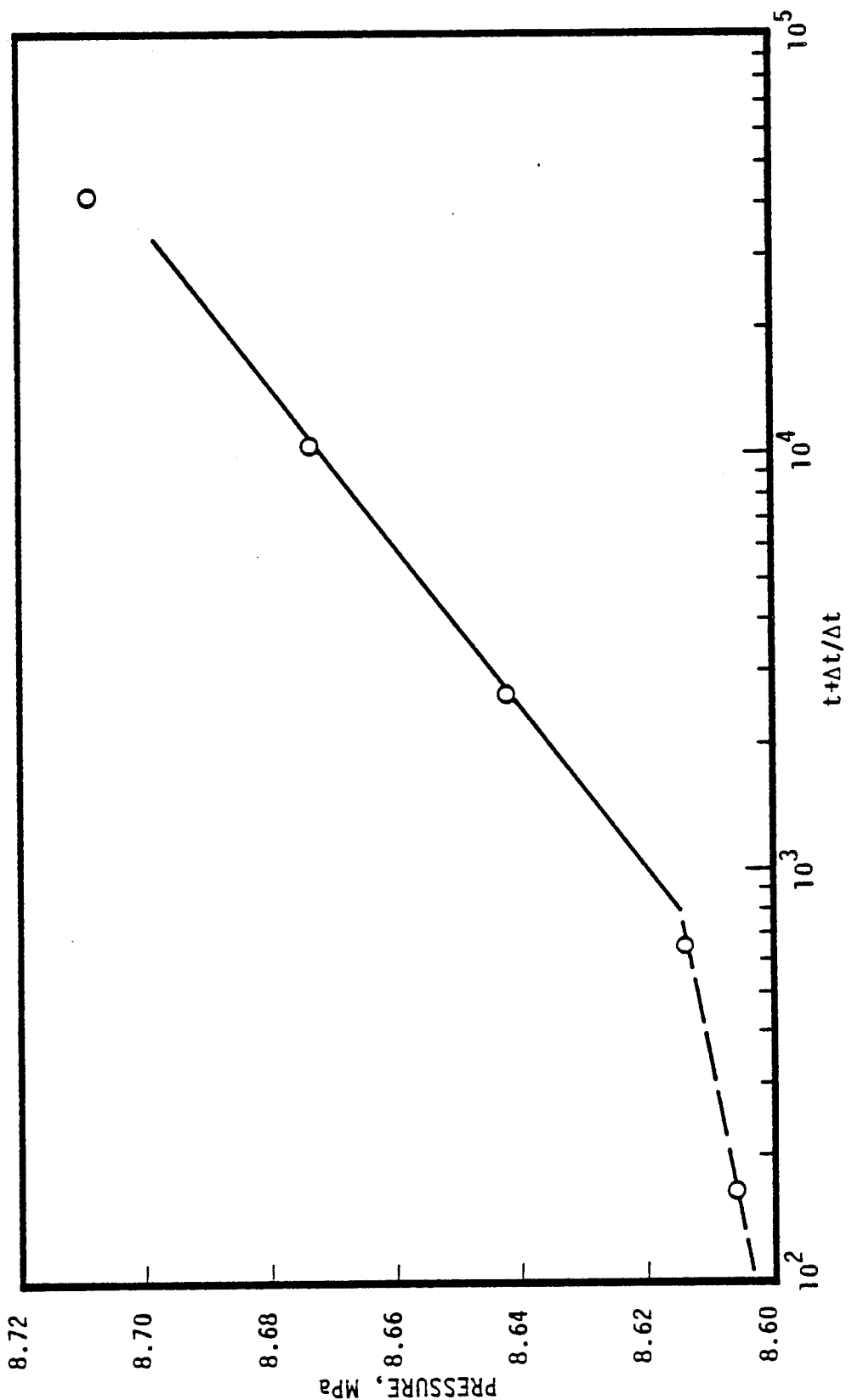


Figure 3.11. Early pressure fall-off data for case C.2.

in the above calculation for r_e) are liable to be dominated by wellbore storage, and it may well be impossible to identify the time at which the well starts exhibiting "semi-steady" response.

An examination of the numerical results shows that at the end of the first part of the fall-off curve, the pressure gradient in the single-phase (condensed) region is essentially zero whereas the pressure at the edge of the condensation front remains at its value at $\Delta t = 0$ (start of shut-in period). Also, the edge of the condensation front is stationary throughout this initial period (Figures 3.6 and 3.7 - See steam saturation profiles for $t = 5.868 \times 10^5$ s to $(t + \Delta t)/\Delta t = 2610$ in Figure 3.6, and 653 in Figure 3.7)).

During the middle fall-off period, the condensation front starts moving towards the wellbore. This part of the well response is characterized by an essentially constant pressure. At the end of this period, the condensation front becomes coincident with the edge of the thermal front (see e.g., steam saturation curve labeled $(t + \Delta t)/\Delta t \sim 3.43$ in Figure 3.7). The condensation front once again becomes stationary at this point.

For large fall-off times (i.e., for the third fall-off period), the well response is governed by the two-phase region. As can be seen from Figures 3.8 and 3.9, the pressure fall-off data do not, however, asymptote to a straight line. It is convenient to plot the fall-off data in a somewhat different manner. Figures 3.12 and 3.13 are plots of $\log \Delta p$ ($\Delta p = |p_w(\Delta t) - p_f|$ where p_f is the last flowing pressure) versus $\log \Delta t$. Referring to Figure 3.13, it may be seen that the two-phase fall-off data lie on the unit slope line. A unit slope line can also be identified on Figure 3.12. It is well known that the presence of a unit slope line indicates that the well response is controlled by storage effects; this part of the fall-off data is useless for analysis purposes in the absence of data regarding the location of the condensation front (\sim effective wellbore radius for two-phase fall-off regime). For

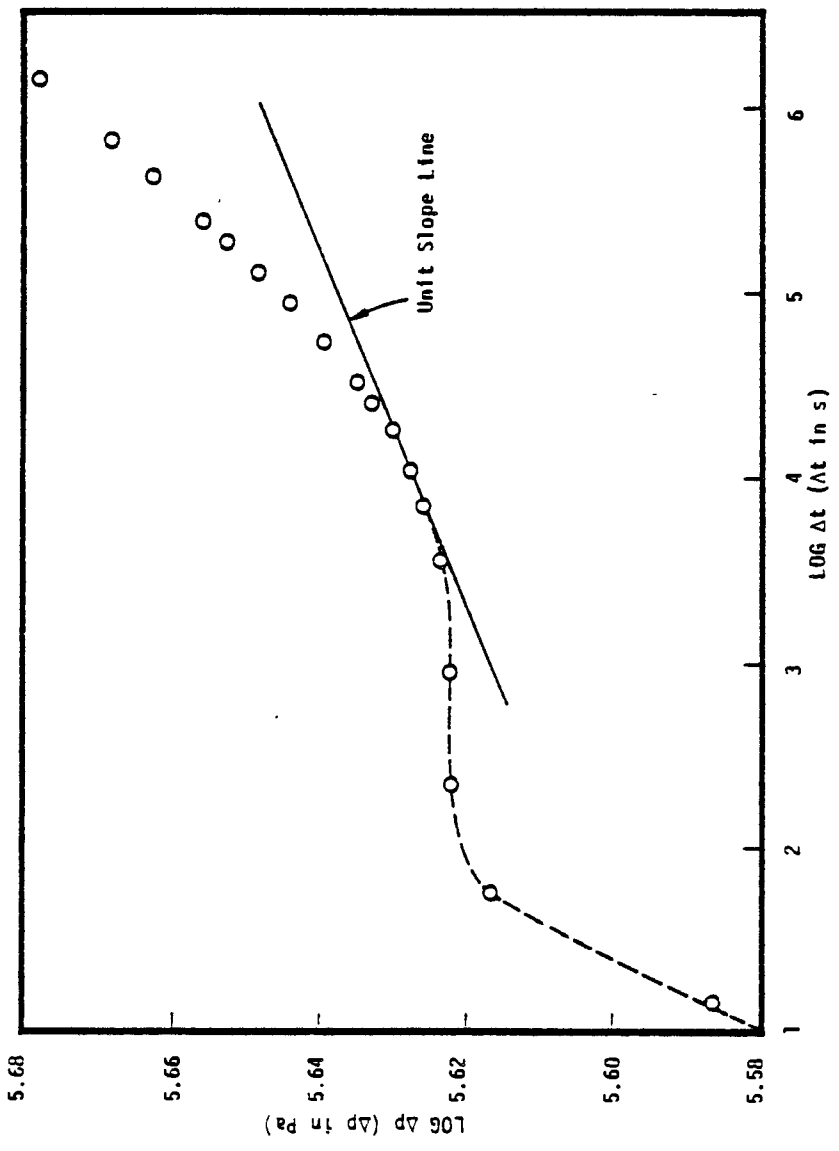


Figure 3.12. Plot of $\log \Delta p$ versus $\log \Delta t$ for case C.1. ($\Delta p = |p_w - p_f|$; p_w is the well pressure at Δt and p_f is the last flowing pressure.) Note that the vertical and horizontal scales are different.

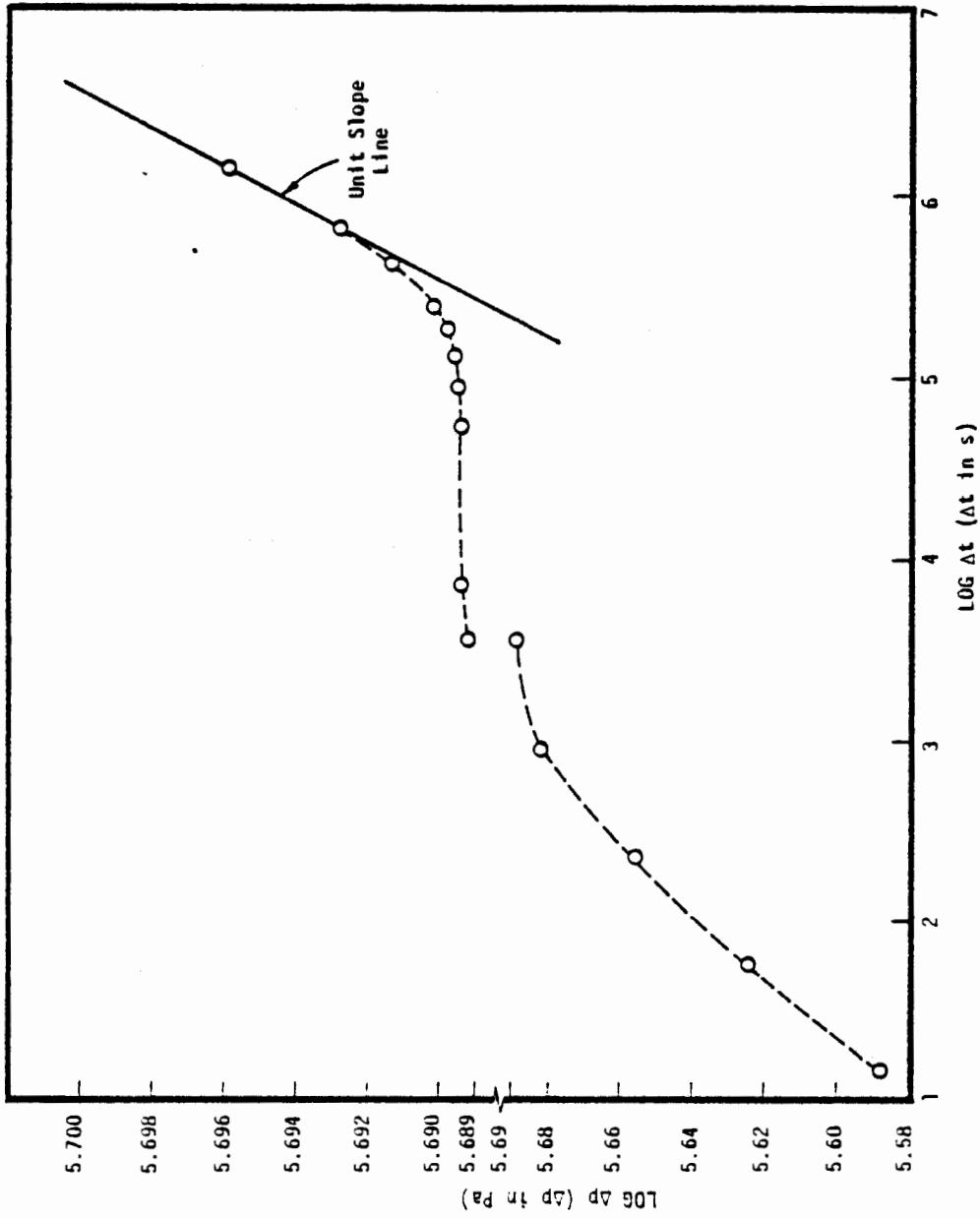


Figure 3.13. Plot of $\log \Delta p$ versus $\log \Delta t$ for case C.2. ($\Delta p = |p_w - p_f|$; p_w is the well pressure at Δt and p_f is the last flowing pressure.) Note that (1) the vertical and horizontal scales are different, and (2) the vertical scale is discontinuous.

single-phase flow, a rough rule of thumb is that the semi-log straight line starts at a time which is one and one-half log cycles removed from the time at which the pressure data begins to deviate from the unit slope straight line. Utilizing the latter criterion, it is seen from Figure 3.12 that only the last point or two may be expected to lie on the semi-log line. In view of the nonlinear nature of two-phase flow in porous media, especially prior to the start of semi-log straight line, it would very likely be futile to try to analyze the two-phase fall-off data of Figure 3.12 to derive kinematic mobility.

REFERENCES

- EARLOUGHER, R. C., Jr., Advances in Well Test Analysis, Monograph Series, Vol. 5, Society of Petroleum Engineers, Dallas, TX, 1977.
- GARG, S. K., "Pressure Transient Analysis for Two-Phase (Water/Steam) Geothermal Reservoirs," Society of Petroleum Engineers, Paper No. 7479, 1978. Also SPEJ, pp. 206-214, June 1980.
- GRANT, M. A., "Two-Phase Linear Geothermal Pressure Transients: A Comparison With Single-Phase Transients," New Zealand J. Sci., Vol. 21, pp. 355-364. 1978.
- GRANT, M. A., "Quasi-Analytic Solutions for Two-Phase Flow Near a Discharging Well," Applied Mathematics Division - DSIR, New Zealand, Report No. 86, June 1979a.
- GRANT, M. A., "Interpretation of Downhole Measurements in Geothermal Wells," Applied Mathematics Division - DSIR, New Zealand, 1979b.
- MATTHEWS, C. S. and D. G. Russell, Pressure Buildup and Flow Tests in Wells, Monograph Series, Vol. 1, Society of Petroleum Engineers, Dallas, TX, 1967.
- MOENCH, A. F. and P. G. Atkinson, "Transient Pressure Analysis in Geothermal Steam Reservoirs With an Immobile Vaporizing Liquid Phase - Summary Report," Proc. Third Stanford Workshop on Geothermal Reservoir Engineering, Stanford, CA, pp. 64-69, 1977.
- O'SULLIVAN, M., "A Similarity Method for Geothermal Well Test Analysis," to appear in Water Resources Research, 1980.
- PRITCHETT, J.W., "Geothermal Reservoir Engineering Computer Code Comparison and Validation Calculations Using MUSHRM and CHARGR Geothermal Reservoir Simulators," Systems, Science and Software Report SSS-R-81-4749, November 1980.
- SOREY, M. L., M. A. Grant and E. Bradford, "Nonlinear Effects in Two-Phase Flow to Wells in Geothermal Reservoirs," Water Resources Research, August 1980.

Union Geothermal Company of New Mexico

4100 Southern Blvd. SE

P. O. Box 15225

Rio Rancho, New Mexico 87174

Telephone (505) 897-1776

ROE9-089

union

October 15, 1979

Mr. Carl Ulvog
New Mexico Energy Resources Board
Oil Conservation Commission
P.O. Box 2088
Santa Fe, New Mexico 87501

Dear Mr. Ulvog:

Enclosed are location data, lithologic summaries, and geophysical logs for our wells in the Redondo Creek area of the Valles Caldera. These data may be made available upon request to interested parties as per Union's agreement with the U. S. Department of Energy. Data for two wells outside Redondo Creek, Baca 7 and Baca 8, are also included.

Very truly yours,



R. O. Engebretsen
Area Manager

RD:dp

Enclosure

#4
5-A
6
7
8
9
10
11
12
13
14
15
16
17

Operator: Union Geothermal Company of New Mexico
Lease: Baca
Well No.: Baca 4
Location: 1,778,980'N 404,915'E NM State Plane Co-ordinates
Elevation: 9318'
County: Sandoval
Total Depth of Well: 6376'

Lithologic Units

<u>Formation</u>	<u>Age</u>	<u>Interval - Feet</u>	
		<u>Measured Depth</u>	<u>Elevation Above Sea Level</u>
Caldera Fill	Quaternary	0-200	9318-9135
Bandelier Tuff	Quaternary	200-5980	9135-3355
Paliza Canyon	Tertiary	5980-6376	3355-2959

Operator: Union Geothermal Company of New Mexico

Lease: Baca

Well No.: Baca 5A

Location: 1,774,670'N 403,285'E NM State Plane Co-ordinates

Elevation: 9320'

County: Sandoval

Total Depth of Well: 6973'

Lithologic Units

<u>Formation</u>	<u>Age</u>	<u>Interval - Feet</u>	
		<u>Measured Depth</u>	<u>Elevation Above Sea Level</u>
Caldera Fill	Quaternary	0-450	9320-8870
Bandelier Tuff	Quaternary	450-6610	8870-2710
Paliza Canyon	Tertiary	6610-6973	2710-2347

Operator: Union Geothermal Company of New Mexico

Lease: Baca

Well No.: Baca 6

Location: 1,778,490'N 401,580'E NM State Plane Co-ordinates

Elevation: 8726'

County: Sandoval

Total Depth of Well: 4810'

Lithologic Units

<u>Formation</u>	<u>Age</u>	<u>Interval - Feet</u>	
		<u>Measured Depth</u>	<u>Elevation Above Sea Level</u>
Caldera Fill	Quaternary	0-500	8726-8226
Bandelier Tuff	Quaternary	500-4750	8226-3976
Paliza Canyon	Quaternary	4750-4810	3976-3916

Operator: Union Geothermal Company of New Mexico

Lease: Baca

Well No.: Baca 7

Location: Projected: NE1/4, SE1/4, NW1/4 Sec 26; T20N; R 3E NMPM

Elevation: 8724'

County: Sandoval

Total Depth of Well: 5532'

Lithologic Units

<u>Formation</u>	<u>Age</u>	<u>Interval - Feet</u>	<u>Elevation Above Sea Level</u>
		<u>Measured Depth</u>	
Valles Rhyolite	Quaternary	0-1400	8724-7324
Caldera Fill	Quaternary	1400-2300	7324-6424
Bandelier Tuff	Quaternary	2300-3300	6424-5424
Sediments-Undivided	Tertiary	3300-3960	5424-4764
Red Beds	Permian	3960-4840	4764-3884
Limestone, Sandstone	Pennsylvanian	4840-5460	3884-3264
Granite	Pre-Cambrian	5460-5532	3264-3192

Operator: Union Geothermal Company of New Mexico

Lease: Baca

Well No.: Baca No. 8

Location: Projected NE $\frac{1}{4}$, SE $\frac{1}{4}$, SW $\frac{1}{4}$ Sec 35; T20N; R3E NMPM

Elevation: 8631'

County: Sandoval

Total Depth of Well: 4384'

Lithologic Units

<u>Formation</u>	<u>Age</u>	<u>Interval - Feet</u>	
		<u>Measured Depth</u>	<u>Elevation Above Sea Level</u>
Caldera Fill	Quaternary	0-580	8631-8070
Bandelier Tuff	Quaternary	580-3100	8070-5550
Sediments-Undivided	Tertiary	3100-4000	5550-4650
Red Beds	Permian	4000-4384	4650-4226

Operator: Union Geothermal Company of New Mexico
Lease: Baca
Well No.: Baca 9
Location: Approximately 1,776,400'N 400,270'E NM State Plane Co-ordinates
Elevation: 8605'
County: Sandoval
Total Depth of Well: 5303'

Lithologic Units

<u>Formation</u>	<u>Age</u>	<u>Interval - Feet</u>	<u>Elevation Above Sea Level</u>
		<u>Measured Depth</u>	
Caldera Fill	Quaternary	0-80	8605-8525
Bandelier Tuff	Quaternary	80-5303	8525-3302

Operator: Union Geothermal Company of New Mexico
 Lease: Baca
 Well No.: Baca 10
 Location: 1,777,860'N 400,715'E NM State Plane Co-ordinates
 Elevation: 8735'
 County: Sandoval
 Total Depth of Well: 6001'

Lithologic Units

<u>Formation</u>	<u>Age</u>	<u>Interval - Feet</u>	<u>Elevation Above Sea Level</u>
		<u>Measured Depth</u>	
Caldera Fill	Quaternary	0-520	8735-8235
Bandelier Tuff	Quaternary	520-5220	8235-3555
Paliza Canyon	Tertiary	5220-5390	3555-2848
Sediments-Undivided	Tertiary	5390-6001	2848-2777

Geophysical Logs

<u>Type</u>	<u>Interval (ft. KB)</u>	<u>Date</u>
Temperature	50-2421	9-14-79
Gamma Ray	2445-surface	9-12-79

Operator: Union Geothermal Company of New Mexico

Lease: Baca

Well No.: Baca 11

Location: 1,781,120'N 403,450'E NM State Plane Co-ordinates

Elevation: 9065'

County: Sandoval

Total Depth of Well: 6924'

Lithologic Units

<u>Formation</u>	<u>Age</u>	<u>Interval - Feet</u>	
		<u>Measured Depth</u>	<u>Elevation Above Sea Level</u>
Caldera Fill	Quaternary	0-320	9605-8765
Bandelier Tuff	Quaternary	320-5300	8765-3811
Paliza Canyon	Tertiary	5300-6560	3811-2585
Sediments-Undivided	Tertiary	6560-6924	2585-2239

Operator: Union Geothermal Company of New Mexico
 Lease: Baca
 Well No.: Baca 12
 Location: 1,773,160'N 399,360'E NM State Plane Co-ordinates
 Elevation: 8430'
 County: Sandoval
 Total Depth of Well: 9212'

Lithologic Units

<u>Formation</u>	<u>Age</u>	<u>Interval - Feet</u>	Elevation Above Sea Level
		<u>Measured Depth</u>	
Caldera Fill	Quaternary	0-160	8430-8290
Bandelier Tuff	Quaternary	160-6460	8290-1998
Paliza Canyon	Tertiary	6460-7380	1998-1080
Abiquiu Tuff	Tertiary	7380-7575	1080-886
Red Beds	Permian	7575-9210	886-(-) 750

Geophysical Logs

<u>Type</u>	<u>Interval (ft. KB)</u>	<u>Date</u>
Temperature	1453-3495	7-7-74

Operator: Union Geothermal Company of New Mexico
 Lease: Baca
 Well No.: Baca 13
 Location: 1,781,685'N 405,725'E NM State Plane Co-ordinates
 Elevation: 9292'
 County: Sandoval
 Total Depth of Well: 8228'

Lithologic Units

<u>Formation</u>	<u>Age</u>	<u>Interval - Feet</u>		<u>Elevation Above Sea Level</u>
		<u>Measured Depth</u>		
Caldera Fill	Quaternary	0-560		9292-8752
Bandelier Tuff	Quaternary	560-5712		8752-3686
Paliza Canyon	Tertiary	5712-8090		3686-1340
Red Beds	Permian	8090-8228		1340-1204

Geophysical Logs

<u>Type</u>	<u>Interval (ft. KB)</u>	<u>Date</u>
Induction	3485-1470	9-18-74
Induction	6813-3494	10-28-74
Temperature	1150-3499	9-18-74
Temperature	2640-8228	10-27-74
Sonic	7240-3494	10-28-74
Neutron/Density	6809-3494	10-28-74

Operator: Union Geothermal Company of New Mexico
 Lease: Baca
 Well No.: Baca 14
 Location: 1,776,450'N 400,320'E NM State Plane Co-ordinates
 Elevation: 8605'
 County: Sandoval
 Total Depth of Well: 6824'

Lithologic Units

<u>Formation</u>	<u>Age</u>	<u>Interval - Feet</u>	
		<u>Measured Depth</u>	<u>Elevation Above Sea Level</u>
Caldera Fill	Quaternary	0-280	8605-8345
Bandelier Tuff	Quaternary	280-5800	8345-3060
Paliza Canyon	Tertiary	5800-6140	3060-2736
Undivided-Sediments	Tertiary	6140-6700	2736-2204
Red Beds	Permian	6700-6824	2204-2085

Geophysical Logs

<u>Type</u>	<u>Interval (ft. KB)</u>	<u>Date</u>
Temperature	470-5300	10-7-75
Neutron/Density	5830-3068	2-10-75

Operator: Union Geothermal Company of New Mexico
Lease: Baca
Well No.: Baca 15
Location: 1,780,590'N 402,160'E NM State Plane Co-ordinates
Elevation: 9117'
County: Sandoval
Total Depth of Well: 5505'

Lithologic Units

<u>Formation</u>	<u>Age</u>	<u>Interval - Feet</u>	
		<u>Measured Depth</u>	<u>Elevation Above Sea Level</u>
Caldera Fill	Quaternary	0-140	9117-8997
Bandelier Tuff	Quaternary	140-5300	8997-4003
Paliza Canyon	Tertiary	5300-5505	4003-3833

Operator: Union Geothermal Company of New Mexico

Lease: Baca

Well No.: Baca 16

Location: 1,784,290'N 405,630'E NM Plane Co-ordinates

Elevation: 9622'

County: Sandoval

Total Depth of Well: 7002'

Lithologic Units

<u>Formation</u>	<u>Age</u>	<u>Interval - Feet</u>	
		<u>Measured Depth</u>	<u>Elevation Above Sea Level</u>
Caldera Fill	Quaternary	0-380	9622-9242
Redondo Creek Rhyolite	Quaternary	380-880	9242-8742
Bandelier Tuff	Quaternary	880-5560	8742-4155
Paliza Canyon	Tertiary	5560-6880	4155-2931
Undivided-Sediments	Tertiary	6880-7002	2931-2820

Operator: Union Geothermal Company of New Mexico
 Lease: Baca
 Well No.: Baca 17
 Location: 1,782,690'N 402,980'E NM State Plane Co-ordinates
 Elevation: 9361'
 County: Sandoval
 Total Depth of Well: Original Hole: 5791'
 Redrill: 6254'
 Lithologic Units

<u>Formation</u>	<u>Age</u>	<u>Interval - Feet</u>	
		<u>Measured Depth</u>	<u>Elevation Above Sea Level</u>
<u>Original Hole:</u>			
Redondo Creek Rhyolite	Quaternary	0-400	9361-8982
Caldera Fill	Quaternary	400-980	8982-8402
Bandelier Tuff	Quaternary	980-5500	8402-3931
Paliza Canyon	Tertiary	5500-5791	3931-3647
<u>Redrill:</u>			
Bandelier Tuff	Quaternary	3175-5520	6211-3949
Paliza Canyon	Tertiary	5520-6254	3949-3266

Geophysical Logs

<u>Type</u>	<u>Interval (ft. KB)</u>	<u>Date</u>
Induction	1168-238	8-31-78
Induction	2763-1171	9-22-78
Induction	5801-3000	10-12-78
Induction (Redrill)	6270-3000	11-10-78
Temperature	250-2755	9-22-78
Temperature	100-4615	10-12-78
Borehole Geometry	2755-1181	9-22-78
Caliper	3500-3000	10-12-78